



Faculté des sciences de la vie

Thèse réalisée en co-tutelle avec
l'Université de Bâle

Présentée pour obtenir le grade de
Docteur de l'Université Louis Pasteur
Strasbourg I

Discipline: Sciences du vivant
Spécialité: Aspects moléculaires et cellulaires de la biologie

par Sophie Schlumberger

Caractérisation des récepteurs de l'hormone de mélanocortine (MCH)

Soutenue le 26 juillet 2002 à 14 heures, devant le jury composé de:

Directeur de Thèse: M. A.N. EBERLE, Professeur, Université de
Bâle
Co-Directeur de Thèse: Mme M-J. FREUND-MERCIER, Professeur, ULP
Rapporteur Interne: M. P. PEVET, Directeur de Recherche, ULP
Rapporteur Externe: Mme T.J. RESINK, Professeur, Université de Bâle
Rapporteur Externe: M. H. VAUDRY, Professeur, Université de
Rouen

Table of contents

	Page
Table of contents _____	1
Abbreviations _____	6
Abstract _____	7
1. Introduction _____	8
1.1. Melanin-concentrating hormone (MCH) _____	8
1.1.1. Structure and localisation _____	8
1.1.2. Functions _____	12
a. In teleost fish _____	12
b. In mammals _____	12
c. MCH / α -MSH / NEI antagonism _____	13
1.1.3. MCH knockout mouse model _____	13
1.1.4. MCH transgenic mouse model _____	13
1.2. MCH-R ₁ _____	14
1.2.1. MCH-R ₁ cloning _____	14
1.2.2. MCH-R ₁ mRNA expression _____	15
1.2.3. Binding characteristics of MCH to MCH-R ₁ _____	16
1.2.4. MCH-R ₁ signalling pathway _____	17
a. In cellular models of MCH-R ₁ ectopic expression _____	17
b. In cells endogenously expressing MCH-R ₁ _____	18
1.2.5. MCH-R ₁ knockout mouse model _____	19
1.2.6. MCH / α -MSH antagonism at MCH-R ₁ _____	19
1.2.7. Implication of MCH-R ₁ in a human autoimmune disease _____	19
1.3. MCH-R ₂ _____	20

1.4.	Putative MCH receptors on melanophores and melanoma cells_____	22
1.5.	Aims of the thesis_____	23

2. Methods	24
2.1. Cell culture	24
2.1.1. Cell lines used during this thesis work	24
2.1.2. Cell culture conditions and media	25
2.2. Peptides used during this thesis work	26
2.3. Binding assay	27
2.3.1. Binding assay with cell lines	27
a. Preparation of radioligand	27
b. Receptor binding assay	28
c. Stability of radioligand after incubation	29
2.3.2. Binding assay with porcine brain membranes	29
a. Membrane preparation	29
b. Binding assay	29
2.3.3. Binding assay with embryonic rat neurons	30
a. Isolation and culture of the rat embryonic hypothalamic cells	30
b. Binding assay	30
2.4. Cross-linking of [¹²⁵ I]-MCH	31
2.4.1. Cross-linking assay prior to 2-D electrophoresis	31
2.5. Two-dimensional gel electrophoresis	32
2.6. Autoradiographic localisation of MCH binding sites in the central nervous system of the rat	33
2.7. Semi-quantitative RT-PCR	34
2.8. Immunofluorescence studies	35

2.8.1.	External staining	35
2.8.2.	Internal staining	35
2.9.	Western blotting	35
2.10.	FLIPR assay	36

3.Results	37
3.1. Detection of MCH binding sites	37
3.1.1. A well established model: ^{125}I -[DPhe ¹³ , Tyr ¹⁸]-MCH binding to the G4F-Cl1 melanoma cells	37
3.1.2. Binding assays with neuroblastoma cell lines	38
3.1.3. Binding assays with porcine brain membranes	40
3.1.4. Binding assay with human primary melanocytes	45
3.1.5. Binding assays with rat embryonic primary hypothalamic neurons	46
3.1.6. Autoradiographic localisation of MCH binding sites in the central nervous system of the rat	47
3.1.7. Cross-linking of MCH radioligand to neuroblastoma cell lines	47
3.2. Can the 50 kDa cross-linked band be isolated by two-dimensional electrophoresis ?	49
3.2.1. Establishment of the technique with unlabeled proteins	49
3.2.2. 2-D electrophoresis of radioligand cross-linked sample	50
3.3. Structure-activity of MCH derivatives on cells overexpressing rat MCH-R ₁	52
3.3.1. Verification of transgene expression by RT-PCR and immunofluorescence	52
a. Flag-rat MCH-R ₁ mRNA production	52
b. Expression and localisation of Flag-rat MCH-R ₁	53

3.3.2.	Binding assays_____	54
3.3.3.	FLIPR assays_____	56
3.3.4.	Cross-linking assays_____	60
3.3.5.	Western blotting assay_____	61

3.4.	The Kelly neuroblastoma cell line endogenously expresses MCH-R ₁	61
3.4.1.	RT-PCR for MCH, MCH-R ₁ and -R ₂	61
3.4.2.	MCH-R ₁ immunofluorescence staining	63
3.4.3.	Western blotting	64
3.4.4.	Competition assay with [¹²⁵ I]-MCH	65
3.4.5.	Cross-linking assay	66
3.4.6.	FLIPR assay	66
4.	Discussion	68
4.1.	Choice of the radioligand to find novel MCH binding sites	68
4.2.	Structure/activity of MCH derivatives on MCH-R ₁ overexpressing cells	69
4.3.	The case of G4F-Cl1 mouse melanoma binding site	71
4.3.1.	Binding site	71
4.3.2.	Isolation of the \approx 50 kDa cross-linked band	71
4.4.	Advantages of FLAG TM tag	72
4.5.	MCH-R ₁ regulation by MCH or leptin	73
4.6.	Presence of MCH-R ₁ in Kelly human neuroblastoma cell line	74
4.7.	MCH: a promising drug target for obesity and/or anorexia?	75
4.7.1.	Example of a neuropeptide administration that induced body fat loss in humans	75

4.7.2. Tools to study MCH-MCH-R₁ axis in humans _____76

5. Conclusion	78
5.1. Conclusion	78
5.2. Perspectives (proposal for future experiments)	79
5.2.1. With the Kelly human neuroblastoma cell line	79
5.2.2. With MCH-R ₁ and -R ₂ coding sequences	79
a. Intracellular localisation of MCH-R ₁ and -R ₂	79
b. Study of intracellular dynamics of MCH-R ₁ and -R ₂	80
c. Study of MCH-R ₁ and -R ₂ homo- or heterodimerisation	80
d. Mapping of the [¹²⁵ I]-MCH contact point on MCH-R ₁ and R ₂	81
5.2.3. With the G4F-Cl1 mouse melanoma cells	81
6. References	82
7. Appendix	89
7.1. Acknowledgements	89
7.2. Curriculum vitae	90
7.2.1. Personal information	90
7.2.2. Education	90
7.2.3. Lectures attended during the Ph.D. fellowship	91
7.3. Original publications	92

Abbreviations

α -MSH	α -melanocyte-stimulating hormone
bp	basepair (s)
BSA	bovine serum albumin
CHAPS	3-[(3-cholamidopropyl)dimethyl-ammonio]-1-propane-sulfonate
CHO	Chinese hamster ovary
cpm	count (s) per minute
DTT	dithiothreitol
ECL	enhanced chemoluminescence
EDTA	ethylenediamine tetraacetic acid
FLIPR	fluorimetric imaging plate reader
Fluo-3	1-[2-Amino-5-(2,7-dichloro-6-hydroxy-3-oxy-9-xanthenyl)-phenoxy]-2-[2-amino-5-methylphenoxy]ethane-N,N,N',N'-tetraacetic acid
GPCR	G protein-coupled receptor
HEK	human embryonic kidney
HEPES	N-(2-hydroxyethyl-1-piperazine-N'-ethane)-sulfonic acid
HPLC	high pressure liquid chromatography
IP	intra peritoneal
kDa	kilodalton (s)
MCH	melanin-concentrating hormone
MCH-R ₁	melanin-concentrating hormone receptor 1
MCH-R ₂	melanin-concentrating hormone receptor 2
NP-40	nonidet P-40
PBS	phosphate-buffered saline
PCR	polymerase chain reaction
PMSF	phenylmethylsulfonylfluoride
Ponceau S	3-hydroxy-4-(2-sulfo-4-[4-sulfophenylazo]-phenylazo)-2,7-naphthalenedisulfonic acid
PP	polypropylene
Probenecid	p-[Dipropylsulfamoyl]benzoic acid
RACE	rapid amplification of cDNA ends
RT	reverse transcriptase
SDS-PAGE	sodium dodecyl sulfate poly acrylamide gel electrophoresis
SEM	standard error of the mean
TEMED	N,N,N',N'-tetramethylethylenediamine
TFA	trifluoroacetic acid

1. Introduction

A factor promoting the aggregation of melanin granules within chromatophores has been suspected in teleost fishes since 1926. In 1931 Hogben and Slome hypothesised that a second principle, a melanin-concentrating hormone (MCH), acted in conjunction with melanocyte-stimulating hormone (MSH) to control the rapid changes in skin colour seen in some lower vertebrates. In 1955 Enami presented the initial evidence that this principle might be a neurohypophyseal hormone produced in hypothalamic neurons and transported to the pars nervosa of the pituitary gland. In 1958 Imai prepared a pituitary extract with MCH-like activity. Thirty years later, Kawauchi et al. isolated and sequenced a 17-amino acid peptide with MCH activity from salmon pituitary glands: analysis of MCH could now begin [1].

I will start by introducing the melanin-concentrating hormone, its two cloned receptors MCH-R₁ and MCH-R₂, the putative melanophores and melanoma receptor and then present the aims of my thesis.

1.1. Melanin-concentrating hormone (MCH)

Even after the demonstration of a melanin-concentrating and a melanin-dispersing activity in the teleost pituitary gland, the characterisation of MCH would not have been possible without the help of a reliable bioassay. This was achieved by Baker and Rance [2] whose research led to the fish-scale melanophore assay. Carp melanophores were used to test bioactivity of fractionated pituitary extracts [3].

The latest and more complete review covering MCH is to be found in "Cell and Molecular Cell Biology of Melanin-concentrating Hormone" by B. Griffond and B.I. Baker [4].

1.1.1. Structure and localisation

MCH is a cyclic neuropeptide composed of 19 amino acids in human, cat, rat and mouse (Fig. 1), and 17 amino acids in the salmonids, tilapia, and bonito. Compared to fish MCH, the mammalian molecule has two additional and three mutated amino acids (see below). Mammalian MCH is positively charged at pH 7 (net charge: $-3 + 4 = +1$); fish MCH is also positively charged at pH 7 (net charge: $-3 + 4 = +1$).

Mammalian MCH:

Asp¹-Phe²-Asp³-Met⁴-Leu⁵-Arg⁶-

Cys⁷-Met⁸-Leu⁹-Gly¹⁰-Arg¹¹-Val¹²-Tyr¹³-Arg¹⁴-Pro¹⁵-Cys¹⁶-Trp¹⁷-Gln¹⁸-Val¹⁹

Fish MCH:

Asp¹-Thr²-Met³-Arg⁴-

Cys⁵-**Met⁶**-Val⁷-Gly⁸-Arg⁹-Val¹⁰-Tyr¹¹-Arg¹²-Pro¹³-Cys¹⁴-Trp¹⁵-Gln¹⁶-Val¹⁷

(Amino-acid residues identical to the ones of mammalian MCH are in bold)

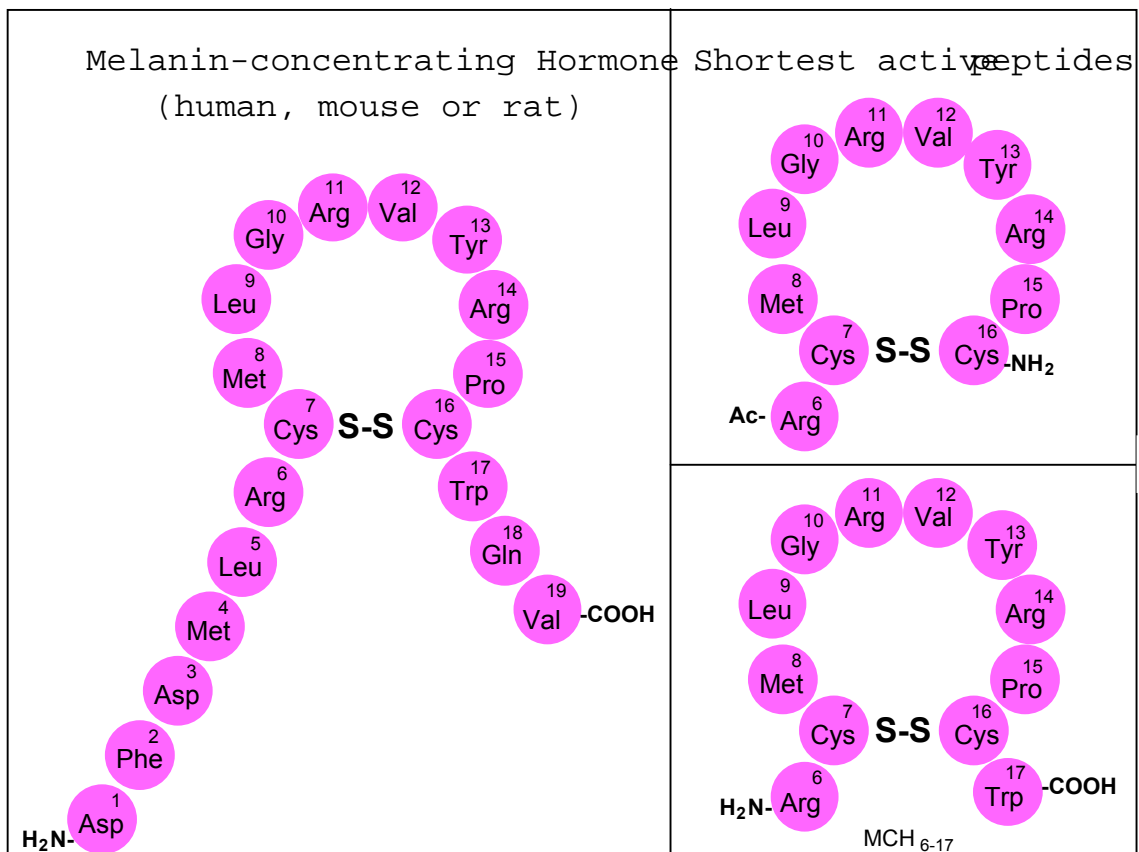


Figure 1. Schematic representation of MCH and its shortest active equivalents. Upper right analogue [91]; MCH₆₋₁₁ [46].

MCH was first isolated in 1983 using its melanin-aggregating properties observed in teleost fish melanophores [5]. The discovery of salmon MCH (sMCH) and the availability of an antiserum against it made it possible to characterise MCH counterparts in mammals. The first mammalian MCH molecule to be characterised was the rat MCH (rMCH), the human and mouse MCH were later deduced from the cDNA sequences (for details see the review [6]).

In humans two distinct gene systems were discovered, one corresponding to the authentic gene, highly homologous to its rodent counterparts and the other defined as the variant gene on the basis of partial sequence homology with the authentic gene (the variant genes lack exon 1 and are thus truncated forms of authentic MCH). In contrast to the salmonid gene, which is intronless, the mammalian gene has two introns and three exons (Fig. 2). Authentic human MCH gene was mapped by fluorescence *in situ* hybridisation to locus 12q23-q24, two copies of the variant gene are located to 5p14 and 5q12-q13 [7].

MCH is derived by posttranslational cleavage from the C-terminal end of a 165 amino-acid precursor molecule, pre-proMCH (Fig. 2). Concomitantly two other peptides are putatively produced: neuropeptide glutamic acid (E), isoleucine (I), also called NEI and neuropeptide glycin (G), glutamic acid (E) or NGE. In rodents NEI is cleaved by pro-hormone convertase PC2 and was shown to be secreted with MCH by cultured rat hypothalamic cells [8] but NGE release is still unproven in mammals.

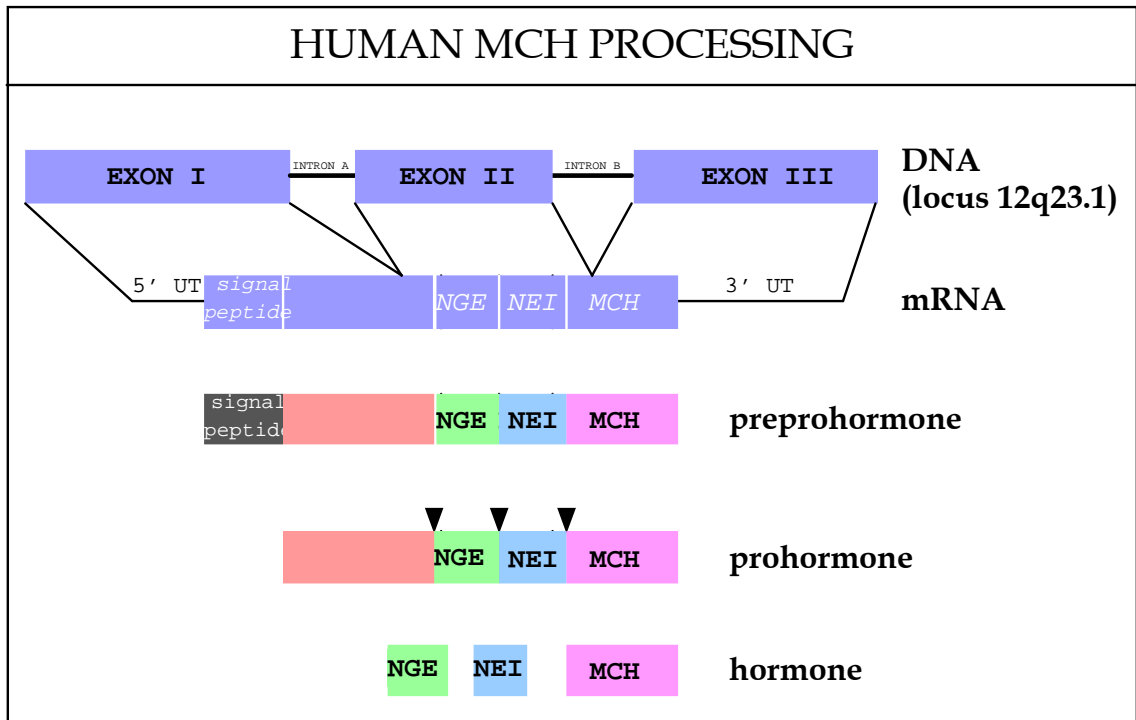


Figure 2. Schematic representation of human MCH gene organisation and hormone processing.

MCH mRNA and MCH peptide are synthesised in neurons of the dorso-lateral hypothalamus of adult human brain, precisely in:

- Lateral hypothalamus area (LHA)
- Zona incerta (ZI) (Fig. 3)

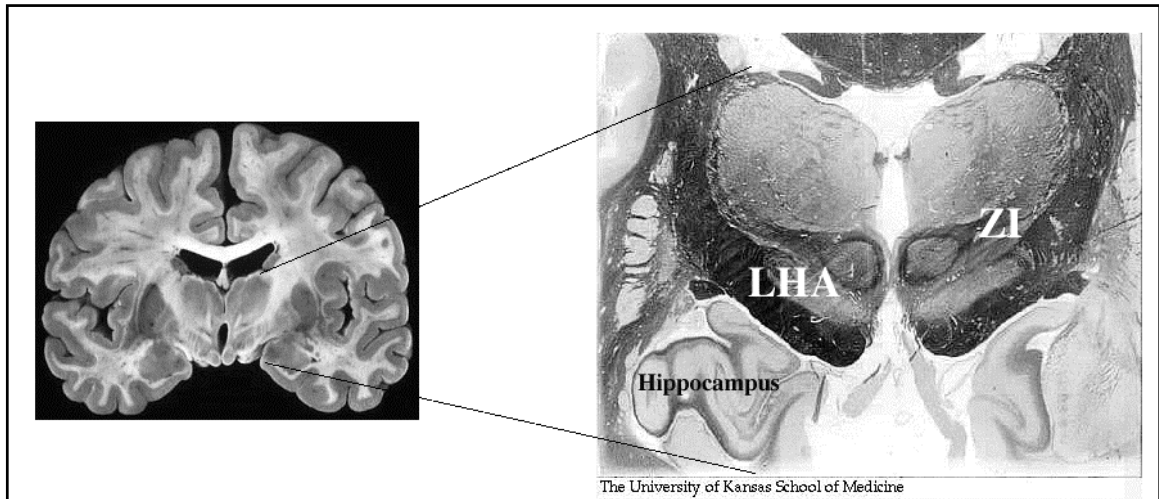


Figure 3. Coronal section of human brain through mamillary bodies (left) and enlargement of hypothalamic area (right). Hippocampus, zona incerta (ZI) and lateral hypothalamic area (LHA) are labelled. Left picture is from the University of Iowa Virtual Hospital®; right picture is from the University of Kansas School of Medicine brain collection.

By reverse transcriptase-polymerase chain reaction (RT-PCR), MCH transcript was also amplified from various organs obtained from human neonates [7]:

- Spleen +
- Thymus +++
- Brown fat ++
- Medulla oblongata +
(lower portion of the brain stem)
- Duodenum +
- Adrenal gland +
- Bone marrow +
- Testis +
- Lymphatic gland +

Abbreviations used:

- +++ 2 fold less MCH mRNA than in hypothalamus
- ++ 8 fold less MCH mRNA than in hypothalamus
- + 20 fold less MCH mRNA than in hypothalamus

1.1.2. Functions

a. In teleost fish

In teleost fish, MCH serves as a neurohypophyseal hormone that is released by the pituitary into the circulation when fish move onto a pale background. This in turn causes rapid aggregation of the pigment granules within melanophores of fish scale, resulting in skin palor [5].

b. In mammals

The physiological roles of MCH are numerous in mammals, rat and mouse being the best-studied organisms; almost nothing is known about the role of MCH in humans. The more frequently cited roles for MCH are:

- Central regulation of feeding behaviour: MCH is a potent orexigenic hormone i.e. stimulating food intake when injected into the brain [9], [10].
- Regulation of the hypothalamo-pituitary adrenal axis during stress [11].
- Modulation of water and electrolyte fluxes in the gastrointestinal tract [12].
- Stimulation of oxytocin secretion from isolated rat neurohypophysis [13].
- Regulation of sensory processing (auditory stimuli) [14].
- Modulation of the activity of monoaminergic systems in the medial preoptic area [15].
- Stimulation of sexual behaviour in the female rat [16].
- Antagonistic to MSH and NEI in grooming and locomotor activities in the rat [17].
- Effects on metabolic axes such as insulin release [18], and leptin secretion from rat adipocytes [19].
- Suppression of thyroid stimulating hormone (TSH) release [20].

MCH is also thought to be involved in:

- Modulation of other hormones regulating food intake [21].
- Modulation of memory retention [22].
- Modulation of hormones regulating sexual behaviour [23].
- Prevention of pentylenetetrazole (PTZ)-induced seizure in rat and guinea pig [24].
- Anxiety (MCH is anxiolytic) [25].
- Control of energy homeostasis via inhibition of the thyroid axis [20].

c. MCH / α -MSH / NEI antagonism

MCH and α -MSH (α -melanocyte-stimulating hormone) show antagonistic effects on pigmentary aggregation in teleost fish [26]. This antagonism is also observed in the mammalian central nervous system with respect to feeding [27], to the hypothalamic-pituitary-adrenal-axis [27], to grooming [17], [16] and to auditory gating [14].

In human melanocytes MCH seems to antagonise α -MSH as there is a partial inhibition of α -MSH-induced melanogenesis. Furthermore, MCH can reduce the increase in cyclic AMP that occurs in response to α -MSH in human melanocytes (Poster #15 presented by Hoogduijn et al. at the British Society for Investigative Dermatology Annual Meeting, Warwick, 9-11 April 2001 [28]).

MCH and NEI act as functional antagonists in the activation of the hypothalamus-pituitary-adrenal gland axis after an acute stress in the rat [29].

1.1.3. MCH knockout mouse model

MCH deficient mice are born with the expected mendelian frequency and are viable and fertile. However, from 5 week of age, they are leaner than the wild-type mice and their weight deficit is about 25% at 4 months of age [30]. This decrease in body weight is associated with a reduced food intake during the dark (i.e. activity) period. However, their locomotor activity remains unchanged but their rate of oxygen consumption expressed per kg body weight is augmented by 20%. The weight loss results therefore from hypophagia and alteration in metabolic rate. In terms of functioning, mutant mice have a normal feeding response after food deprivation. They are however, more sensitive to fasting as demonstrated by greater weight loss and even death if it is prolonged [31].

1.1.4. MCH transgenic mouse model

Transgenic mice overexpressing MCH (MCH-OE) in the lateral hypothalamus at approximately twofold higher levels than normal mice were studied. When fed on a high-fat diet, mice gained significantly more weight than wild-type mice, with a difference of 12.6% by age 13 weeks. The reason was that the food intake of the transgenic animals was about 10% higher than that of the wild-type mice. These animals were also fatter than wild-type littermates (21.9 ± 1.4 vs. 16.7 ± 1.4 % body fat). This obese phenotype did not appear when mice were fed on standard chow. Blood glucose levels were

higher in transgenic mice (181 ± 4 vs. 161 ± 5 mg/dl preprandially). MCH-OE mice were insulin-resistant, as demonstrated by a 5% decrease in blood glucose after insulin administration compared to a 31% decrease in wild-type animals [32].

1.2. MCH-R₁

1.2.1. MCH-R₁ cloning

The SLC-1 or GPR24 orphan receptor was identified as MCH-R₁ using the so-called “reverse pharmacology” techniques. In this approach, the target receptor is expressed in the appropriate animal cell line and the material obtained from tissue extracts or known compound libraries are applied to the cells to investigate whether they may be the potential ligand of the receptor. By exposing the cells to biological extracts or compounds libraries, the matching ligand will induce changes in intracellular second messenger levels in response to orphan receptor activation. These changes in level serve as a monitoring system for the purification of the ligand [33].

SLC-1 orphan receptor was first characterised in 1996 by customised search of human expressed sequence tags database [34]. The sequence found corresponds to an intronless gene in its open reading frame and encodes a G protein-coupled receptor (GPCR) of 402 amino acids. This receptor shares 40% amino acid identity in the transmembrane regions to the five known human somatostatin receptors and was therefore called SLC-1 for “somatostatin-like clone 1”. It was shown by northern blotting to be expressed in human forebrain and hypothalamus.

In 1998, with the same aim to isolate new G protein-coupled receptors, a Belgian group used a different approach: PCR amplification on rat brain cortex mRNA with degenerate oligonucleotides corresponding to consensus sequences present in the third and seventh transmembrane segment of 26 GPCRs. The search led to the isolation of a rat gene containing one 1217 bp intron that encodes a 353 amino acid protein sharing 91% overall identity with the previously cloned human SLC-1. A corrected 353 amino acids sequence for the human receptor was deduced at the same time, which shares 96% amino acid identity with the rat ortholog [35].

Using the “corrected” human SLC-1 sequence, five groups [36], [37], [38], [39] and [40] published more or less simultaneously (mid July to September 1999) the identification of MCH as the cognate ligand for SLC-1 (reviewed in [41]). The “long” form of human SLC-1 responds very weakly to MCH

stimulation, it is even postulated that this unspliced form is hardly expressed [36].

Human SLC-1 gene was assigned to chromosome 22q13.3 and comprises two exons. A rat [35] and a mouse [42] ortholog were also identified. The genomic organisation of the mouse SLC-1 gene seems to parallel that of rat and human, with an intron of approximately 1,2 kb in length spanning the entire coding region. The three molecules show striking homology at the amino acid level: 98% identity between rat and mouse and 91% between rat and human. The three protein products are all 353 amino acid long. This high degree of conservation among species at both mRNA and protein levels is not unexpected knowing that the ligand structure is identical in human, rat and mouse.

1.2.2. MCH-R₁ mRNA expression

The expression of MCH-R₁ in the central nervous system coincides with the distribution of prominent fields of MCH-expressing nerve terminals. The localisation of MCH-R₁ mRNA in the rat and human species is summarised in tables 1 and 2:

Table 1: MCH-R₁ mRNA in the brain^a

Brain region	Rat	Human
Hippocampus	++	++
Amygdala	++	++
Substantia nigra	++	++
Hypothalamus	++	++
Nucleus accumbens	++	?
Locus coeruleus	++	?
Olfactory system	+	?
Cerebellum	?	++
Reference:	[43], [38]	[44], [45]

^aAbbreviations used: ++ abundant; + detectable; - not detectable; ? not investigated.

Table 2: MCH-R₁ mRNA in peripheral tissues^a

Peripheral organ	Rat	Human
Skeletal muscle	++	-

Adipose tissue	+	++
Ovary	++	++
Testis	+	++
Prostate	?	+
Placenta	?	+
Liver	-	++
Small intestine	?	+
Colon	?	+
Pituitary	?	+
Reference:	[46]	[44]

^aAbbreviations used: ++ abundant; + detectable; - not detectable; ? not investigated; * C. Talke-Messerer, unpublished.

Tumours or cell lines were also tested for MCH-R₁ expression, the following were positive:

- Primary porcine ciliary pigmented epithelial cells [47].
- Human nonpigmented ciliary epithelial cell line, ODM-2 [47].
- Tumour tissues of human pheochromocytoma, ganglioneuroblastoma and neuroblastoma [45].
- IMR-32 human neuroblastoma cells [45].
- NB69 human neuroblastoma cells [45].
- BeWo human choriocarcinoma cells [45].
- SW-13 human adrenocortical cells [45].
- DLD-1 human colorectal adenocarcinoma cells [45].
- SK-MEL-37 human melanoma cells [48].
- Rat islets of Langerhans, CRI-G1 and RINm5F insulinoma cell lines [18].
- Human melanocytes, human and mouse melanoma cell lines (Poster #15 presented at the British Society for Investigative Dermatology Annual Meeting, Warwick, 9-11 April 2001 [28]).

In contrast, no MCH-R₁ mRNA could be detected by RT-PCR or northern blot in B16F1 mouse melanoma cells [41], [49], [50] or in SVK14 human keratinocytes. Human keratinocytes and fibroblasts were also devoid of MCH-R₁ expression (Poster #15 presented at the British Society for Investigative Dermatology Annual Meeting, Warwick, 9-11 April 2001 [28]).

1.2.3. Binding characteristics of MCH to MCH-R₁

Discoverers of MCH-R₁ performed binding experiments with iodinated MCH as radioligand and the former orphan receptor bound the iodinated authentic MCH satisfactorily. Values for MCH K_d and K_i (Table 3) varied depending on the cell type under investigation and the experimental procedure (intact cells or membranes from either cells or brain tissue).

Table 3: [¹²⁵I]-MCH displacement by MCH

Cell line	MCH affinity (K _i)	Reference
HEK293 + rat MCH-R ₁	0.043 nM	[36]
CHO + human MCH-R ₁	0.1 nM	[51]

Cell line/tissue	[¹²⁵ I]-MCH affinity (K _d)	Reference
HEK293 + human MCH-R ₁	0.2 nM	[36]
HEK293 + human MCH-R ₁	0.46 nM	[52]
CHO + human MCH-R ₁	1.3 nM	[51]
Human brain	0.2 nM	[53]

1.2.4. MCH-R₁ signalling pathway

a. In cellular models of MCH-R₁ ectopic expression

In Chinese hamster ovary (CHO) cells stably expressing MCH-R₁, the K_d for MCH was 1.3 nM and the binding capacity was 3.6 pmol/mg protein. All three subfamilies of G protein α subunits i.e. G_i, G_o, and G_q were assessed for MCH-R₁ coupling [51].

MCH inhibits forskolin-stimulated cAMP production in a pertussis toxin-(PTX)-sensitive manner (EC₅₀ = 100 pM) indicating that MCH-R₁ couples to members of the G_i subfamily of G proteins (Fig. 4).

MCH stimulates increases in phosphoinositide metabolism (EC₅₀ = 50 nM) and intracellular free Ca⁺⁺ levels (EC₅₀ = 10 nM). It also stimulates inositol phosphate production and increases in intracellular free Ca⁺⁺ that are partially inhibited (60% and 40% respectively) by PTX treatment (PTX can ADP-ribosylate the α subunit of G_i/G_o proteins and thus inhibit signalling mediated through G_i/G_o proteins but has no effect on signalling mediated by G_q). This demonstrates that there are both G_i/G_o and G_q components in MCH-R₁ signalling (Fig. 4).

To distinguish G_i vs. G_0 coupling, mitogen-activated protein (MAP) kinase activity on MCH stimulation was examined (protein kinase C, PKC activity is essential in the G_i -dependent MAP kinase signalling pathway but is not required in the G_0 -dependent MAP kinase signalling pathway). In this cellular model PKC inhibition by bisindolmaleimide pre-treatment only decreased MCH-induced MAP kinase activation by 50%, indicating that both G_i and G_0 are involved (Fig. 4).

Furthermore, experiments involving the use of a G-protein chimera indicate that MCH- R_1 couples to $G\alpha_{i3}$ with a higher affinity than to $G\alpha_q$ [37].

It must be noted that other groups found different MCH potencies (EC_{50}), depending on the cellular model used (CHO or HEK293) and the experimental procedure (see comparative table II in B. Griffond's review [4]).

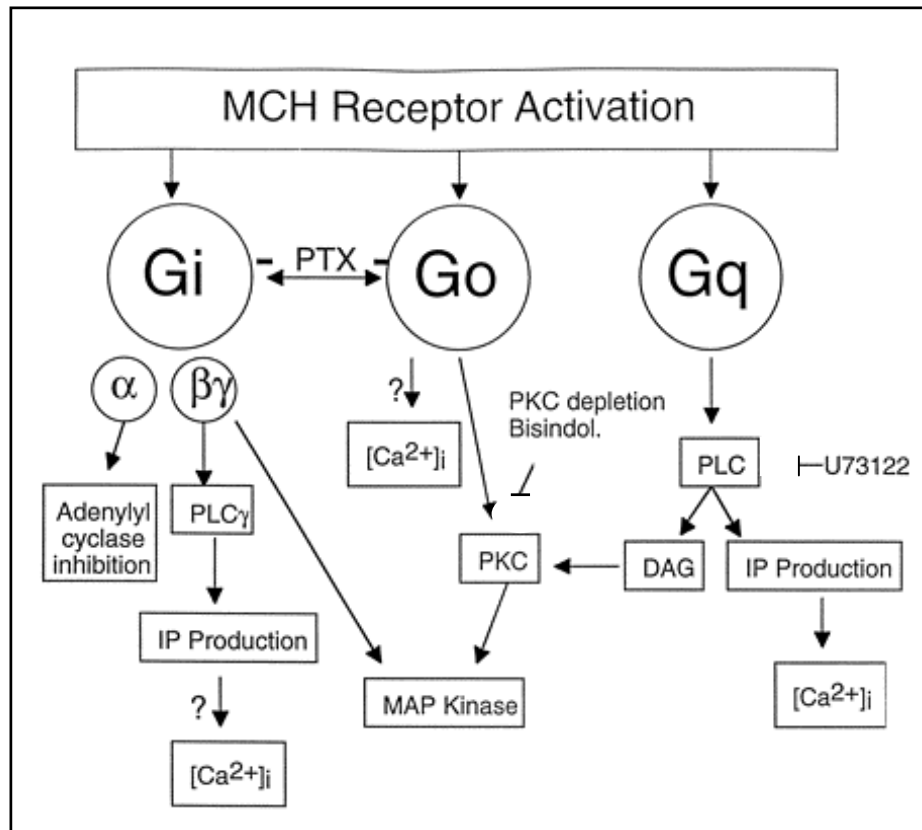


Figure 4. Model of the intracellular signalling pathways coupled to MCH-R₁ activation in CHO-MCH-R₁ cells. Proposed by Brian E. Hawes et al. [51]. Bisindolmaleimide or prolonged pretreatment with PMA block PKC activity. PTX inhibits G_i and G_o activity. U73122 inhibits PLC activity.

b. In cells endogenously expressing MCH-R₁

In the human melanoma cell line SK-MEL-37, MCH-R₁ is only coupled to PTX-sensitive G α_i /G α_0 . Experimentally, MCH inhibited forskolin-stimulated cyclic AMP accumulation and induced mitogen-activated protein (MAP) kinase in a pertussis toxin-(PTX)-sensitive manner. The MAP kinase activity led then to the production of phosphorylated forms of p42/44 MAP kinase. However, no increase in the intracellular free Ca⁺⁺ concentration could be elicited by MCH in these cells [48].

A preliminary report showed that MCH causes a rapid and sustained elevation of calcium levels in human melanocytes. MCH is also reported to reduce the increase in cyclic AMP that occurs in response to α -MSH in human melanocytes (Poster #15 presented at the British Society for Investigative Dermatology Annual Meeting, Warwick, 9-11 April 2001 [28]).

1.2.5. MCH-R₁ knockout mouse model

MCH-R₁^{-/-} mice have normal body weight, yet are lean and have a reduced fat mass ($\approx 50\%$ less fat mass and $\approx 7\%$ more lean mass than wild types). Surprisingly, MCH-R₁^{-/-} mice are hyperphagic when maintained on regular chow (they ate 12 to 15% more chow than littermate controls, due to an increased feeding duration associated with a concomitant increase in drinking). Their leanness is a consequence of hyperactivity and altered metabolism (greater metabolic rate and preference for the oxidation of fatty acids rather than glycolysis). Consistent with this hyperactivity, MCH-R₁^{-/-} mice are less susceptible to diet-induced obesity (DIO); interestingly, maintenance on the high-fat diet abolished the hyperphagia observed with regular chow (due to a taste preference?). More importantly, chronic central infusions of MCH (that induce hyperphagia and mild obesity in wild-type mice) did not have any effect in MCH-R₁^{-/-} mice, demonstrating that MCH-R₁ is indeed a physiologically relevant MCH receptor [54].

1.2.6. MCH / α -MSH antagonism at MCH-R₁

Since α -MSH did not block the activation of MCH-R₁ by MCH in cells overexpressing MCH-R₁ [36], [37], α -MSH does not exert antagonistic activity by competing with MCH for MCH-R₁.

1.2.7. Implication of MCH-R₁ in a human autoimmune disease

Vitiligo is a depigmenting disorder characterised by circumscribed depigmented macules resulting from the loss of cutaneous melanocytes. The pathogenesis of this disease remains obscure although an autoimmune etiology has been suggested because the disease is frequently associated with other disorders that have an autoimmune origin such as autoimmune thyroiditis and type 1 diabetes mellitus.

9 out of the 55 vitiligo patients tested (= 16.4%) exhibited an immunoreactivity against MCH-R₁ and the frequency of MCH-R₁ antibodies in the vitiligo patient group was significantly greater than normal ($p = 0.025$). IgG from MCH-R₁ antibody-positive vitiligo patients inhibited [¹²⁵I]-MCH binding on membranes of CHO cells transfected with MCH-R₁ by $45\% \pm 4\%$ compared to $16\% \pm 14\%$ with IgG from healthy controls. Analysis of the MCH-R₁

antibody-positive vitiligo patients revealed no obvious association between the presence of MCH-R₁ antibodies and either age or gender, duration of the disease, clinical subtype of vitiligo or the presence of another autoimmune disorder (tyrosinase, TRP-1, TRP-2, Pmel17 or SOX10 immunoreactivity). It is proposed that MCH-R₁ autoantibodies by binding MCH-R₁ might adversely affect the functioning of the receptor, leading to the disruption of normal melanocyte behaviour. In this disease, antibodies against MCH-R₁ might also indicate the presence of autoreactive anti-MCH-R₁ T lymphocytes that are capable of destroying pigment cells [55].

1.3. MCH-R₂

Six groups published almost concomitantly the identification of a second human MCH receptor in spring 2001. It was designated: MCHR2 [56], MCH-2R [57], MCH₂ [58], MCH-R2 [59], SLT [44] or MCH2 [60]. In this manuscript I will use the terminology MCH-R₂.

This second MCH receptor is 340 amino acid long and was identified thanks to bioinformatic and molecular cloning approaches (human gene databank searching and 5'/3' rapid amplification of cDNA ends or RACE). It exhibits a high degree of homology with the MCH-R₁ receptor i.e. 38 % overall and 44% amino acid identity in the transmembrane regions (Fig. 5). It has no greater protein sequence homology to any other G-protein-coupled receptor (GPCR), the closest homologue being the somatostatin receptor 1 (SSTR1) with 32% overall amino acid identity. MCH-R₂ belongs to class 1 subfamily (rhodopsin-like) of the G-protein-coupled receptors and contains several features common to GPCRs including:

- Seven putative transmembrane domains (TM1 to TM7 boxed in figure 5).
- Two putative N-linked glycosylation sites in the N-terminal region.
- A DRY motif located after TM3 (important for receptor-G protein complex formation).
- An aspartate residue in TM3 (D123 in MCH-R₁ and D113 in MCH-R₂) which is thought to be involved in ligand binding [61].

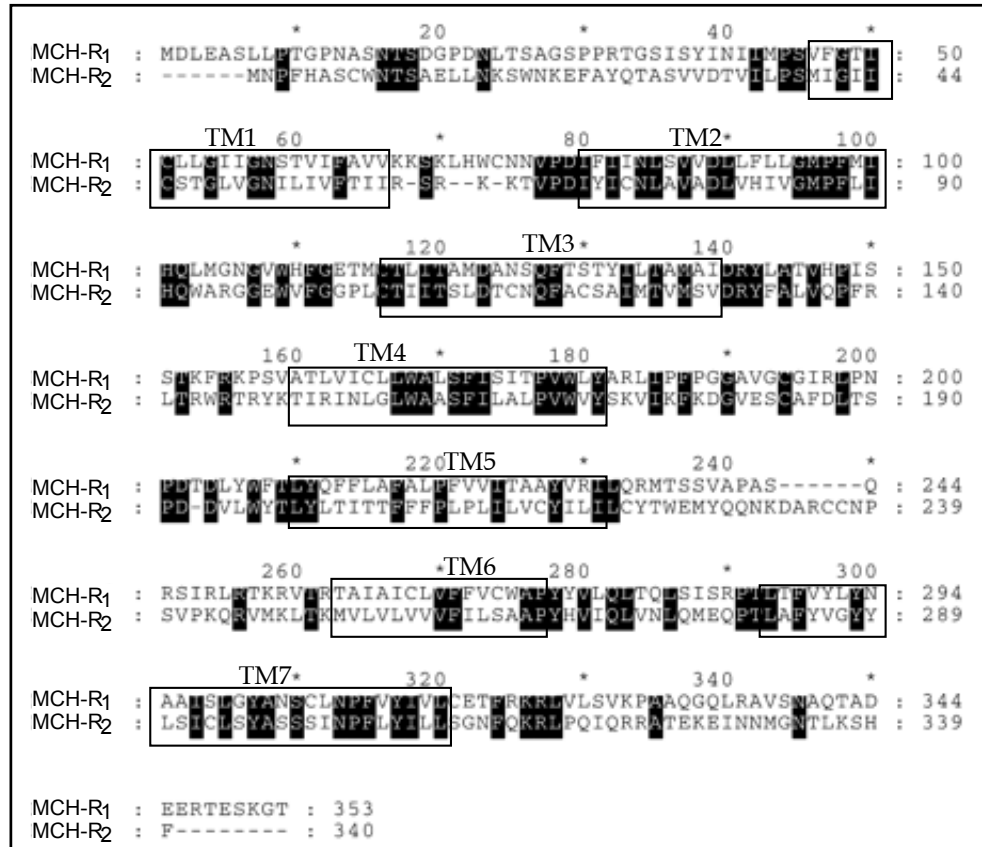


Figure 5. Amino acid sequences comparison of the human MCH-R₁ and MCH-R₂. Identical residues are highlighted in black. Predicted transmembrane domains are boxed (based on Hill et al. [58] and Sailer et al. [57]).

MCH-R₂ gene spans more than 23 kilobase pairs (kb) and comprises five exons interrupted by four large introns (1 to 9 kb). This genomic structure is very different from the one of the MCH-R₁ gene, which has only a small intron. MCH-R₂ gene is mapped on the long arm of human chromosome 6, precisely 6q14.3-q15 by fluorescence *in situ* hybridisation [60] or 6q16.2-q16.3 by the radiation hybrid method [57]. A rat or a mouse ortholog has not yet been reported.

In humans, the distribution of MCH-R₂ mRNA in the brain almost overlaps that of MCH-R₁, although the expression of MCH-R₂ in the hypothalamus is lower than that of MCH-R₁. Human MCH-R₂ mRNA is specifically detected in the hippocampus, amygdala, caudate nucleus, accumbens nucleus and frontal lobe. As a general feature, MCH-R₂ mRNA expression is restricted to cortical regions of the human brain. In the periphery, a weak signal has been reported in adipocytes, pituitary, pancreas, testis and small intestine.

In mammalian cells transfected with MCH-R₂, MCH stimulated increased levels of inositol phosphates ($EC_{50} = 3.4 \pm 0.2$ nM) and intracellular free Ca^{++} ($EC_{50} = 0.1 \pm 0.1$ to 5.65 ± 1.78 nM). This effect was insensitive to pertussis toxin (PTX) treatment which implies that MCH-R₂ couples primarily to G_q (PTX can ADP-ribosylate the α subunit of G_i proteins and thus inhibit signalling mediated through G_i proteins but has no effect on signalling mediated by G_q). MCH stimulation had no effect on basal or forskolin-stimulated cAMP production. The difference in G protein coupling between MCH-R₁ and MCH-R₂ can be explained by a high sequence divergence in the third intracellular loop (only three out of 31 residues are identical). This loop was shown to be implicated in G protein coupling in other GPCRs. MCH affinity for MCH-R₂ is slightly lower than the one for MCH-R₁ ($IC_{50} = 1.5 \pm 0.9$ to 5.0 ± 1 nM compared to 0.3 ± 0.1 to 3.0 ± 1 nM for MCH-R₁).

Proposed roles for MCH-R₂ are:

- Mediation of the cognitive and emotional representation of food intake (due to the presence of MCH-R₂ mRNA in cortical regions of the brain) [59].
- Involvement in the regulation of nutritional homeostasis by MCH (due to expression of both MCH mRNA and MCH-R₂ mRNA in the digestive tract) [60].

1.4. Putative MCH receptors on melanophores and melanoma cells

Other MCH receptors, particularly from fish, are still to be cloned. As there is a clear function for MCH in fish melanophores a receptor should integrate the melanin-aggregating signal. Similarly, a pigment cell receptor must also exist. In B16 mouse melanoma, rat PC12 pheochromocytoma and human SVK-14 keratinocytes a high-affinity binding site for ¹²⁵I-[Phe¹³, Tyr¹⁹]-MCH was found (Table 4). 1,000 receptors per melanoma cell [62] and 10,000 receptors per keratinocyte [63] were estimated from scatchard plots.

During initial studies on melanoma cells, [Phe¹³, Tyr¹⁹]-MCH analogue was designed by our group [62] because first attempts to demonstrate MCH binding

sites in brain sections or on cells encountered problems due to the high MCH lipophilicity (MCH octanol/buffer partition coefficient is 0.091 ± 0.004 [64]) and also because MCH is readily degraded enzymatically. The natural radioligand, with an ^{125}I atom placed in the tyrosine¹³, showed a marked reduction in bioactivity on fish melanophores (the only bioassay available at that time), while ^{125}I -[Phe¹³, Tyr¹⁹]-MCH exhibited full biological potency in this assay. This analogue was afterwards used in many laboratories and allowed the detection of high affinity binding sites on various cell lines.

Table 4: ^{125}I -[Phe¹³, Tyr¹⁹]-MCH displacement by MCH

Cell line	MCH affinity (IC_{50} ^a)	Reference
G4F-7 mouse melanoma	12 ± 4.5 nM	[62]
G4F mouse melanoma	120 ± 12 nM	[62]
B16-F1 mouse melanoma	14 ± 5.3 nM	[62]
PC12 rat pheochromocytoma	120 ± 7.8 nM	[62]
SVK-14 human keratinocytes	65-93 nM	[63]

^a Inhibitory concentration₅₀ (IC_{50}) is the peptide concentration inhibiting 50% of specific radioligand binding.

1.5. Aims of the thesis

From summer 1999 onwards, numerous publications brought new facts to the MCH field. Thus, the aims of this thesis: the characterisation of MCH receptors, evolved with the continuous availability of fresh information

After developing stable and potent MCH radioligands: ^{125}I -[Phe¹³, Tyr¹⁹]-MCH and ^{125}I -[DPhe¹³, Tyr¹⁹]-MCH, our first aim was to find cells “richer” in MCH binding sites than G4F-C11 cells in order to possibly clone the MCH receptor. For this purpose, we chose cells and membranes of “neuronal” origin assuming that since MCH is released by hypothalamic neurons, target cells of MCH should also be neurons (discussed in part 3.1).

In another approach we tried to characterise and isolate biochemically the binding site present on the G4F-C11 mouse melanoma cells with the help of two-dimensional electrophoresis (discussed in part 3.2).

After publication of the first MCH receptor sequence, we included in our work a structure-activity analysis of numerous MCH-related peptides using HEK-T cells transfected with rat MCH-R₁ [65] (discussed in part 3.3).

Taking advantage of the gene and cDNA sequences of MCH-R₁ and -R₂, we were able to track cells expressing these MCH receptors by RT-PCR, and thus extend the analysis of the most promising cell line in this respect, namely the human Kelly neuroblastoma [66] (discussed in part 3.4).

2. Methods

2.1. Cell culture

2.1.1. Cell lines used during this thesis work

Human neuroblastoma cell lines:

SMS-KAN: gift from M. Langer (ETH, Zürich)
SH-SY5Y: ATCC #CRL 2266 [67]
SK-N-MC: ATCC # HTB 10 [67]
LAN-5: ICLC # HTL96022 [68], [69]
KELLY: DSMZ # ACC 355 [70]

Mouse neuroblastoma cell lines:

N1E115: ATCC # CRL-2263 [71], [72]
N-18: [71]

Mouse brain tumor cell line:

CATH.a: gift from Dona M. Chikaraishi [73]

Human primary melanocytes:

W400: white melanocytes
M407: type V, mexican heritage melanocytes
B 141: black melanocytes

Kind gifts from Bryan B. Fuller (University of Oklahoma Health Sciences Center, Oklahoma City)

Other cell lines used during this thesis work:

HeLa: ATCC #CCL 2 [74], [75]
CHO: ICLC # ATL95003 [76]
HEK293-T: ATCC # CRL 1573 [77]
HEK #33: HEK transfected with N-terminus Flag-tagged rat MCH-R₁.
G4F-C11: Clone # 1 of B16-G4F mouse melanoma, a variant of B16-F1 that do not express MSH receptors [78]

2.1.2. Cell culture conditions and media

Cells were maintained at 37°C in a humidified atmosphere with 5% CO₂. All media and supplements were from Gibco (Paisley, UK) unless stated.

Table 5: Description of the cell culture media adapted to the different cell lines

Cell line	Culture medium
SMS-KAN SH-SY5Y	Dulbecco's modified Eagle's medium / Nut. Mix F12 1:1 15 % fetal calf serum (FCS) 4 mM L-glutamine 50 U/ml penicillin 50 µg/ml streptomycin 1% MEM non-essential amino acids
SK-N-MC	Modified Eagle's medium (MEM) with Earl's salts 10% FCS 2 mM L-glutamine 50 U/ml penicillin 50 µg/ml streptomycin 1% MEM non-essential amino acids 1 mM sodium pyruvate
LAN-5 Kelly	RPMI 1640 containing folic acid (40 mg/L) 10% FCS 2 mM L-glutamine 50 U/ml penicillin 50 µg/ml streptomycin 1% MEM non-essential amino acids 1 mM sodium pyruvate
N1E115 N-18 CATH.a	Dulbecco's modified Eagle's medium 10% FCS 2 mM L-glutamine 50 U/ml penicillin 50 µg/ml streptomycin
G4F-C11 CHO	Modified Eagle's medium with Earl's salts 10% FCS 2 mM L-glutamine 50 U/ml penicillin 50 µg/ml streptomycin 1% MEM non-essential amino acids 1.5% MEM vitamin solution

Primary melanocytes	HAM's F ₁ 5% FCS 10% Horse serum 50 U/ml penicillin 50 µg/ml streptomycin 32 nM 12-0-Tetradecanoylphorbol 13-Acetate; TPA (Sigma, Saint Louis, MI) 0.1 mM 3-Isobutyl-1-Methylxanthine; IBMX (Sigma, Saint Louis, MI) 5 µg / ml insulin (Novo Nordisk, Bagvaerd, Denmark)
HEK-T HeLa	Dulbecco's modified Eagle's medium containing 4.5 g/L glucose 10% FCS 2 mM L-glutamine 50 U/ml penicillin 50 µg/ml streptomycin 1 mM sodium pyruvate
HEK-T #33	Dulbecco's modified Eagle's medium containing 4.5 g/L glucose 10% FCS 2 mM L-glutamine 50 U/ml penicillin 50 µg/ml streptomycin 1 mM sodium pyruvate 250 µg / ml Zeocin™ (Cayla, Toulouse, France)

2.2. Peptides used during this thesis work











Peptides used during the thesis are listed in the table below (Table 6). They are either peptides used in previous publications and whose synthesis has already been described (see reference papers), from commercial source (Bachem, Bubendorf, Switzerland) or are peptides synthesised for this study by classical solid phase synthesis.

In brief, solid phase synthesis was carried out on a Pioneer™ automated peptide synthesiser (PerSeptive Biosystems, Framingham, MA) using continuous flow technology with TentaGel-based (Rapp) NovaSyn TGA resin (Calbiochem-Novabiochem, La Jolla, CA) containing 4-hydroxymethylphenoxyacetyl linker as well as Fmoc-protection of α -amino groups. The following protecting groups were used for ω -protection: Trt for Cys and Gln, Boc for Trp, tBu for Tyr, Pbf for Arg, OtBu for Asp and Glu. Cleavage from the resin was carried out in 87% TFA/ 5% anisol/ 2.5%

thioanisol/ 0.5% ethane dithiol/ 5% water. Cyclisation of the linear peptides was performed by iodine oxidation using a solution of iodine in glacial acetic acid (30- to 40-fold excess). The peptides were purified by conventional chromatography and semipreparative HPLC. They were then analysed by analytical HPLC and ESI mass spectrometry.


All peptides were stored at -20°C and allowed to equilibrate at room temperature before weighting on the microbalance. For competition binding experiments, 10^{-4} M stocks were dissolved in 2% acetic acid and also stored at -20°C .

Table 6: List of the peptides used in the thesis work

Compound	Sequence	Reference
Amino-acid positions	1 3 5 * 9 11 13 15 * 17 19	
H/m/r MCH	Asp Phe Asp Met Leu Arg Cys Met Leu Gly Arg Val Tyr Arg Pro Cys Trp Gln Val	
salmon MCH	Asp Thr Met Arg Cys Met Val Gly Arg Val Tyr Arg Pro Cys Trp Gln Val	
linear MCH	Asp Phe Asp Met Leu Arg Cys Met Leu Gly Arg Val Tyr Arg Pro Cys Trp Gln Val	
[DPhe ¹³]-MCH	Asp Phe Asp Met Leu Arg Cys Met Leu Gly Arg Val D _{phe} Arg Pro Cys Trp Gln Val	
[Phe ¹³ ,Tyr ¹⁹]-MCH	Asp Phe Asp Met Leu Arg Cys Met Leu Gly Arg Val Phe Arg Pro Cys Trp Gln Tyr	[62] 
[DPhe ¹³ ,Tyr ¹⁹]-MCH	Asp Phe Asp Met Leu Arg Cys Met Leu Gly Arg Val D _{phe} Arg Pro Cys Trp Gln Tyr	[79]
[des1,2,Phe ¹³ ,Tyr ¹⁹]-MCH	Asp Met Leu Arg Cys Met Leu Gly Arg Val Phe Arg Pro Cys Trp Gln Tyr	
[Val ⁹ ,Phe ¹³ ,Glu ¹⁸ ,Tyr ¹⁹]-MCH	Asp Phe Asp Met Leu Arg Cys Met Val Gly Arg Val Phe Arg Pro Cys Trp Glu Tyr	
[Ser ^{4,6} ,DPhe ¹³ ,Tyr ¹⁹]-MCH	Asp Phe Asp Ser Leu Ser Cys Met Leu Gly Arg Val D _{phe} Arg Pro Cys Trp Gln Tyr	
[MetO ^{4,8} ,Phe ¹³ ,Tyr ¹⁹]-MCH	Asp Phe Asp Met _O Leu Arg Cys Met _O Leu Gly Arg Val Phe Arg Pro Cys Trp Gln Tyr	[79]
[Ser ^{7,16}]-MCH	Asp Phe Asp Met Leu Arg Ser Met Leu Gly Arg Val Tyr Arg Pro Ser Trp Gln Val	
[Lys ¹⁹]-MCH	Asp Phe Asp Met Leu Arg Cys Met Leu Gly Arg Val Tyr Arg Pro Cys Trp Gln Lys	

* indicates the cysteines that are oxidised and form a disulfide bridge in all cases except for linear MCH.

 Bachem (Bubendorf, Switzerland)

 Synthesised in our lab.

2.3. Binding assay

2.3.1. Binding assay with cell lines

a. Preparation of radioligand

20 or 10 μg of MCH (Bachem, Bubendorf, CH) or peptide analogue were resuspended in 20 μl of 2% acetic acid and incubated at room temperature for 50 min with 1 mCi [Na^{125}I] (ICN, Irvine, CA), 50 μl 0.3M Na-phosphate buffer, pH 7.4, 100 mU Lactoperoxidase-biotin (Sigma, St Louis, MO), 200 mU Glucoseoxidase-biotin (Sigma, St Louis, MO), and 10 μl of 80 mM β -D glucose to start the reaction. Then 25 μl streptavidin magnetic beads (PerSeptive Biosystems, Framingham, MA) were added for 5 min and the reaction finally stopped with 30 μl saturated ascorbic acid in water. The reaction medium was completed with 250 μl 0.1% porcine thyroglobulin (Sigma, St Louis, MO) and the enzymes pelleted with a microcentrifuge tube magnetic separator (Polysciences, Warrington, PA).

Supernatant was transferred on a HBL extraction cartridge (Oasis™ Waters, Milford, MA) previously equilibrated with 2 x 1 ml methanol and 2 x 1 ml dH₂O. Cartridge was washed twice with 1 ml dH₂O, once with 1 ml 5% methanol, radioligand was then eluted in 1 ml methanol and stored at -70°C.

The radiopeptide was further purified by analytical HPLC on a C₁₈ column (Symmetry 3.5 µm, 2.1x150 mm, Waters Corporation, Milford, MA) with a flow rate of 0.3 ml/min, using a stepwise gradient of acetonitrile/ 0,01% TFA and H₂O/ 0.01% TFA. Peak identification of monoiodinated peptide was done with a Packard Radiomatic Instrument (Packard, Meriden, CT), relevant collected fraction was mixed with 200 µl BSA/lactose (4 mg/ml each) and lyophilized overnight. The radioligand was used the next day.

Table 7: Detailed HPLC gradient:

Time (min)	Flow (ml / min)	H ₂ O / 0.01% TFA (%)	Acetonitrile / 0.01% TFA (%)
0	0.3	90	10
0.5	0.3	90	10
7	0.3	65	35
15	0.3	44	56
18	0.3	0	100
39	0.3	0	100
40	0.3	90	10

b. Receptor binding assay [79]

The competition binding reaction was started by adding 40 µl (0.05 pmol = 200,000 cpm) of monoiodinated peptide to prelubricated 1.7 ml polypropylene tubes (Sorenson™, BioScience Inc., Salt Lake City, UT) containing 500 µl of cell suspension (2 x 10⁶ cells/ml) and 60 µl of competitor peptide in a 1:3 dilution series. In saturation binding experiment, the concentration of competitor peptide was constantly 1 µM and 0.005-0.4 pmoles of radioligand were added. Incubation lasted for 2 h at 10, 15 or 20°C. Cells, cold peptides and radioligand were diluted in binding medium which consisted of modified Eagle's medium (Gibco, Paisley, UK) containing 25 mM HEPES, supplemented with 0.2% gelatin (Inotech AG, Dottikon, Switzerland), 0.3 mM 1,10-phenanthroline (Merck, Darmstadt, FRG) and 0.16 mM PMSF. After incubation, triplicate aliquots (150 µl) were layered onto 150 µl ice-cold AR-20 silicon oil (Wacker Chemie, München, FRG). Unbound radioactivity was

removed by centrifugation at 13,400 g and 4°C for 2 min. Radioactivity associated with the cell pellet was measured in a γ -counter and data were further analysed using Prism (GraphPad Software, San Diego, CA).

c. Stability of radioligand after incubation

Reaction tube was centrifugated to pellet cells, one volume of supernatant was mixed with two volumes of methanol to precipitate the proteins, after a 2-min centrifugation at 14,000 rpm an aliquot of the supernatant was loaded on HPLC for analysis.

2.3.2. Binding assay with porcine brain membranes

a. Membrane preparation [80]

Porcine brains were dissected at 4°C as soon as possible after collection, and specific regions stored in cryotubes at -80°C until use. Brain regions were overlaid with ice-cold lysis buffer (20 mM Tris buffer, pH 7.5, 1 mM EDTA, 0.25 M sucrose, 1 mg/ml bacitracin, 0.1 mg/ml soybean trypsin inhibitor, 0.125 mg/ml PMSF; enzyme inhibitors were purchased from Sigma., St Louis, MO), and homogenized with a polytron homogeniser. The lysates were centrifuged at 500 g and 4°C for 5 min in order to remove unbroken cells, nuclei and cell debris and the supernatants were ultracentrifuged at 40,000 g and 4°C for 50 min. The pelleted membranes were resuspended in binding medium without gelatin (modified Eagle's medium with Earle's salts containing 25 mM HEPES, supplemented with 0.3 mM 1,10-phenanthroline and 0.16 mM PMSF) and the protein content was determined by the method of Bradford (BioRad, Hercules, CA) using BSA as standard. Membrane preparations were kept at -80°C until use.

For membrane fractionation, a first ultracentrifugation run was performed at 20,500 rpm (= 40,000 g) for 20 min to pellet the plasmic membranes. The supernatant was subjected to a one-hour ultracentrifugation at 40,800 rpm (= 158,000 g) to pellet the internal vesicles.

b. Binding assay

50 µg membranes (in 350 µl binding medium) were incubated with either 50 µl 1.2×10^{-5} M cold MCH (non-specific binding) or 50 µl binding medium (total binding) and 50 µl radioligand (200,000 cpm) at 10°C for 2 h. Membranes, cold MCH and radioligand were diluted in binding medium which consisted of modified Eagle's medium (Gibco, Paisley, UK) containing 25 mM HEPES, supplemented with 0.2% gelatin (Inotech AG, Dottikon, Switzerland), 0.3 mM 1,10-phenanthroline (Merck, Darmstadt, FRG) and 0.16 mM PMSF. The reaction was stopped by incubation on ice for 10 min, and the reaction medium transferred to thin tubes. After a 2-min centrifugation at 13,400 g and 4°C, pellets were extensively washed with cold PBS (without resuspending the membranes), and radioactivity associated with the pellet was measured in a γ -

counter. Data were further analysed using Prism (GraphPad Software, San Diego, CA).

2.3.3. Binding assay with rat embryonic hypothalamic neurons

Performed under the expertise of D. Di Scala-Guenot at the "Laboratoire de physiologie cellulaire et intégrée" UMR7519 CNRS/ULP -I.P.C.B- STRASBOURG (06/15→21/2000)

a. Isolation and culture of the rat embryonic hypothalamic cells

Pregnant wistar rats at day 16 of gestation were anaesthetised with an IP injection of 2 ml 25% urethane, the embryos aseptically exposed and their brains removed. The hypothalami were isolated and placed in ice-cold Earle's balanced salt solution (EBSS) without Ca^{++} and Mg^{++} (to avoid adhesion of the cells), the meningeal membranes removed and the tissues placed in a tube containing 5 ml DMEM high glucose (DMEM, Life Technologies supplemented with 5 g/l glucose, 2 g/l NaHCO_3 , 50 mg streptomycine, 500 UI penicilline, pH 7.4). The tissues were mechanically dissociated by passing through a glass pipet several times and the supernatant filtered through a 40- μm nylon mesh (that retains astrocytes) and spun down at 800-1,000 rpm at room temperature for 10 min. The cells were resuspended in DMEM containing 6 g/l glucose supplemented with 20 % FCS, and seeded in 12-well Costar dishes precoated with poly-L-lysine (1 g/l in 0.1 M borate buffer, pH 8.4). The cells were plated at a density of 1:2 hypothalamus per well. The cultures were incubated at 37 °C in a humidified 5% CO_2 atmosphere. Five or twenty four hours after seeding, the serum-rich medium was replaced by a serum-free chemically defined medium by Bottenstein and Sato [81]; this favours neurons instead of astrocytes (DMEM containing 6 g/l glucose supplemented with 5 $\mu\text{g}/\text{ml}$ insulin, 100 $\mu\text{g}/\text{ml}$ transferrin, 100 μM putrescine and 30 nM selenium).

b. Binding assay

After five days of culture *in vitro*, the attached cells were washed twice with 37°C Tris/BSA buffer (170 mM Tris-HCl, pH 7.4, 5 mM MgCl_2 , 0.1% BSA) and equilibrated in 2 ml buffer at 37°C for 20 min. [^{125}I]-MCH was then added to every well, at a concentration of 0.1 nM (260,000 cpm), non-specific binding was determined by adding an excess of cold MCH (1 and 5 μM). After incubation at 37°C (15 min, 30 min or 1 h), the dishes were placed on ice cold devices, the medium was removed and the cells washed during 10 min with 1 ml Tris/BSA, three times. Then 1 ml 0.05% SDS was added per well and left at room temperature for 5 min, detached cells were collected in 4-ml PP tubes and radioactivity counted in a γ -counter.

2.4. Cross-linking of [¹²⁵I]-MCH

Cells were washed twice in PBS and resuspended at a concentration of 5×10^6 cells per ml binding medium (modified Eagle's medium with Earl's salts (Gibco, Paisley, UK) containing 25 mM HEPES supplemented with 0,2 % gelatin (Inotech AG, Dottikon, Switzerland), 0,3 mM 1,10-phenantroline (Merck, Darmstadt, FRG) and 0,16 mM PMSF). The binding reaction consisted of 0,5 ml cell suspension, 0,25 pmol [¹²⁵I]-MCH (1×10^6 cpm), with or without 1 μ M MCH and lasted 2 h at 10°C. The cross-linker, disuccinimidyl suberate (Pierce Chemical Co, Rockford, IL) was then added to a final concentration of 1,85 mM. After a second 2-h incubation at 10°C, 20 mM Tris-Cl pH 7,5 was added to quench the reaction, and left at 10°C for 15 min. Tubes were centrifuged at 5,000 rpm and 4°C for 4 min, pellet was washed with 1 ml cold PBS and resuspended in 1 ml 10 mM Tris-Cl pH 7,5 and incubated 10 min on ice. After a 10-min centrifugation at 15,300 rpm and 4°C, the pellet was incubated in 1 ml 2 mM Tris-Cl pH 7,5 containing 0,2 mM PMSF and 0,15 mM 1,10-phenanthroline on ice for 10 min and for a further 10 min at -80°C (dry ice) . The solution was rapidly thawed at 37°C and centrifuged at 15,300 rpm and 4°C for 10 min. The proteins were extracted 1 h at 4°C in extraction buffer (150 mM Tris-Cl pH 7,5, 300 mM NaCl, 1 mM MgCl₂, 1% Triton X-100, 10% glycerol, 1 mM PMSF, 5 μ g/ml leupeptin hemisulfate, 5 μ g/ml aprotinin), debris were pelleted by centrifugation at 15,300 rpm and 4°C for 15 min. Lysates were mixed with one volume 2 X SDS sample buffer (100 mM Tris-HCl pH 6,8, 4% SDS, 0,2% bromophenol blue, 20 % glycerol, 200 mM DTT), boiled at 95°C for 8 min and subjected to SDS-PAGE in a 10% gel under reducing conditions. After electrophoresis the gel was coomassie stained, air dried in a gel drying system (Labforce, Nunningen, Switzerland) and submitted to autoradiography for 2 days in a storage phosphor screen at room temperature. Phosphor screen was scanned in a Phosphor Imager and image processed with ImageQuant software (all from Amersham Pharmacia Biotech, Dübendorf, Switzerland).

2.4.1. Cross-linking assay prior to 2-D electrophoresis

Some modifications to previous protocol were made in order to analyse the proteins in a 2-dimensional manner. The cells were resuspended at a concentration of 20×10^6 cells per ml and processed under the same conditions as previously. After the PBS wash, cells were spun down and washed 3 times with 10 mM Tris-Cl pH 7,5, pellet was lysed with urea lysis buffer (8 M urea, 4% w/v CHAPS, 40 mM Tris base, 2 mM PMSF), nucleic acid digested with RNase/DNase mix (1 mg/ml DNase I, 0,5 mg/ml RNase A, 50 mM MgCl₂.6H₂O, 500 mM Tris, pH 8,0) on ice for 8 min. Debris were pelleted by centrifugation at 14,000 rpm, 4°C for 5 min, supernatant was loaded

on desalting column (NAP-5 Column, Amersham Pharmacia Biotech, Dübendorf, Switzerland), sample eluted in 0.5% CHAPS and protein content determined by the method of Bradford (BioRad, Hercules, CA) using BSA as standard. Aliquots were lyophilized and stored at -80°C until use.

2.5. Two-dimensional gel electrophoresis

I was introduced to this technique by Dr Sandrine Besson (Biozentrum Abteilung Pharmakologie /Neurobiologie; Klingelbergstrasse 70; 4056 Basel). Horizontal isoelectric focusing with immobilized pH gradient (IPG) was carried on Multiphor II apparatus. All solutions, material and equipment were from Amersham Pharmacia Biotech (Dübendorf, Switzerland) and procedure performed under manufacturer's instructions.

Sample, resuspended in 450 µl rehydration solution [8 M urea, 2% w/v CHAPS, 0.28% w/v DTT, 2% IPG buffer (ampholytes pH 3-10 non-linear), traces of bromophenol blue in sulfone form] was pipetted into an Immobiline DryStrip Reswelling Tray slot, covered with an Immobiline DryStrip (180 mm, pH 3-10 non linear) and overlaid with IPG cover fluid (paraffin oil). Rehydration took place overnight at room temperature. Isoelectric focussing was carried out during 31 hours in Multiphor II according to the following program.

Table 8: Isoelectric focussing program

Phase	Time	Voltage	mA
1	1 min	increase to 150 V	1
	3 hours	150 V	1
2	1 min	increase to 300 V	1
	3 hours	300 V	1
3	5 hours	increase to 3,500 V	1
	20 hours	3,500 V	1
Total	31 hours and 2 min	80,900 Vh	

After isoelectric focussing, strips were placed individually in petri dishes and stored at -80°C . Equilibration started with a 15-min incubation at room temperature in 15 ml equilibration buffer (6 M urea, 2% w/v SDS, 50 mM Tris pH 8.5, 30% w/v glycerol) supplemented with 1% w/v DTT; followed by a second incubation in the same buffer supplemented with 5% w/v iodoacetamide and few grains bromophenol blue dye instead of DTT. Strip was sealed on top of a 1 mm thick 10% SDS gel (10% acrylamide:bis acrylamide mix (37.5:1), 375 mM Tris pH 8.8, 0.05% ammonium persulfate, 33 µl/ 100 ml TEMED) with 0.5% agarose dissolved in running buffer (25 mM Tris base, 190 mM glycine, 0.1% SDS). After electrophoresis at 20 mA

per gel for 5 h, in Hoefer SE 600 unit, the proteins were stained using the colloidal staining method described by Anderson et al. [82] based on coomassie blue G250. Gel was fixed over night in 150 ml orthophosphoric acid/ethanol solution (2 volumes of 1.38% w/v orthophosphoric acid : 1 volume ethanol) and washed three times 30 min in dH₂O.

Post-fixing-step consisted in a 1-h incubation in 3 volumes 1.38% w/v orthophosphoric acid solution / 1 volume methanol supplemented with 12,7 mg/ml ammonium sulfate. Staining was performed in the same buffer as before, supplemented with 0.5 mg/ml coomassie blue G250 for a few hours to 3 days at room temperature on a rocking platform. Gel was then air dried in a gel drying system (Labforce, Nunningen, Switzerland) and submitted to autoradiography for 2 days in a storage phosphor screen at room temperature. Phosphor screen was scanned in a Phosphor Imager and image processed with ImageQuant software (all from Amersham Pharmacia Biotech, Dübendorf, Switzerland).

2.6. Autoradiographic localisation of MCH binding sites in the central nervous system of the rat

Performed under the expertise of MJ Freund-Mercier and E. Waltisperger at the "Laboratoire de physiologie cellulaire et intégrée" UMR7519 CNRS/ULP -I.P.C.B-STRASBOURG (05/26 → 06/19/2000)

Male wistar rats, weighing ca 260 grams were sacrificed, their brains frozen in dry-ice cooled isopentane and stored at -20°C until sectioning. Frontal sections (20 µm thick) were cut at -16°C on a cryostat, thaw-mounted on gelatine-coated slides and stored at -20°C until use. Frozen sections were preincubated at room temperature for 20 min in Tris buffer (170 mM Tris-HCl, 5 mM MgCl₂.6H₂O, 0.1% bovine serum albumin; pH 7.4). The sections were then incubated either at 4°C for 24 h or at room temperature for 90 min in the same buffer containing 0.05 or 0.1 nM [¹²⁵I]-MCH (= 4.26 or 8.52 × 10⁶ cpm). Non-specific binding was determined in presence of 10⁻⁸ M MCH. After incubation, sections were washed in cold Tris buffer, then in cold distilled water and dried overnight with a cold air stream. Film autoradiographs were generated by exposing labelled sections to Hyperfilms (Amersham Pharmacia Biotech, Dübendorf, Switzerland) in X-ray cassettes (Eastman Kodak Company, Rochester, NY). After 3-5-7 days exposure at 4°C the films were developed for 5 min in Kodak D19 (Eastman Kodak Company, Rochester, NY) at 18°C, washed in tap water and fixed at room temperature for 10 min in Hypam fixer (Ilford, Cheshire, UK).

2.7. Semi-quantitative RT-PCR

Total RNA was extracted from cultured cells with a kit (RNeasy; Qiagen, Chatsworth, CA) and subjected to DNase I digestion (DNA-free kit; Ambion, Austin, TX) according to manufacturers' instructions. Human adult normal brain total RNA was obtained from BioChain Institute (Hayward, CA). Total RNA (1 µg) was denatured at 65°C for 5 min in presence of 0.2 µg oligo (dT)₁₅; first-strand cDNA was produced at 37°C for 60 min in presence of 200 U of M-MLV reverse transcriptase (Promega, Madison, WI), 1 mM dNTP and 0.5 U ribonuclease inhibitor (Promega, Madison, WI), in a total volume of 20 µl, followed by a denaturation step of 5 min at 94°C. Multiplex PCR was performed with cDNA corresponding to 25 ng total RNA, 200 µM dNTP, 0.05 µM of each beta-actin primer, 1µM of each other primer (Table 9), 1.5 mM MgCl₂, and 1 U HotStarTaq DNA polymerase (Qiagen, Chatsworth, CA) in a total volume of 20 µl. After a polymerase activation step of 15 min at 94°C, 40 or 50 cycles of 94°C (40 s), 62°C (45 s), and 72°C (45 s) were performed and followed by a final extension at 72°C for 2 min. PCR products were resolved on a 1.5% agarose gel and visualised by ethidium bromide staining. Bands intensity quantification was performed with a digital imaging system (Multi-Analyst® Bio-Rad, USA) and results standardised with corresponding beta-actin value. The results were expressed as mean ± SEM and statistical inference of the data was determined by an analysis of variance (ANOVA) test with GraphPad Prism software. All PCR-amplified fragments were sequenced by Microsynth (Balgach, Switzerland) and corresponded to the targeted region.

Table 9: Sequence of oligonucleotide primers used for RT-PCR, expected size (bp) of amplified products depending on the template. When possible primers are designed to span an intron to distinguish between genomic and cDNA sequence.

Targets	5' primer (5'-3')	3' primer (5'-3')	cDNA size (bp)	Genomic DNA size (bp)
β-actin	CAGCTCACCATGGATGATGAT	CTCGGCCGTGGTGGTGAAGCT	623	1,180
Flag-rat MCH-R ₁	GGACTACAAAGCACGATGACG	GTGATGAGGGTGCACATGG	379	no amplification ^a
MCH-R ₁	CCCCGATAACCTCACTTCG	GTGATGAGGGTGCACATGG	300	1,517
MCH-R ₂	CTGCCAGTGTGGTGGATACAG	AACGIGTCAGTCGAAATGGTTG	347	> 12,000
MCH	ATAAAGTITCAAAGAACACAGG CT	ATACATCTGAGCATGTCAAATC T	226	no amplification ^b

^a Forward primer is complementary to the FLAG sequence that is unique.

^b Forward primer is complementary to end of exon I and beginning of exon II; reverse primer is complementary to end of exon II and beginning of exon III of MCH gene.

2.8. Immunofluorescence studies

2.8.1. External staining

The cells were detached from culture flask with PBS/EDTA and from this step on, all the procedures were done on ice. The cells were washed twice with wash medium (PBS, 1% BSA, 0.02% NaN₃), distributed at 300,000 cells per well in U bottom 96-well plate (Falcon®, Becton Dickinson, Lincoln Park, NJ), and pelleted at 1,100 rpm and 4°C for 3 min. The supernatant was discarded and cells resuspended with 20 µl first antibody solution (anti-Flag M2 monoclonal antibody, Sigma, St. Louis, MI; 22µg/ml wash medium). After a 30-min incubation, cells were washed twice with 200 µl wash medium and finally incubated 20 min in the dark in 20 µl of the second antibody solution (FITC-labeled goat anti-mouse Ig, Southern Biotechnology Associates, Birmingham, AL; 20 µg/ml wash medium). After two washes, the cells were mounted with 10 µl Fluorsave™ Reagent (Calbiochem, San Diego, CA) and examined under a Zeiss Axiophot Photomicroscope using a 40 x objective.

2.8.2. Internal staining

Anti MCH-R₁ polyclonal antibody was raised in rabbit by our laboratory. The antigenic peptide H₂N-SNAQTADERTESKG-COOH is located at the C-terminus of the receptor, a part that is identical in rat and human MCH-R₁.

The cells were grown in 8-well glass slides (Lab-Tek® Chamberslide, Nalge Nunc International, Naperville, IL) and washed twice with wash buffer (PBS, 10% FCS, 10 mM NaN₃), fixed in 50% acetone + 50% methanol at -20°C for 20 min, washed again and incubated at room temperature for 30 min with 1:100 total IgG solution (IgG being purified from either pre-immune or MCH-R₁- immunised serum). Cells were then washed 5 times, incubated for 20 min with Alexa Fluor®488-conjugated goat anti-rabbit IgG (H+L) 1:200, Molecular Probes, Leiden, The Netherlands), washed twice, mounted with Fluorsave™ Reagent (Calbiochem, San Diego, CA) and examined under a Zeiss Axiophot Photomicroscope using a 40 x objective.

2.9. Western blotting

Cells or membranes were washed in PBS and proteins extracted in extraction buffer (150 mM Tris-Cl pH 7.5, 300 mM NaCl, 1 mM MgCl₂, 1% Triton X-100, 10% glycerol, 1 mM PMSF, 5 µg/ml leupeptin hemisulfate, 5 µg/ml aprotinin) at 4°C for 1h, debris were pelleted by centrifugation at

15,300 rpm and 4°C for 15 min. Lysates were mixed with one volume 2 X SDS sample buffer (100 mM Tris-HCl pH 6.8, 4% SDS, 0.2% bromophenol blue, 20% glycerol, 200 mM DTT, 10% v/v β -mercaptoethanol), boiled at 95°C for 8 min and subjected to a 10% SDS-PAGE under reducing conditions.

Migration proceeded in SDS-PAGE running buffer (25 mM Tris-base, 190 mM glycine, 1% SDS) at 19 V/cm for 1 h. Transfer on 0.45 μ m nitrocellulose membrane (porablot NCL, Machery-Nagel, Düren, Germany) was performed in transfer buffer (48 mM Tris-base, 40 mM glycine, 0.037% SDS, 20% methanol) at 50 mA/cm for 1 h. Transfer efficiency was accessed by Ponceau S staining (0.2% w/v Ponceau S, 3% w/v trichloroacetic acid, 3% w/v sulfosalicylic acid), molecular weight standards were marked with waterproof black ink and membrane was washed with deionized water. Blocking was performed at room temperature for 1 h in TBS-T (50 mM Tris-HCl pH 7.5, 150 mM NaCl, 0.05 % v/v Tween-20) + 10% w/v non-fat dry milk, anti-Flag M2 mouse monoclonal antibody (Sigma, St Louis, MO) was diluted to 0.88 μ g/ml in the same solution and incubated either at room temperature for 1 h or overnight at 4°C. Membranes were washed three times 10 min in TBS-T, and goat anti-mouse IgG horseradish peroxidase conjugated antibody (Southern Biotechnology Associates, Birmingham, AL) diluted 1:10,000 in TBS-T + 0.5 % w/v non-fat dry milk was incubated at room temperature for 1 h. After three 10-min washes, the peroxidase reaction was performed with ECL plus kit (Amersham Pharmacia Biotech, Dübendorf, Switzerland) according to manufacturer's instructions. Chemoluminescent signal was subsequently detected on a Kodak Biomax film (Eastman Kodak Company, Rochester, NY). For a second blotting with the same sample, the membrane was washed in TBT-T for 20 min, stripped at 65°C for 40 min in strip-buffer (2% SDS, 63 mM Tris-HCl pH 6.8, 0.7% v/v β -mercaptoethanol). A 20 min saturation in TBS-T + 10% w/v milk preceded the second immunoblotting.

2.10. Fluorimetric imaging plate reader (FLIPR) assay

Performed at Axovan (Innovation Center; Gewerbestrasse 16, CH-4123 Allschwill, Switzerland; <http://www.axovan.com>) under the expertise of Dr. Thomas Giller, Managing Director.

Cells were detached from culture flask with PBS/EDTA, washed with PBS and loaded at 37°C for 1 h with Fluo-3 calcium indicator dye (Dulbecco's modified Eagle's medium (DMEM) without phenol red, 20 mM HEPES, 4 μ M Fluo-3). In the case of Kelly cells, 5 mM probenecid (Sigma, Saint Louis, MI) was added to inhibit the extrusion of dye by the multiple drug-resistance pump. Cells were washed in assay buffer (DMEM 50%, Hanks's Balanced Salt Solution (HBSS) 50%, HEPES 10 mM) and seeded at 200,000 cells in 200 μ l per well in clear-bottom black-well Costar 96-well dish. Subsequent studies were performed in 384-well plates and cells were seeded at 50,000 per well in 80 μ l. Changes of Ca⁺⁺ levels were measured after addition of 50 μ l of assay buffer (or 20 μ l in case of 384-well plate) containing the appropriate concentration of tested compound. The FLIPR instrument (Molecular Devices, Sunnyvale, CA)

was used to monitor intracellular free Ca^{++} levels over a 3-min stimulation period. The maximum increase in fluorescence was measured and EC_{50} values were determined by non-linear regression using Prism (GraphPad Software, San Diego, CA).

3. Results

3.1. Detection of MCH binding sites

3.1.1. A well-established model: ^{125}I -[DPhe¹³, Tyr¹⁹]-MCH binding to G4F-Cl1 mouse melanoma cells.

In the 1990's, the major problem to examine MCH binding sites was the development of a satisfactory radioligand. In fact the introduction of an iodine atom onto the tyrosine residue located in the central region of the MCH molecule (Tyr¹³) reduced bioactivity by 500- to 1,000 fold in the fish scale melanophore assay (the only bioassay for MCH available at that time).

For this reason, in 1995, Tyr¹³ was replaced by Phe and Val¹⁹ by Tyr in the human MCH by our laboratory [62]. This replacement did not alter the activity of the peptide when tested in the fish scale melanophore assay, [Phe¹³, Tyr¹⁹]-MCH potency equalled that of the parent human MCH ($\text{EC}_{50} \approx 10^{-11}$ M in both cases). Binding analysis with ^{125}I -[Phe¹³, Tyr¹⁹]-MCH and G4F melanoma cells revealed that these cells showed specific MCH binding and that binding was optimal between 10-15°C using a 60-90 min incubation period.

In addition, to decrease lipophilicity and high susceptibility to oxidative damage of [Phe¹³, Tyr¹⁹]-MCH, numerous analogues were synthesised and tested for mouse melanoma binding [79]. Among them, the one in which the L-enantiomer of Phe¹³ is substituted by the D-enantiomer gave the most promising result. [DPhe¹³, Tyr¹⁹]-MCH had the highest relative receptor-binding potency with $K_i = 2.4 \pm 1.0$ nM. It is the most potent MCH analogue synthesised so far. The MCH receptor expressed on mouse melanoma cells has the same affinity for both radioligand ^{125}I -[LPhe¹³, Tyr¹⁹]-MCH and ^{125}I -[DPhe¹³, Tyr¹⁹]-MCH with K_d 's of 118 and 122 pM respectively. All binding characteristics of different MCH analogues were determined following incubation at 10°C for 120 min.

For these reasons, at the beginning of the thesis work we chose to perform binding experiments with the most potent and stable radioligand available at that time, ^{125}I -[DPhe¹³, Tyr¹⁹]-MCH and to use the following incubation conditions: 10°C for 120 min.

3.1.2. Binding assays with neuroblastoma cell lines

Knowing that MCH is produced by neurons of the lateral hypothalamic and zona incerta brain areas, we hypothesized that specific neurons are MCH targets and therefore express the receptor for MCH. As human primary neurons were not a possible source of cells, we analysed neuroblastoma cell lines. Neuroblastoma is a cancer of the sympathetic nervous system. Neuroblastoma cell lines which are derived from postganglionic sympathetic cells of the neural crest are composed of primitive neuroblasts.

We tested the following cell lines with the ^{125}I -[DPhe¹³, Tyr¹⁹]-MCH tracer:

- Five human neuroblastoma cell lines (SMS-KAN, SH-SY5Y, SK-N-MC, LAN-5, and Kelly)
- Two mouse neuroblastoma cell lines (N1E115 and N-18)
- One mouse brain tumour cell line (CATH.a)
- The G4F-C11 cells (mouse melanoma) were used as internal positive control [79]. The non-neuronal Chinese hamster ovary (CHO) cell line was also included as irrelevant control cells.

We observed very low specific binding with three human neuroblastoma cell lines (Fig. 6), SK-N-MC being the one showing the most specific binding (24%). This cell line was further analysed with varying incubation conditions (time and temperature) to optimise the binding of MCH radioligand. Even after trying a wide range of incubation conditions (Fig. 7), the SK-N-MC cell line remained with a non-significant MCH binding compared to G4F-C11 (85% specific binding).

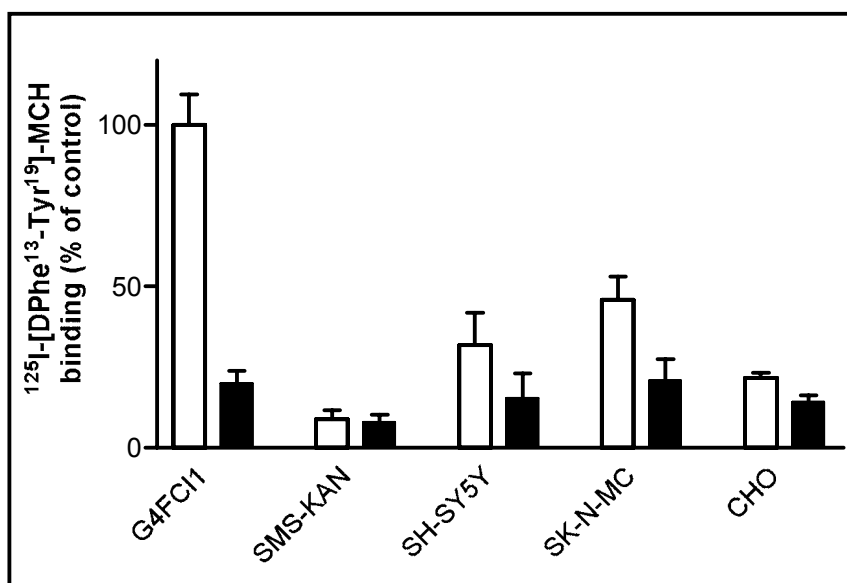


Figure 6. Total (open bars) and non-specific (black bars) binding of ^{125}I -[DPhe¹³, Tyr¹⁹]-MCH on human neuroblastoma, mouse melanoma and Chinese hamster ovary cells. Non-specific binding is obtained with 1 μM MCH. The graph represents the mean \pm SEM of two experiments; incubation conditions are 120 min at 10°C.

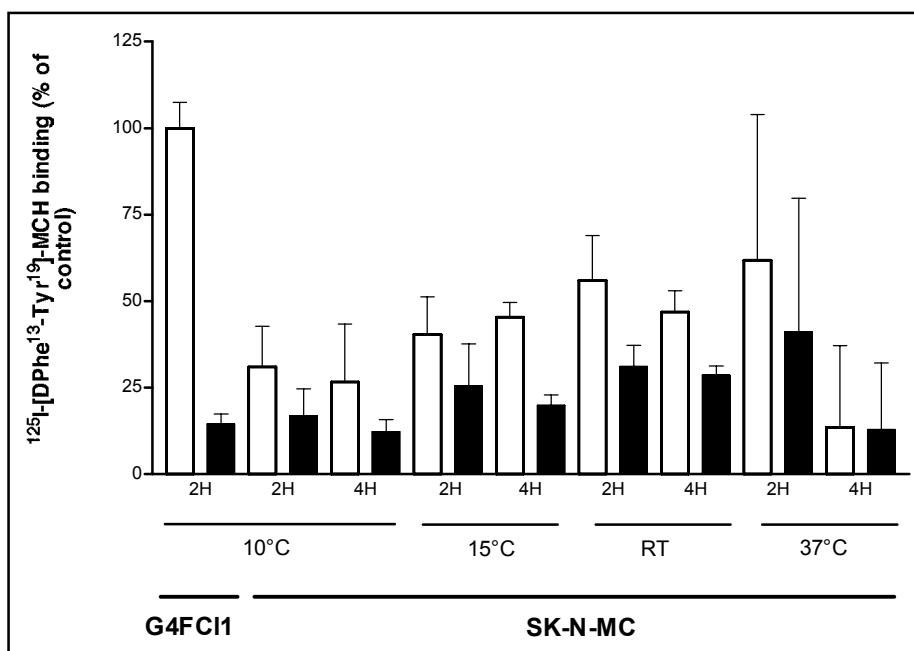


Figure 7. Total (open bars) and non-specific binding (black bars) of ^{125}I -[DPhe¹³, Tyr¹⁹]-MCH on SK-N-MC cells. Non-specific binding is obtained with 1 μM MCH. For incubation conditions see the legend; RT= room temperature ($\approx 21^\circ\text{C}$). Error bars represent SEM of triplicates.

The CATH.a mouse brain tumour cell line did not possess binding sites for MCH either (Fig. 8). The four other neuroblastoma cell lines tested showed very little displacement of radioligand upon addition of cold competitor (Fig. 9). Because of the high overall binding of the radioligand to the mouse neuroblastoma cell lines (N-18 and N1E115), degradation of the radioligand was suspected. Analysis of the radioligand by HPLC after incubation with cells at 10°C for 2 h, revealed that detectable amounts of intact radioligand were still present after incubation with G4F-C11, N-18 and N1E115 cells.

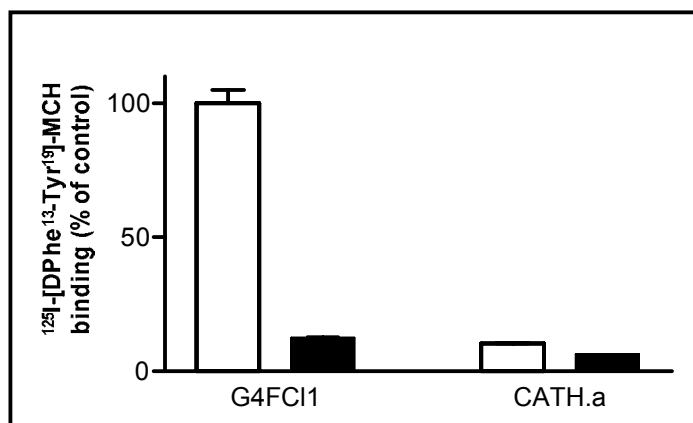


Figure 8. Total (open bars) and non-specific binding (black bars) of ^{125}I -[Dphe¹³, Tyr¹⁹]-MCH on CATH.a cells. Non-specific binding is obtained with 1 μM MCH; incubation conditions are 120 min at 10°C. Error bars represent SEM of triplicates.

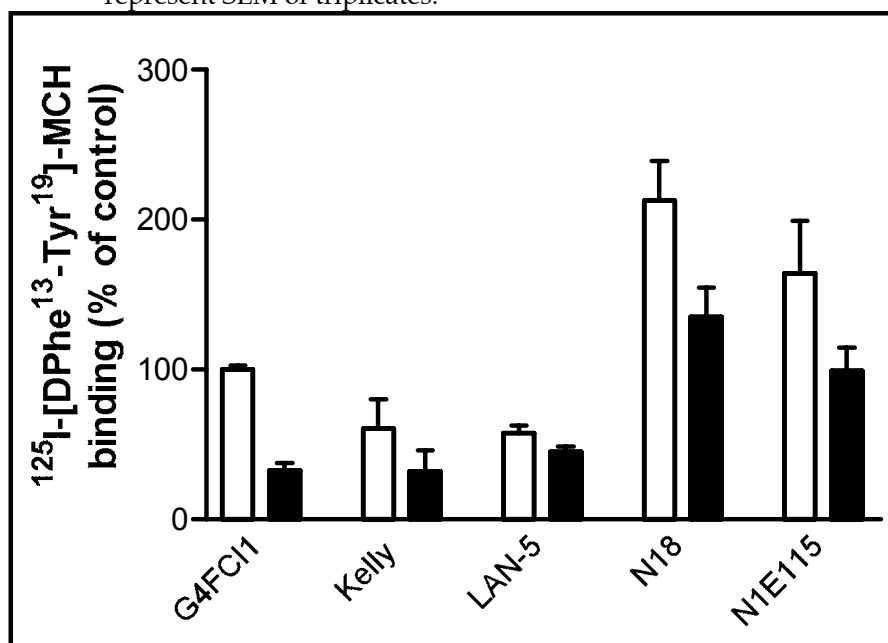


Figure 9. Total (open bars) and non-specific binding (black bars) of ^{125}I -[Dphe¹³, Tyr¹⁹]-MCH on human neuroblastoma (Kelly and LAN-5) and mouse neuroblastoma (N-18 and N1E115). Non-specific binding is obtained with 1 μM MCH. Graph represents the mean of 2 to 4 experiments \pm SEM; incubation conditions are 120 min at 10°C.

3.1.3. Binding assay with porcine brain membranes

The determination of interesting porcine brain regions was based on the table 3 of the review of JL Nahon [6]. The richest MCH immunoreactive fibre-containing regions of the rat brain are nucleus of the diagonal band, bed

nucleus of stria terminalis, medial septum, subzona incerta, hypothalamic medial forebrain bundle, posterior hypothalamic nucleus, and medial mamillary nucleus. On this basis the following porcine brain regions were dissected and subjected to membrane preparation (Fig. 10):

- Bed nucleus of stria terminalis (bed nucl. of s.t.)
- Zona incerta
- Hypothalamus
- Hippocampus
- Mamillary body
- Striatum, as neighbouring control region
- Cerebellum, as negative control region

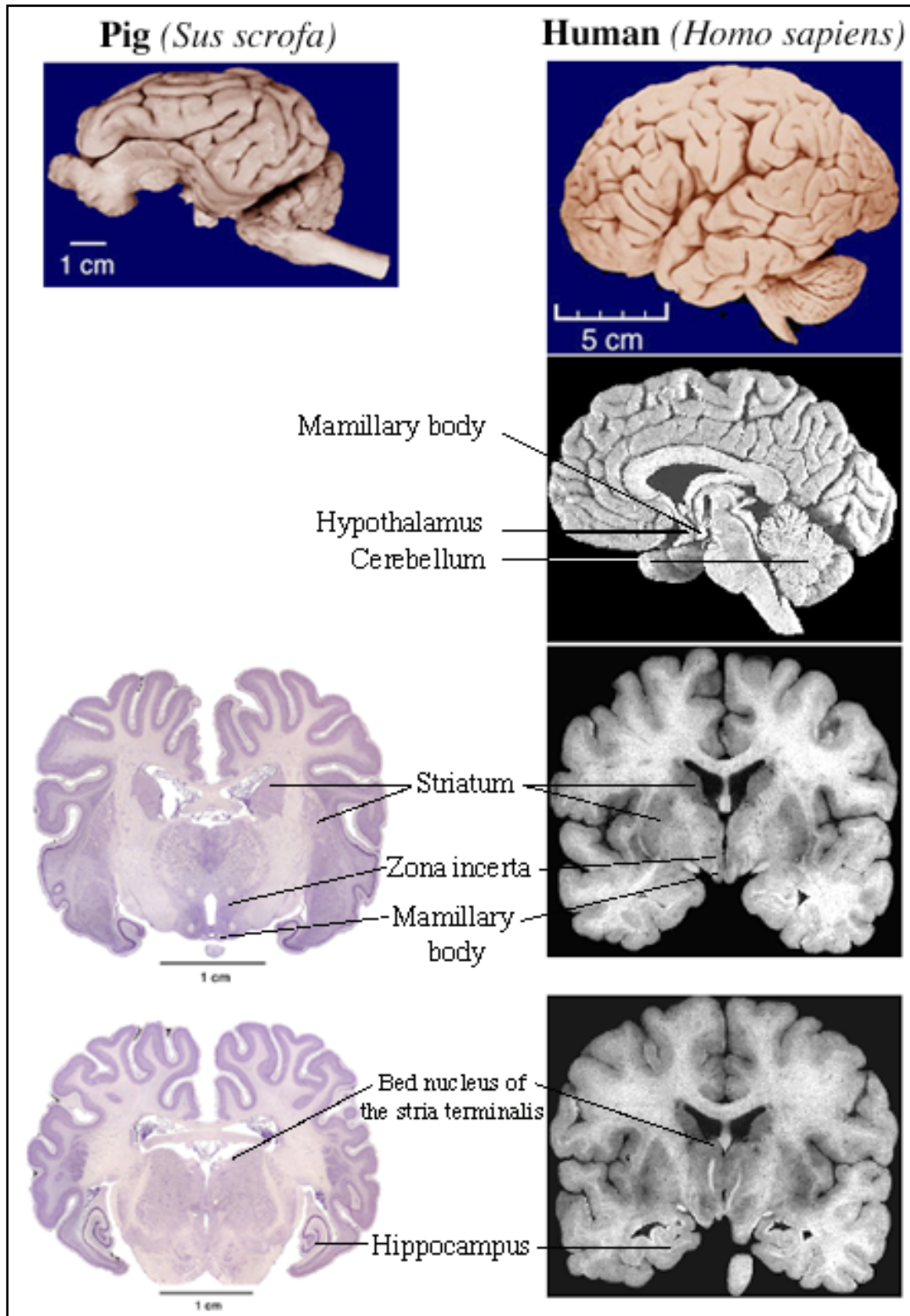


Figure 10. Localisation of excised brain regions on both human and porcine images. Black and white pictures are from the University of Washington digital anatomist program; other pictures are from the University of Wisconsin and Michigan State Comparative Mammalian Brain Collections available at the following web site: <http://brainmuseum.org> ; preparation of images has been funded by the National Science Foundation and the National Institutes of Health.

Due to high hydrophobicity of MCH radioligand, and also high “stickiness” of brain membranes to the filter, the microplate binding assay developed in our laboratory by Dr S. Froidevaux [80] was not applicable. The binding assay was therefore performed in tubes. During the first experiments, no displacement of the radioligand could be seen (Fig. 11); this was due to a high adhesion of the radioligand to the surface of the polypropylene tube. Therefore, for the next attempts two control tubes were included, containing the radioligand in binding medium with or without 1 μ M MCH. These background control figures (5,000 to 10,000 cpm per tube) were subtracted from the ones obtained with the membranes (13,000 cpm to 18,000 cpm per tube). Some specific binding was then detectable, especially in zona incerta, hippocampus and mamillary body (Fig. 12).

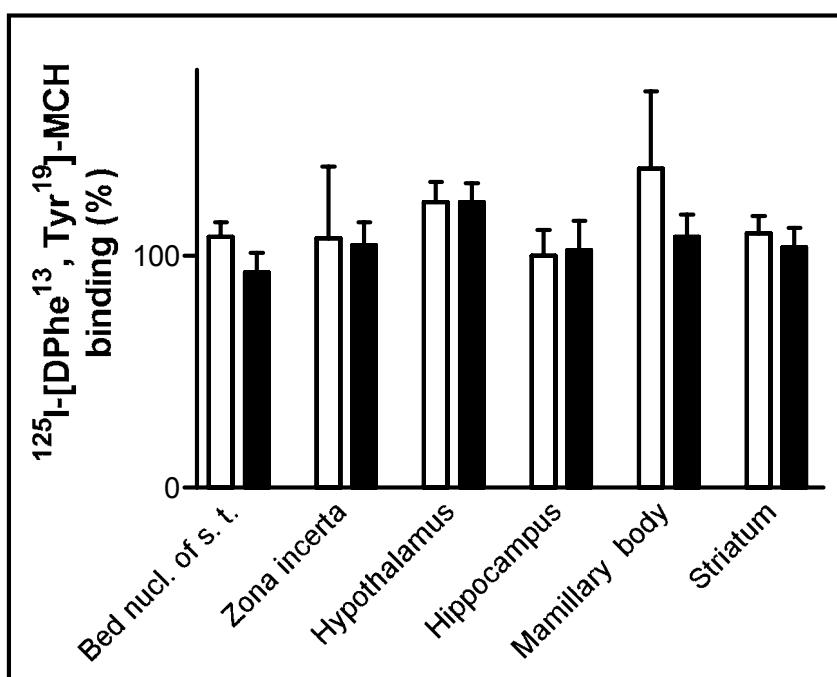


Figure 11. Total (open bars) and non-specific (black bars) of ^{125}I -[DPhe¹³, Tyr¹⁹]-MCH on porcine brain membranes. Non-specific binding is obtained with 1 μ M MCH and data represent the mean of two experiments \pm SEM and are normalised to hippocampus total binding; incubation conditions are 120 min at 10°C.

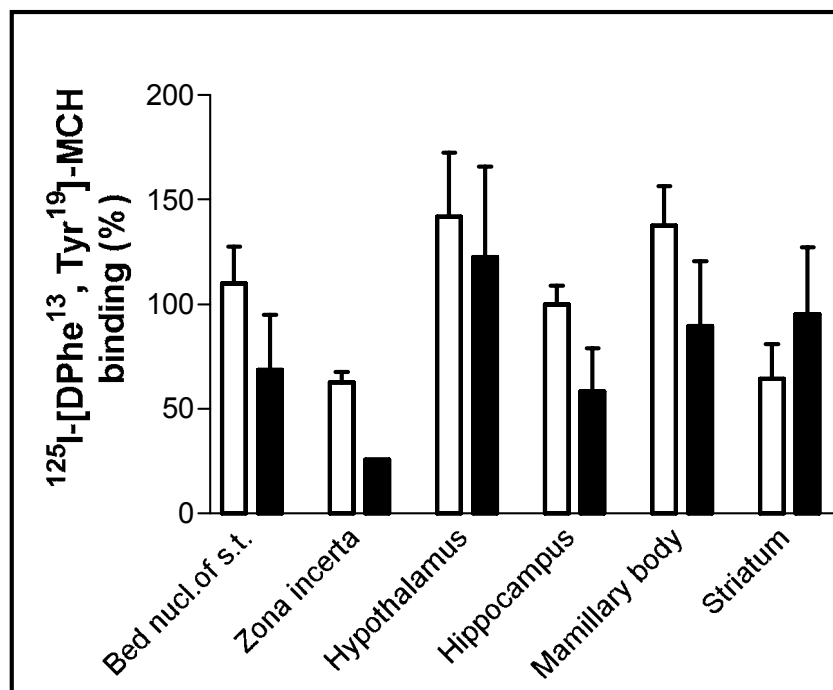


Figure 12. Total (open bars) and non-specific binding (black bars) of ^{125}I -[DPhe¹³, Tyr¹⁹]-MCH on porcine brain membranes. Non-specific binding is obtained with 1 μM MCH and data represent the mean \pm SEM of two experiments and are normalised to hippocampus total binding; incubation conditions are 120 min at 100°C.

To improve the percentage of specific binding, several changes were made such as addition of detergent to the washing buffer, variation of the incubation time and even switch of the radioligand to [^{125}I]-MCH.

To perform these optimisations, hippocampal membranes were chosen due to their relatively high abundance compared to zona incerta and mamillary body regions. Neither the radioligand nor the changes in the conditions of incubation improved the specific binding (Fig. 13). The addition of NP-40 but not Tween20 improved specific binding of the radioligand to porcine hippocampal membranes (Fig. 14).

Because degradation of radioligand during incubation with detergents was feared, radioligand integrity was checked by HPLC, and showed that almost all of the radioligand remained intact after incubation in NP-40-containing binding medium.

Unfortunately this good result (61% specific binding in presence of 0.1% NP-40 in both incubation and washing buffers) was not reproducible (Fig. 15).

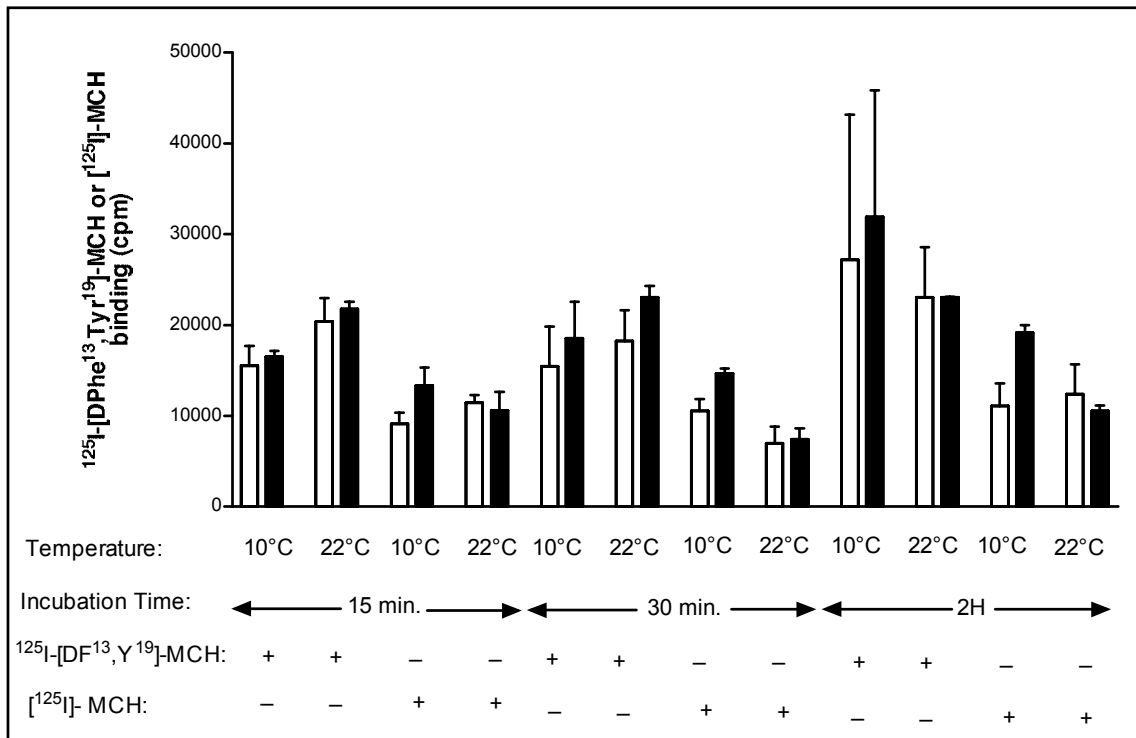


Figure 13. Total (open bars) and non-specific binding (black bars) of ^{125}I -[DPhe 13 ,Tyr 19]-MCH and [^{125}I]-MCH on porcine hippocampal brain membranes (100 $\mu\text{g}/\text{tube}$). Non-specific binding is obtained with 1 μM MCH. For incubation conditions see the legend. Data are from a single experiment \pm SEM of triplicates.

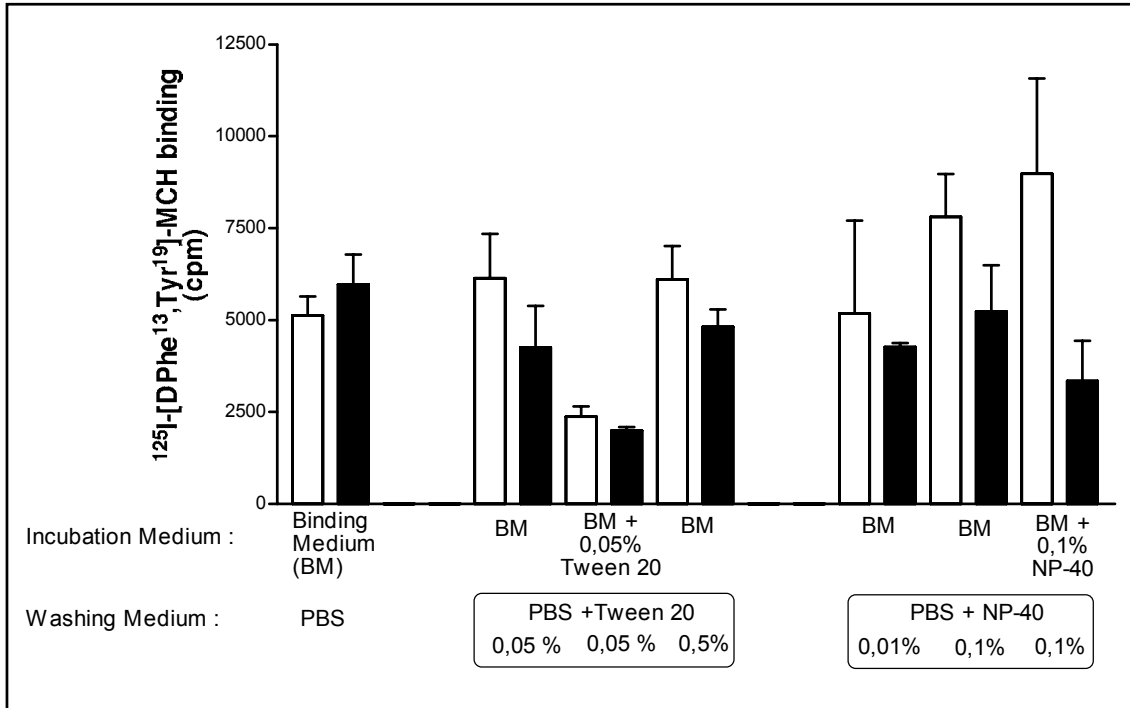


Figure 14. Total (open bars) and non-specific binding (black bars) of ^{125}I -[DPhe¹³, Tyr¹⁹]-MCH on porcine hippocampal membranes (100 $\mu\text{g}/\text{tube}$). Non-specific binding is obtained with 1 μM MCH; incubation conditions are 120 min at 10°C. Data are from a single experiment \pm SEM of triplicates.

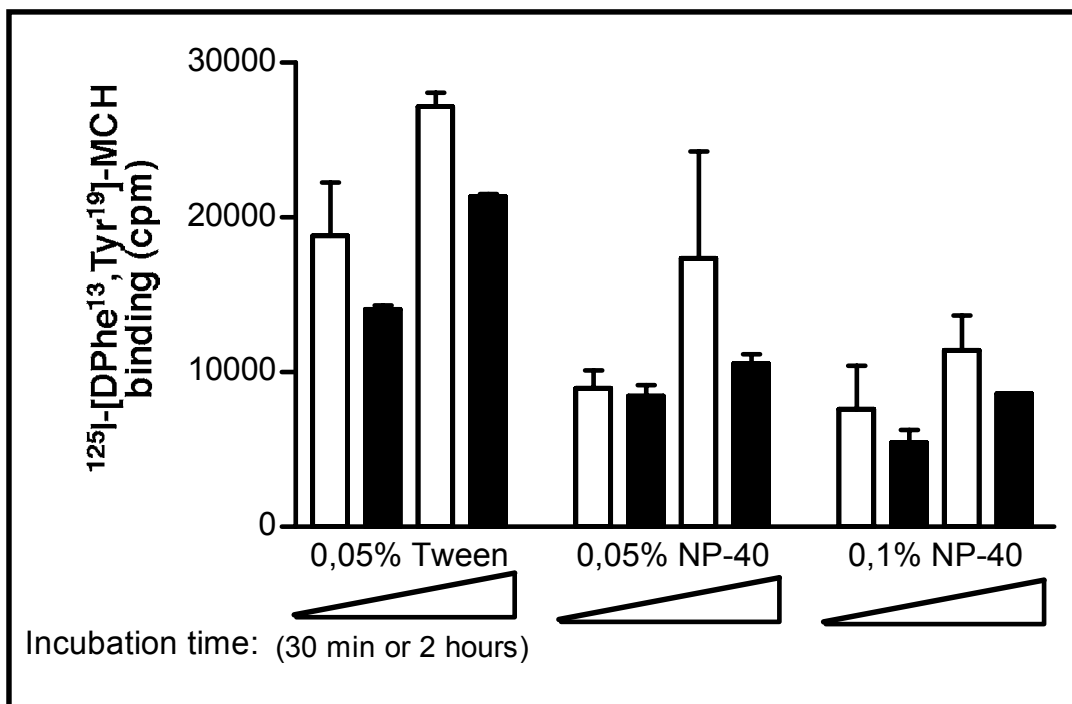


Figure 15. Total (open bars) and non-specific binding (black bars) of ^{125}I -[DPhe¹³, Tyr¹⁹]-MCH on porcine hippocampal membranes (100 $\mu\text{g}/\text{tube}$). Non-specific binding is obtained with 1 μM MCH; incubation conditions are either 30 or 120 min at 10 C. Data are the one of a single experiment \pm SEM of triplicates.

3.1.4. Binding assays with human primary melanocytes

As primary cells hardly grow *in vitro*, it was difficult to expand the primary melanocytes we received in 25 cm² flasks. Only the white melanocytes (W400) reached a sufficient density to perform a binding experiment with them. Compared to G4F-C11, W400 melanocytes did not exhibit significant ¹²⁵I-[Phe¹³, Tyr¹⁹]-MCH binding (Fig. 16).

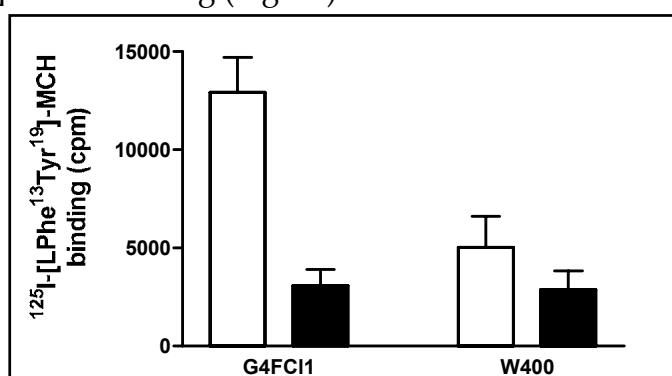


Figure 16. Total (open bars) and non-specific binding (black bars) of ¹²⁵I-[L-Phe¹³, Tyr¹⁹]-MCH on mouse melanoma (G4F-C11) and white human melanocytes (W400). Non-specific binding is obtained with 1 μM MCH; incubation conditions are 120 min at 10°C. Data are from a single experiment ± SEM of triplicates.

3.1.5. Binding assay with rat embryonic primary hypothalamic neurons

Two rat primary embryonic hypothalamic neurons preparations were performed and assayed for [125 I]-MCH binding in presence of 1 or 5 μ M cold MCH competitor (Fig. 17). The results of these two binding experiments are summarised in the following table:

Table 10: [125 I]-MCH specific binding percentage to rat embryonic primary hypothalamic neurons:

5 H serum		24 H serum		Incubation time (37°C)
1 μ M MCH	5 μ M MCH	1 μ M MCH	5 μ M MCH	
-	-	-	-	15 min
-	-	9.6 %	5 %	30 min
30 %	40 %	16 %	30 %	60 min

The specific binding percentages vary between 5 and 40%, result obtained with the 5 h serum rich medium cultivation and 5 μ M cold competitor with an incubation performed at 37°C for 1 h.

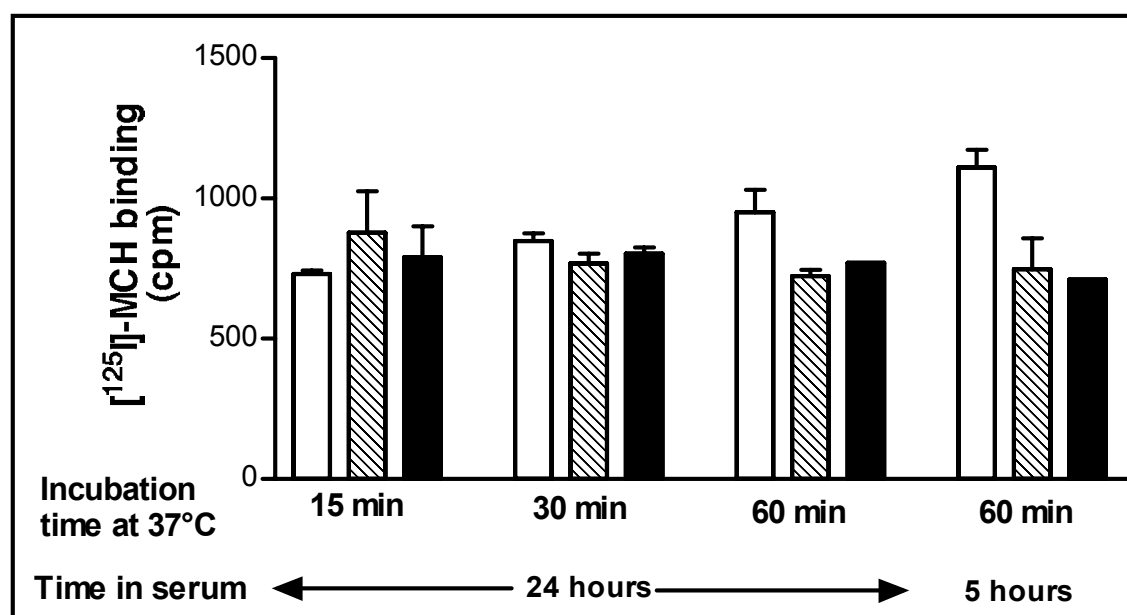


Figure 17. Total (open bars) and non-specific binding (hatched bars=1 μ M MCH, black bars=5 μ M MCH) of [125 I]-MCH on rat embryonic primary hypothalamic neurons. Incubation conditions are indicated on the figure. Data represent the mean of two

3.1.6. Autoradiographic localisation of MCH binding sites in the central nervous system of the rat

Cryostat sections of rat brain covering anterior (interneural - 0.30 mm) to posterior regions (cerebellum) were assayed for [125 I]-MCH binding for either 90 min at room temperature or over night at 4°C, in presence of 10 nM MCH, in the case of non-specific binding determination. We could not stain any specific region with the MCH radioligand, as it was not displaced by the unlabeled analogue (Fig. 18).

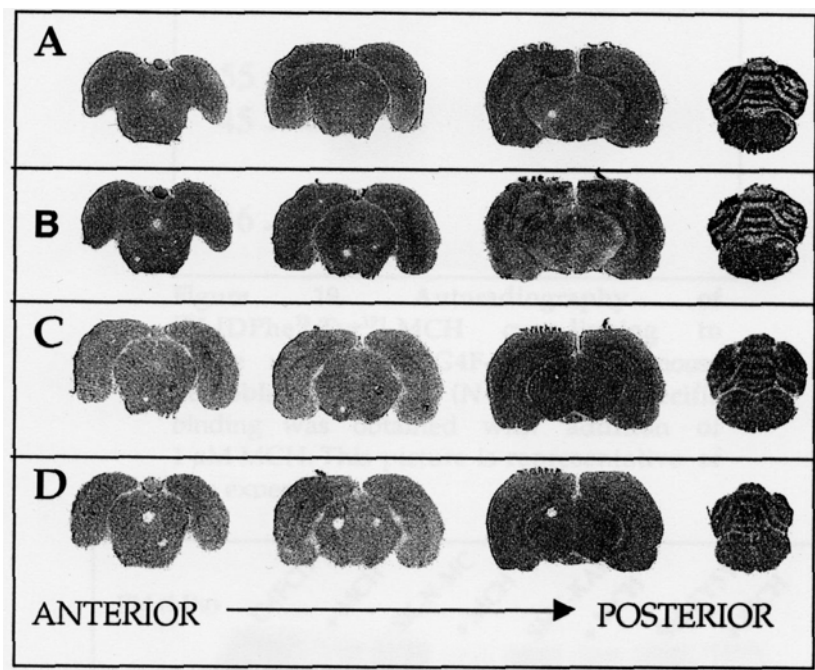


Figure 18. Autoradiographic localisation of [125 I]-MCH binding sites in the central nervous system of the rat. (A) Incubation with 0.1 nM [125 I]-MCH for 90 min at room temperature, total binding ; (B) in presence of 10 nM cold MCH, non-specific binding. (C) Incubation with 0.05 nM [125 I]-MCH over night at 4°C, total binding ; (D) in presence of 10 nM cold MCH, non-specific binding. The film was exposed 3 days at 4°C.

3.1.7. Cross-linking of MCH radioligand to neuroblastoma cell lines

Several cell lines used for binding assays were also subjected to cross-linking assay when possible. The radioligand used is the same as the one used for binding assays i.e. ^{125}I -[DPhe¹³,Tyr¹⁹]-MCH. Both mouse neuroblastoma (N-18; Fig. 19) and human neuroblastoma cells (SK-N-MC, SMS-KAN and SH-SY5Y; Fig. 20) produced a specific 50 kDa cross-linked band when subjected to ^{125}I -[DPhe¹³,Tyr¹⁹]-MCH cross-linking. The same 50 kDa cross-linked band is found in Chinese hamster ovary (CHO) cells (Fig. 21). This radioligand cross-linking could be abolished upon addition of 1 μM unlabeled MCH, but not with 1 μM α -MSH, another neuro-hormone (Fig. 21).

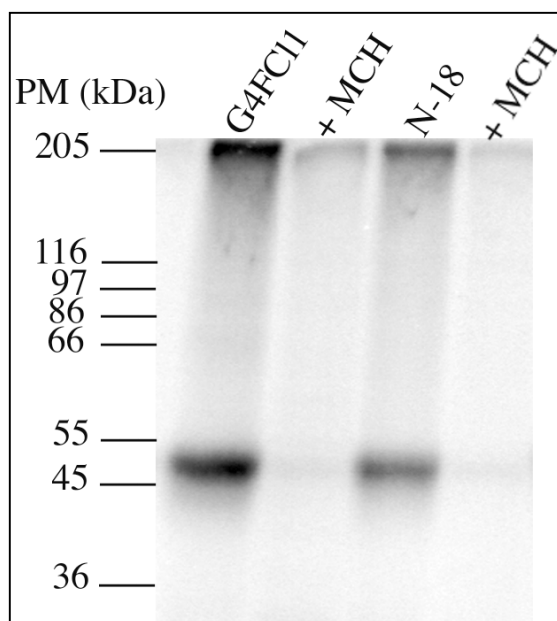


Figure 19. Autoradiography of ^{125}I -[DPhe¹³,Tyr¹⁹]-MCH cross-linking to mouse melanoma (G4F-C11) and mouse neuroblastoma cells (N-18). Non-specific binding was obtained with addition of 1 μM MCH. This picture is representative of two experiments

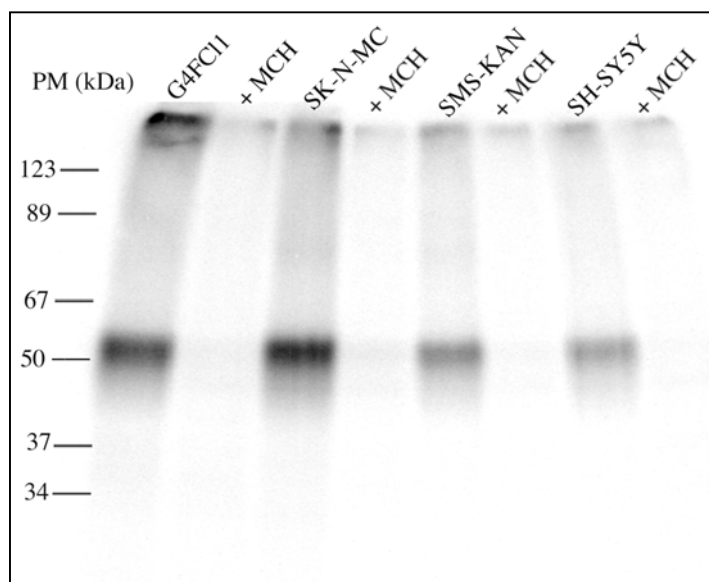


Figure 20. Autoradiography of ^{125}I -[DPhe¹³,Tyr¹⁹]-MCH cross-linking to mouse melanoma (G4F-C11) and human neuroblastoma cells (SK-N-MC, SMS-KAN and SH-SY5Y). Non-specific binding was obtained with addition of 1 μM MCH. This picture is representative of three experiments.

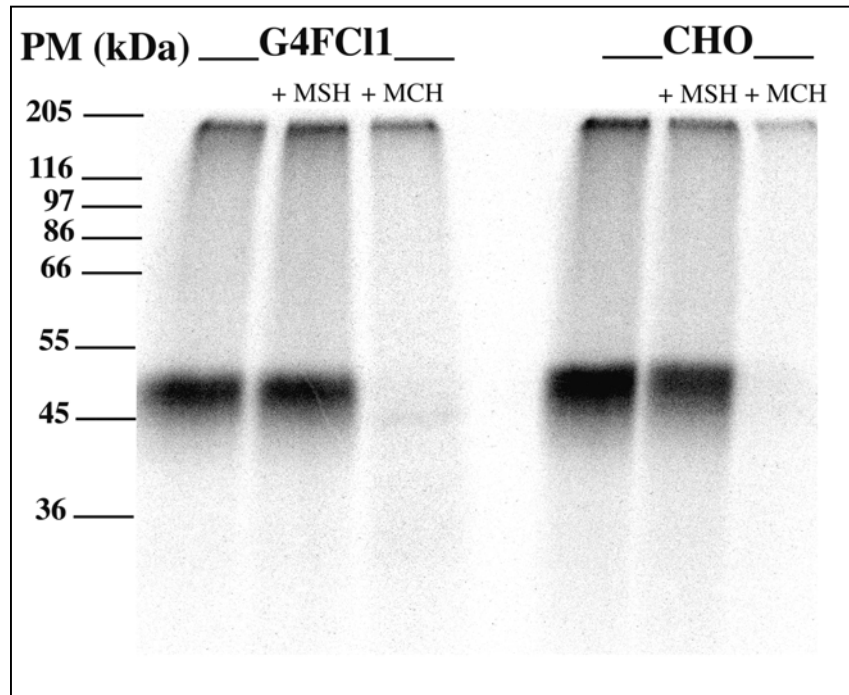


Figure 21. Autoradiography of ^{125}I -[DPhe¹³,Tyr¹⁹]-MCH cross-linking to mouse melanoma (G4F-C11) and Chinese ovary cells (CHO). Non-specific binding was obtained with addition of 1 μM MCH, 1 μM α -MSH were added as control for MCH specificity. This picture represents the data of one experiment.

3.2. Can the 50 kDa cross-linked band be isolated by two-dimensional electrophoresis?

3.2.1. Establishment of the technique with unlabeled proteins

G4F-C11 cells were subjected to either sodium lysis at 95°C for 5 min and at 4°C for 5 min in sodium lysis buffer (0.3% w/v SDS, 50 mM Tris pH 8.0, 200 mM DTT, 30 mM Na₄-Pyrophosphate, 50 mM Na-F, 200 μM Na-Orthovanadate, 5 mM Na-Molybdate) or instant urea lysis at room temperature (8 M urea, 4% w/v CHAPS, 40 mM Tris base, 2 mM PMSF). Isoelectric focussing took place in immobililine non-linear pH 3-10 strips. The strips were then equilibrated and proteins run on a 10% SDS-PAGE gel that was subsequently stained with colloidal coomassie G 250 and dried. Only the urea lysis allowed good G4F-C11 protein separation (Fig. 22).

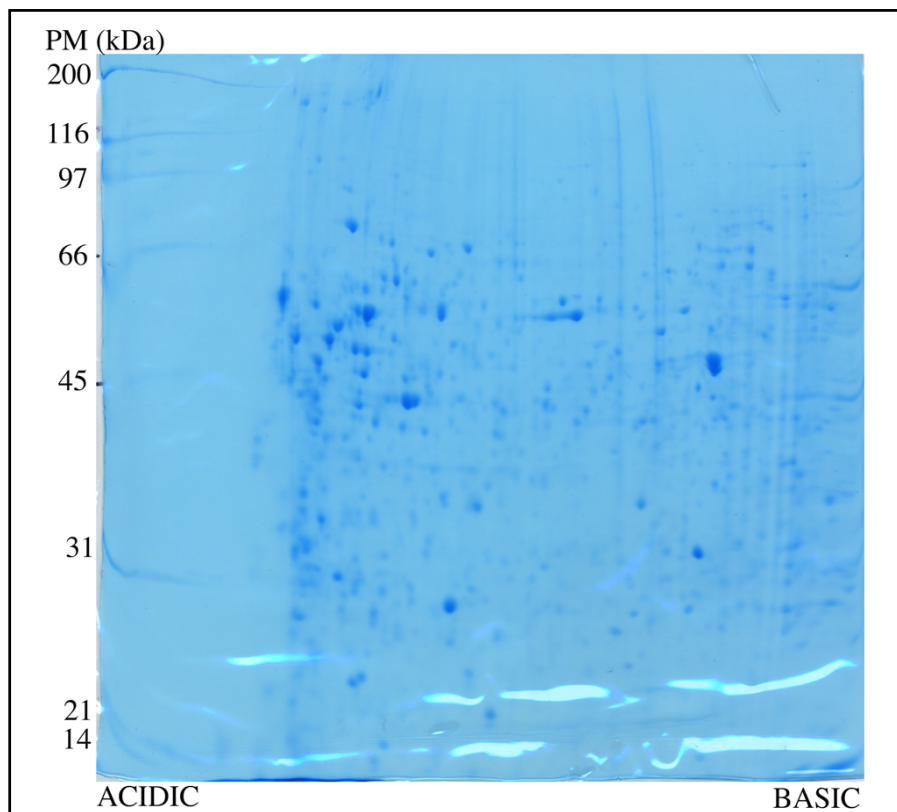


Figure 22. Two-dimensional gel electrophoresis of G4F-C11 proteins. 500 μg proteins were focussed according to their isoelectric point using Immobiline non-linear pH 3-10 strips for 80,900 volthours after desalting of sample on a NAP-5 gel filtration column. The strip was equilibrated and proteins run on a 10% SDS-PAGE gel that was subsequently stained with colloidal coomassie G250 and dried. This picture is representative of two experiments.

3.2.2. 2-D electrophoresis of radioligand cross-linked sample

2-D electrophoresis separation of ^{125}I -[DPhe¹³,Tyr¹⁹]-MCH cross-linked G4F-C11 proteins was performed, first with 500 μg proteins (Fig. 23), then with 5 mg proteins (Fig. 24). The separation of 500 μg proteins gave a strong signal after autoradiography, that was strongly attenuated by addition of 1 μM MCH into incubation medium (Fig. 23). However, the radioactive spot could not be assigned to a particular coomassie blue spot. Lack of coomassie signal was thought to be due to a low protein concentration, which is why a new cross-

linking experiment was performed with 30×10^6 cells (that resulted in a yield of 5 mg total proteins after desalting). The colloidal coomassie G 250 staining revealed some protein spots, but the autoradiography did not result in sufficient staining (Fig. 24).

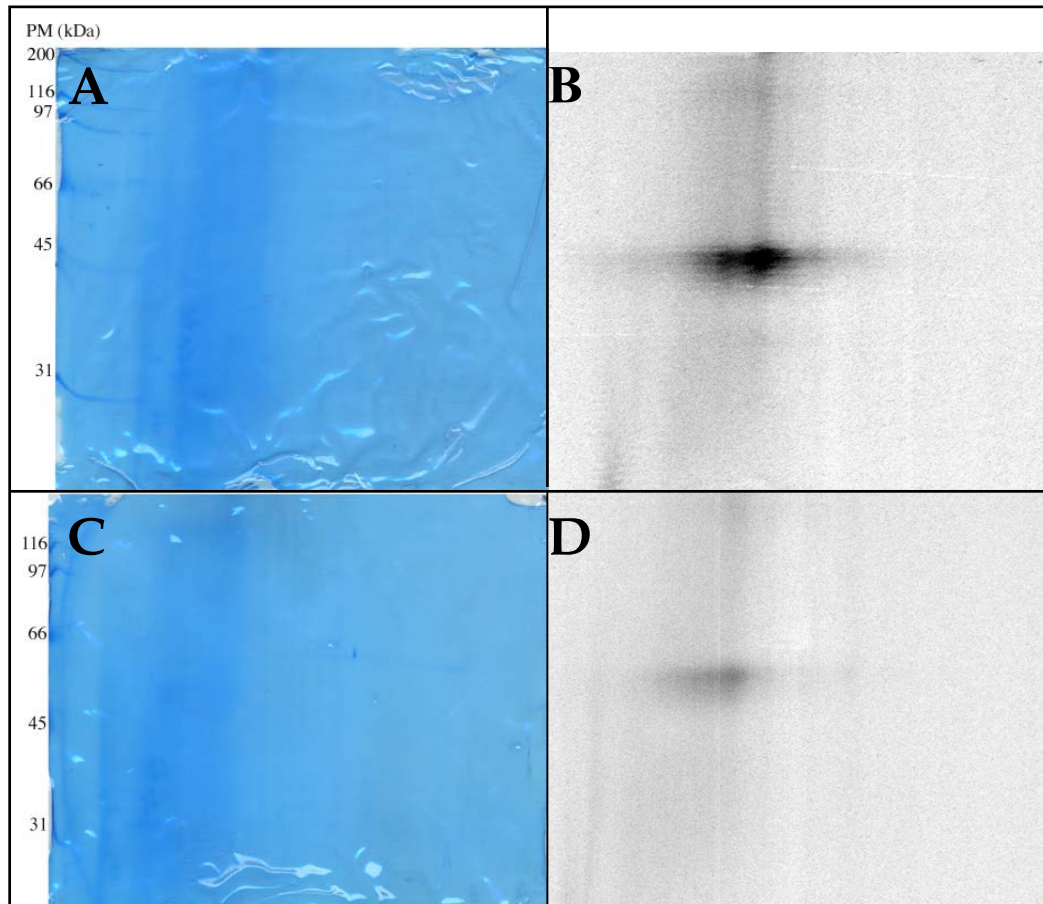


Figure 23. Two-dimensional gel electrophoresis of ^{125}I -[DPhe¹³, Tyr¹⁹]-MCH cross-linked G4F-C11 proteins. 500 μg cross-linked proteins were subjected to 2-D electrophoresis. (A,C), G250 coomassie stain of 2-D gels. (B,D), autoradiographies of gels. A & B, total cross-linking. C & D, non specific cross-linking (in presence of 1 μM MCH).

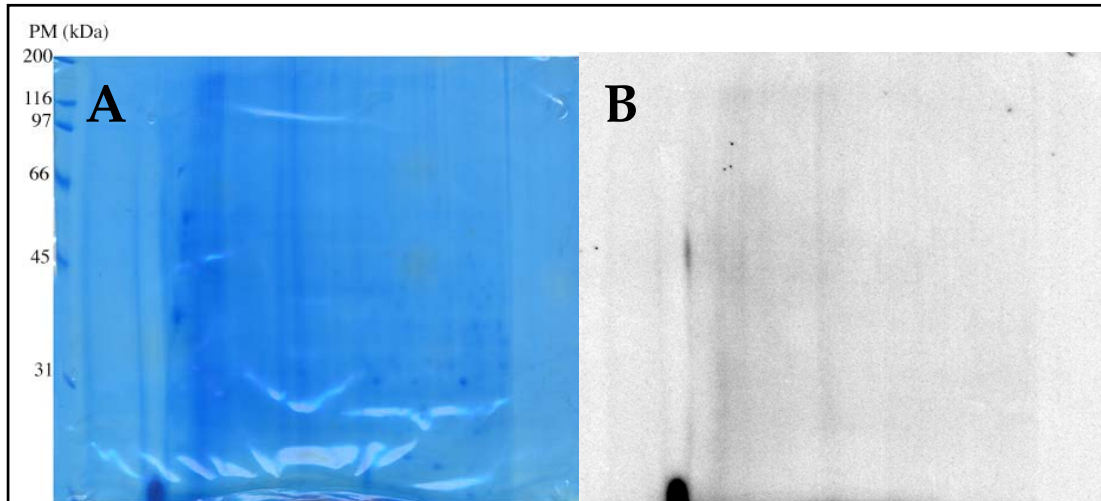


Figure 24. Two-dimensional gel electrophoresis of ^{125}I -[DPhe¹³,Tyr¹⁹]-MCH cross-linked G4F-C11 proteins. 5 mg cross-linked proteins were subjected to 2-D electrophoresis. (A) G250 coomassie stain of 2-D gel. (B) autoradiography of gel A.

3.3. Structure-activity of MCH derivatives on cells overexpressing rat MCH-R₁

3.3.1. Verification of transgene expression by RT-PCR and immunofluorescence

A stable rat MCH-R₁ expressing cell line was kindly provided to us by Dr. Yumiko Saito (Department of Pharmacology, University of California, Irvine). The human embryonic kidney cell line (HEK) expressing simian virus 40 large T antigen (HEK293-T) was transfected with N-terminus Flag-tagged GPR24, subcloned into pcDNA 3.1 neo (+) with EcoR1/Xho1, and among 24 tested clones, the #33 gave the best response for the bioactivity assay. During the rest of the manuscript, this cell line will be referred to as HEK #33.

a. Flag-rat MCH-R₁ mRNA production

Specific primers for Flag-rat MCH-R₁ were designed, the forward primer being complementary to FLAG sequence, the reverse primer being specific for both rat and human MCH-R₁. Primers for human MCH-R₁, MCH-R₂ and beta-actin were also designed to check endogenous expression of MCH receptors and to control cDNA and PCR quality. HEK non-transfected (i.e. wild type, WT) were tested as control cells as well as human cervix adenocarcinoma cell line HeLa.

RT-PCR analysis of these four genes is summarised in figure 25. Flag-rat MCH-R₁ was only detected in HEK #33 cells, starting from 25 PCR cycles. With 35 PCR cycles, endogenous MCH-R₁ and MCH-R₂ could be detected in all three cell lines.

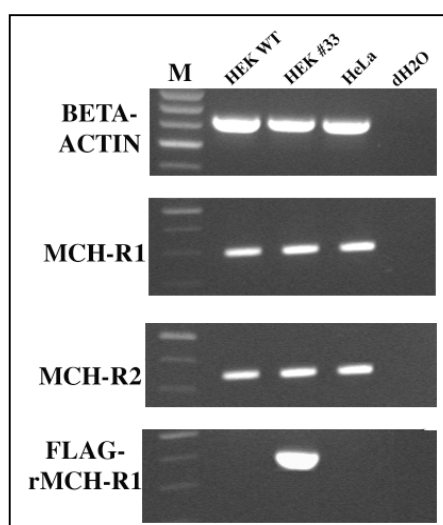


Figure 25. RT-PCR analysis of β -actin (25 PCR cycles), MCH-R₁, MCH-R₂ and Flag-rat MCH-R₁ (all with 50 PCR cycles) of HEK wild type (WT), HEK transfected with Flag-rat MCH-R₁ (#33), and HeLa cells. Negative control was obtained by replacing cDNA by dH₂O, photographs of ethidium bromide-stained agarose gels of PCR products are shown. The more intense band of 100 bp DNA ladder (M) is a 500 bp fragment. Similar results were obtained more than four times.

b. Expression and localisation of Flag-rat MCH-R₁

Immunofluorescence staining of HEK #33 cells with a mouse anti-Flag monoclonal antibody proved that the transgene protein was properly processed and located in the plasmic membrane (Fig. 26).

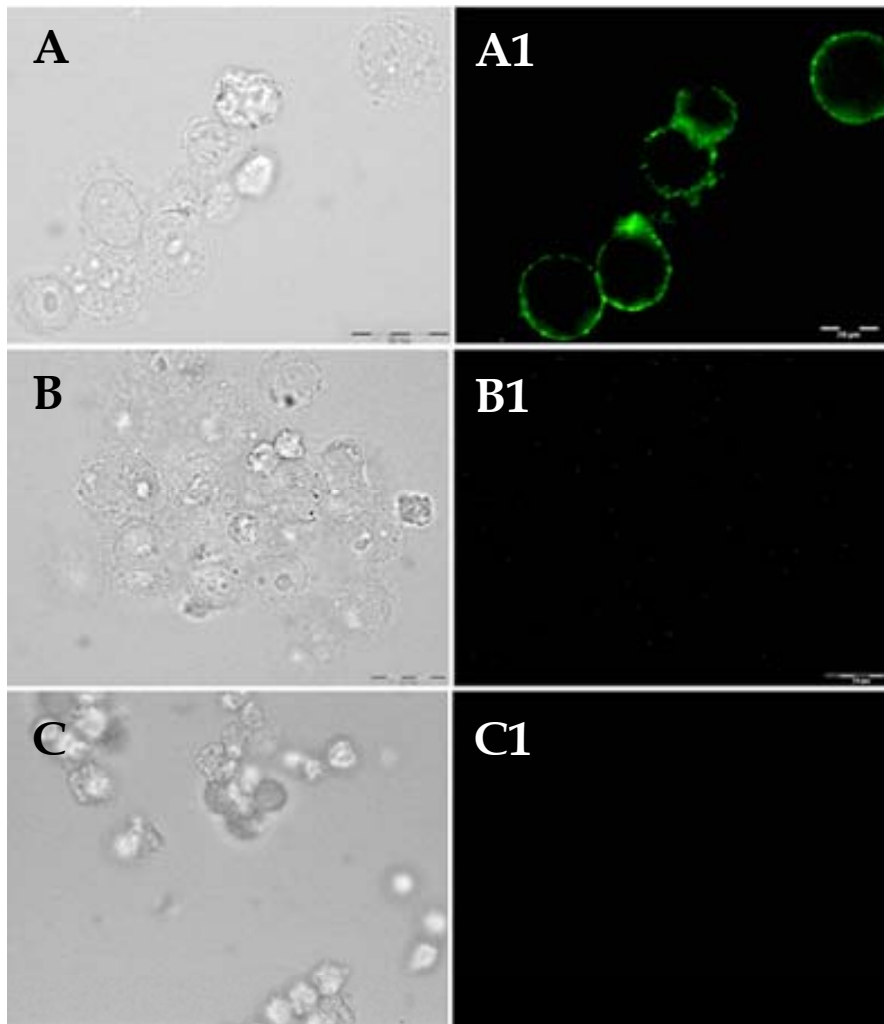


Figure 26. Flag-tagged rat MCH-R₁ visualisation on HEK wild type and #33. (A) immunostaining of HEK #33 with anti-Flag M2 antibody, 22 μ g/ml. (B) immunostaining of HEK #33 with a mouse isotype control monoclonal antibody, 22 μ g/ml. (C) immunostaining of HEK non-transfected with anti-Flag M2 antibody, 22 μ g/ml. The corresponding phase images are presented. *Scale bar, 20 μ m.* Pictures are representative of three experiments.

3.3.1. Binding assays

As early as May 1999, we had received from Dr. Y. Saito (Dr. O. Civelli's lab) Chinese ovary cells (CHO) transfected with rat MCH-R₁, the EC₅₀ of which in FLIPR assay with MCH was 18 nM. ¹²⁵I-[DPhe¹³, Tyr¹⁹]-MCH radioligand did not bind these cells satisfactorily at first, but after several attempts and changes in the incubation conditions (both temperature and time) we found an IC₅₀ of 38.90 ± 10.38 nM (n=3) with ¹²⁵I-[DPhe¹³, Tyr¹⁹]-MCH and its unlabeled counterpart as competitor.

But with the publication of the MCH-R₁, we learned that radioligand-binding studies showed saturable specific binding of [¹²⁵I]-MCH with subnanomolar affinity on MCH-R₁ expressing cells (K_d = 0.214 ± 0.017 nM) [36].

Dr. Y Saito also informed us in September 1999 that [DPhe¹³, Tyr¹⁹]-MCH was not able to elicit a calcium response in FLIPR assay using MCH-R₁ transfected cells. For these two reasons and also thanks to the commercial availability of MCH whereas [DPhe¹³, Tyr¹⁹]-MCH has to be synthesised de novo, we decided to use [¹²⁵I]-MCH as radioligand for future experiments.

Competition binding assays were performed with [¹²⁵I]-MCH and 12 MCH-derived peptides on Flag-rat MCH-R₁ expressed by HEK cells. The mean IC₅₀ of at least three experiments is listed in table 11. All D-enantiomers substituted peptides exhibit very low affinity to MCH-R₁ compared to their L-enantiomers counterparts (Fig. 27).

#	Compound	Sequence	Binding Assay
			IC ₅₀ (nM)
			Mean ± SEM
Amino-acid positions			
		1 3 5 * 9 11 13 15 * 17 19	
1	H/m/r MCH	Asp Phe Asp Met Leu Arg Cys Met Leu Gly Arg Val Tyr Arg Pro Cys Trp Gln Val	170.1 ± 64.8
2	salmon MCH	Asp Thr Met Arg Cys Met Val Gly Arg Val Tyr Arg Pro Cys Trp Gln Val	820.7 ± 115.9
3	linear MCH	Asp Phe Asp Met Leu Arg Cys Met Leu Gly Arg Val Tyr Arg Pro Cys Trp Gln Val	191.9 ± 38.8
4	[DPhe ¹³]-MCH	Asp Phe Asp Met Leu Arg Cys Met Leu Gly Arg Val D ^{Phe} Arg Pro Cys Trp Gln Val	1060
5	[Phe ¹³ ,Tyr ¹⁹]-MCH	Asp Phe Asp Met Leu Arg Cys Met Leu Gly Arg Val Phe Arg Pro Cys Trp Gln Tyr	243.3 ± 66.2
6	[DPhe ¹³ ,Tyr ¹⁹]-MCH	Asp Phe Asp Met Leu Arg Cys Met Leu Gly Arg Val D ^{Phe} Arg Pro Cys Trp Gln Tyr	1636.7 ± 366.3
7	[des1,2,Phe ¹³ ,Tyr ¹⁹]-MCH	Asp Met Leu Arg Cys Met Leu Gly Arg Val Phe Arg Pro Cys Trp Gln Tyr	160.6 ± 40.4
8	[Val ⁹ ,Phe ¹³ ,Glu ¹⁸ ,Tyr ¹⁹]-MCH	Asp Phe Asp Met Leu Arg Cys Met Val Gly Arg Val Phe Arg Pro Cys Trp Glu Tyr	148.2 ± 17.9
9	[Ser ^{4,6} ,DPhe ¹³ ,Tyr ¹⁹]-MCH	Asp Phe Asp Ser Leu Ser Cys Met Leu Gly Arg Val D ^{Phe} Arg Pro Cys Trp Gln Tyr	894.8 ± 48.2
10	[MetO ^{4,8} ,Phe ¹³ ,Tyr ¹⁹]-MCH	Asp Phe Asp Met ^O Leu Arg Cys Met ^O Leu Gly Arg Val Phe Arg Pro Cys Trp Gln Tyr	236.4 ± 132.7
11	[Ser ^{7,16}]-MCH	Asp Phe Asp Met Leu Arg Ser Met Leu Gly Arg Val Tyr Arg Pro Ser Trp Gln Val	nd
12	[Lys ¹⁹]-MCH	Asp Phe Asp Met Leu Arg Cys Met Leu Gly Arg Val Tyr Arg Pro Cys Trp Gln Lys	119.2 ± 97

Table 11. Binding affinities of MCH-derived peptides on HEK cells transfected with Flag-rat MCH-R₁. Binding affinity was accessed by [¹²⁵I]-MCH competition binding assay. Inhibitory concentration 50 (IC₅₀) is the peptide concentration inhibiting 50% of specific radioligand binding and was determined with GraphPad Prism software. * indicates the cysteines that are oxidised and form a disulfide bridge in all cases except for compound # 3.

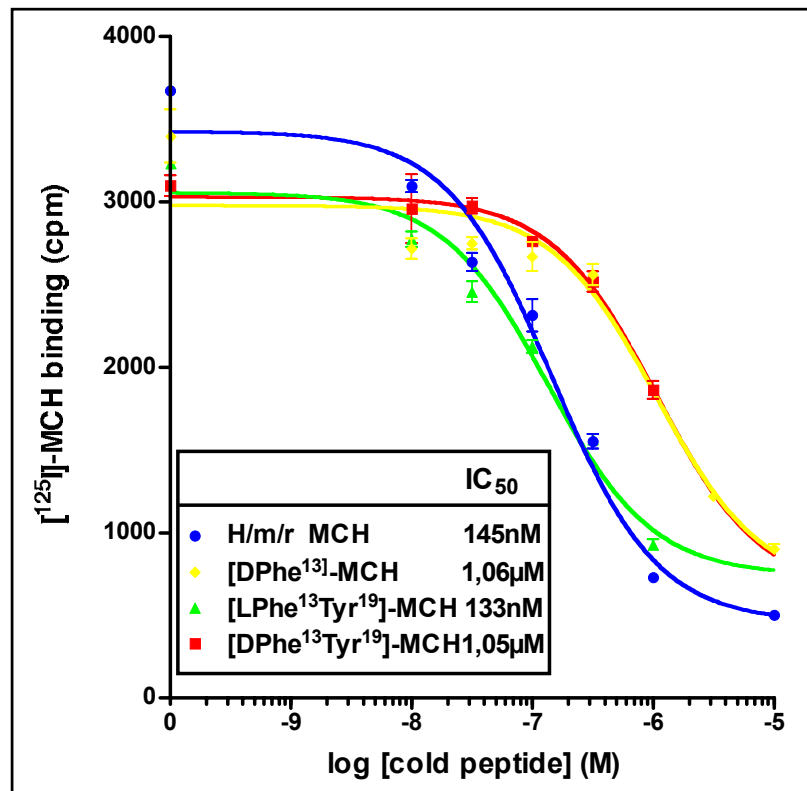


Figure 27. [¹²⁵I]-MCH competition binding assay of MCH-derived peptides on HEK cells transfected with Flag-rat MCH-R₁. Inhibitory concentration 50 (IC₅₀) is the peptide concentration inhibiting 50% of specific radioligand binding and was determined with GraphPad Prism software. Incubation conditions are 120 min at 10 °C. Data are representative of three experiments.

3.3.2. FLIPR assays

Fluorimetric imaging plate reader (FLIPR) assays were performed to monitor Ca^{++} efflux response in Flag-rat MCH-R₁ overexpressing cells (i.e. HEK #33) to stimulation with various peptides. HEK wild type (WT) were also assayed and did not respond to MCH (up to a 1 μM dose), but gave a robust signal upon CaCl_2 addition, our positive control (Fig. 28, lanes 1-4 and Fig. 29, panel A). HEK #33 responded to MCH in a dose dependent manner (Fig. 28, lanes 9-12), it is worth noticing that the 1,000 nM stimulation did not produce a greater response than the one obtained with a 100 nM stimulation (Fig. 29, panel B).

An extensive study of the 12 MCH-derived peptides was made and results summarised in table 12; dose-response curves are shown in figure 30. All peptides were tested at least three times. Four peptides (# 4, 6, 9, and 11) were unable to induce a calcium response in HEK #33 cells, these are D-enantiomers-containing derivatives and artificially linearised MCH (where the cysteines were replaced by serines). The compound # 3 that is a non-cyclised normal MCH peptide had an effect on the cells, which can be explained by spontaneous cyclisation after dissolution of the linear peptide.

An antagonist test was performed with non-agonist peptides # 6 and # 11 (Fig. 31), a 0.1 μM dose was unable to affect MCH potency on calcium response.

A linear regression analysis of both agonist potencies (EC_{50} obtained with the FLIPR assay) and ligand affinities (IC_{50} obtained with competition binding experiments) was performed by GraphPad Prism software (Fig. 32). In the case of 9 peptides (compounds # 1, 3, 4, 5, 6, 7, 8, 9 and 10) a correlation between these two parameters was possible, the correlation coefficient “r” equals 0.891 with a statistical relevance of $p=0.0001$.



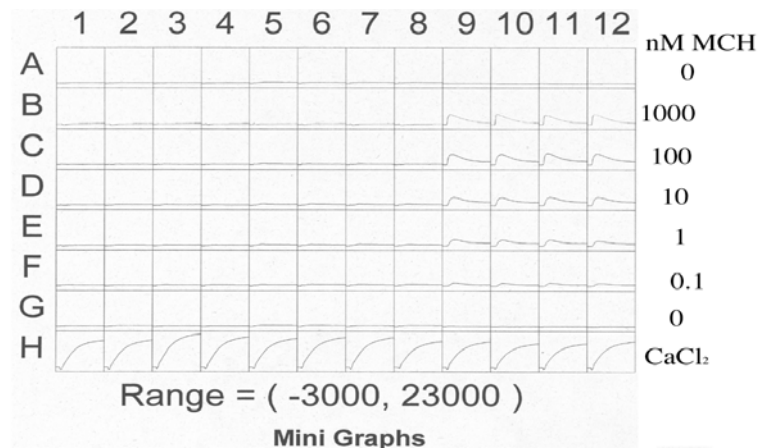


Figure 28. Calcium efflux measurement with fluorimetric imaging plate reader (FLIPR). HEK wild type (lanes 1-4) and HEK transfected with Flag-rat MCH-R₁ (lanes 9-12) were stimulated with CaCl₂ (positive control) and increasing concentrations of MCH.

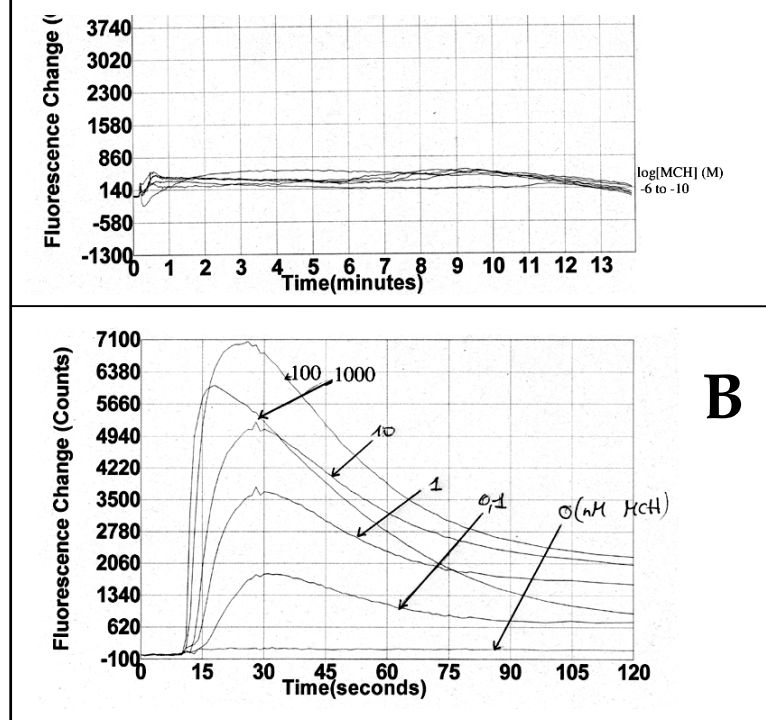


Figure 29. Calcium efflux measurement with fluorimetric imaging plate reader (FLIPR). HEK wild type (A) and HEK transfected with Flag-rat MCH-R₁ (B) were stimulated with increasing concentrations of MCH.

#	Compound	Sequence	FLIPR Assay
			EC ₅₀ (nM)
			Mean ± SEM
Amino-acid positions			
		1 3 5 * 9 11 13 15 * 17 19	
1	H/m/r MCH	Asp Phe Asp Met Leu Arg Cys Met Leu Gly Arg Val Tyr Arg Pro Cys Trp Gln Val	20 ± 4.1
2	salmon MCH	Asp Thr Met Arg Cys Met Val Gly Arg Val Tyr Arg Pro Cys Trp Gln Val	31.8 ± 12.4
3	linear MCH	Asp Phe Asp Met Leu Arg Cys Met Leu Gly Arg Val Tyr Arg Pro Cys Trp Gln Val	67.3 ± 9.9
4	[DPhe ¹³]-MCH	Asp Phe Asp Met Leu Arg Cys Met Leu Gly Arg Val ^D Phe Arg Pro Cys Trp Gln Val	>1000
5	[Phe ¹³ ,Tyr ¹⁹]-MCH	Asp Phe Asp Met Leu Arg Cys Met Leu Gly Arg Val Phe Arg Pro Cys Trp Gln Tyr	25.5 ± 1.4
6	[DPhe ¹³ ,Tyr ¹⁹]-MCH	Asp Phe Asp Met Leu Arg Cys Met Leu Gly Arg Val ^D Phe Arg Pro Cys Trp Gln Tyr	>1000
7	[des1,2,Phe ¹³ ,Tyr ¹⁹]-MCH	Asp Met Leu Arg Cys Met Leu Gly Arg Val Phe Arg Pro Cys Trp Gln Tyr	43.1 ± 7.9
8	[Val ⁹ ,Phe ¹³ ,Glu ¹⁸ ,Tyr ¹⁹]-MCH	Asp Phe Asp Met Leu Arg Cys Met Val Gly Arg Val Phe Arg Pro Cys Trp Glu Tyr	43.8 ± 15
9	[Ser ^{4,6} ,DPhe ¹³ ,Tyr ¹⁹]-MCH	Asp Phe Asp Ser Leu Ser Cys Met Leu Gly Arg Val ^D Phe Arg Pro Cys Trp Gln Tyr	>1000
10	[MetO ^{4,8} ,Phe ¹³ ,Tyr ¹⁹]-MCH	Asp Phe Asp ^{MetO} Leu Arg Cys ^{MetO} Leu Gly Arg Val Phe Arg Pro Cys Trp Gln Tyr	79.5 ± 17.5
11	[Ser ^{7,16}]-MCH	Asp Phe Asp Met Leu Arg Ser Met Leu Gly Arg Val Tyr Arg Pro Ser Trp Gln Val	>1000
12	[Lys ¹⁹]-MCH	Asp Phe Asp Met Leu Arg Cys Met Leu Gly Arg Val Tyr Arg Pro Cys Trp Gln Lys	73.6 ± 26.8

Table 12. Bioactivity of MCH-derived peptides on HEK cells transfected with Flag-rat MCH-R₁. *In vitro* potency was accessed by fluorimetric imaging plate reader (FLIPR) assay. Efficacy dose 50 (EC₅₀) is the peptide concentration producing 50% of maximum Ca⁺⁺ efflux, and was determined with GraphPad Prism software. * indicates the cysteines that are oxidised and form a disulfide bridge in all cases except for compound # 3.

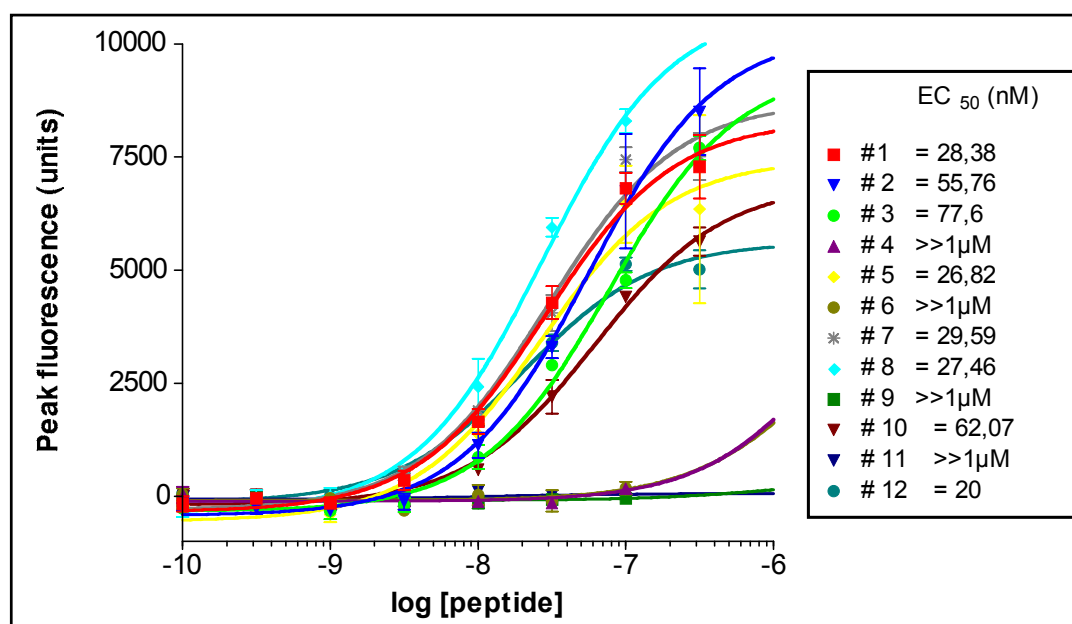


Figure 30. Dose-response curves of 12 peptides on HEK cells transfected with Flag-rat MCH-R₁. Agonist potency was accessed by fluorimetric imaging plate reader (FLIPR) assay and efficacy dose 50 (EC₅₀) determined with GraphPad Prism software. Incubation conditions are 120 min at 10°C.

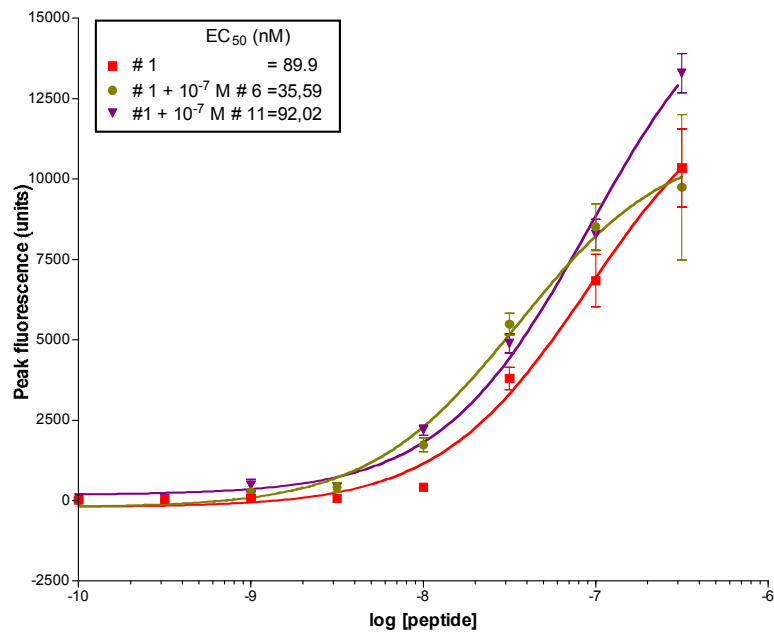


Figure 31. Dose-response curves of MCH (# 1) on HEK cells transfected with Flag-rat MCH-R₁ in presence of 10⁻⁷ M of peptides # 6 or # 11. Agonist potency was accessed by fluorimetric imaging plate reader (FLIPR) assay and efficacy dose 50 (EC₅₀) determined with GraphPad Prism software. Incubation conditions are 120 min at 10°C.

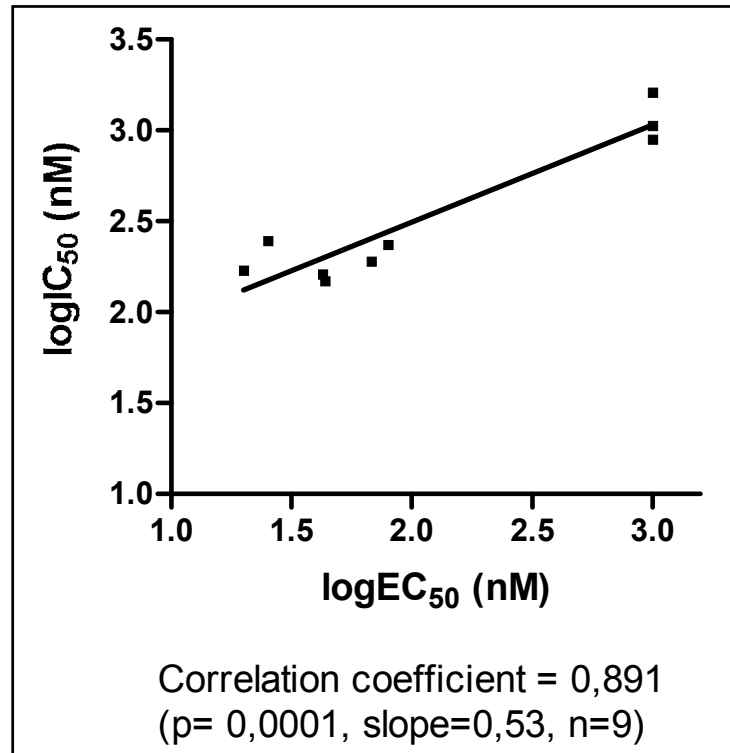


Figure 32. Correlation between agonist potencies and ligand affinities. Agonist potencies (EC_{50}) were determined with the fluorimetric imaging plate reader (FLIPR) assay and ligand affinities with [^{125}I]-MCH radioligand competition binding. Linear regression was performed with GraphPad Prism software.

3.3.4. Cross-linking assays

Cross-linking assay performed with [125 I]-MCH radioligand on HEK wild type (WT), HEK transfected with Flag-rat MCH-R₁ (#33) and HeLa cells allowed the detection of a 45-50 kDa specific band on SDS-PAGE autoradiography (Fig. 33, panel A). Cross-linking with plasmic membranes and internal vesicles was also performed (Fig. 34) and showed specific staining of a 50 kDa cross-linked site in both types of membranes.

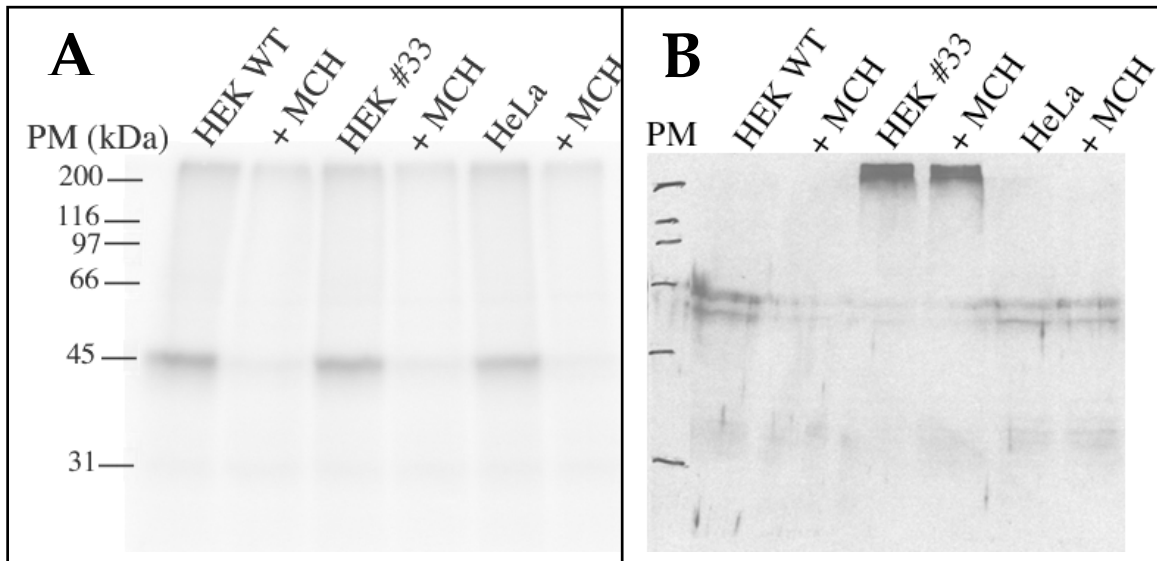


Figure 33. Cross-linking of [125 I]-MCH to HEK wild type (WT), HEK transfected with Flag-rat MCH-R₁ (#33) and HeLa cells. Non-specific binding was obtained by addition of 1 μ M MCH. (A) autoradiography of SDS-PAGE gel; (B) anti-Flag immunoblotting of cross-linked samples.

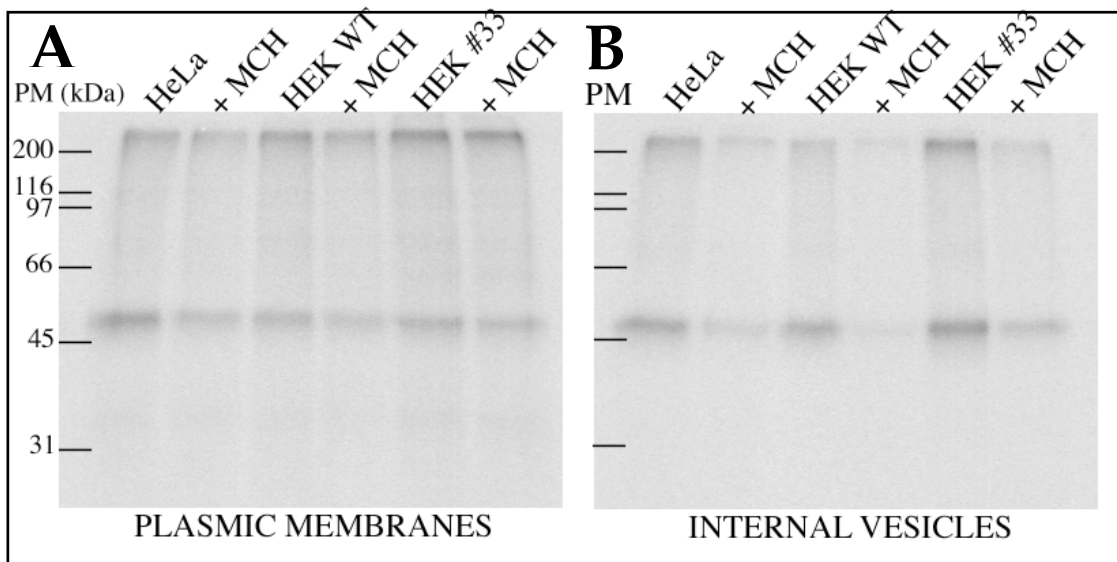


Figure 34. Cross-linking of [125 I]-MCH to HeLa cells, HEK wild type (WT) and HEK transfected with Flag-rat MCH-R₁ (#33). Non-specific binding was obtained by addition of 1 μ M MCH. (A) cross-linking was performed with plasmic membranes; (B) cross-linking was performed with internal vesicles.

3.3.5. Western blotting assay

Anti-Flag western blotting was performed on [¹²⁵I]-MCH cross-linked samples immobilised on nitro-cellulose membrane and Flag-rat MCH-R₁ was detected only in HEK #33 cells, in the form on a > 200 kDa band (Fig. 33, panel B).

3.4. The Kelly neuroblastoma cell line endogenously expresses MCH-R₁

3.4.1. RT-PCR for MCH, MCH-R₁ and -R₂

RT-PCR was performed with total RNA extracted from human embryonic kidney cells (HEK WT), human cervix adenocarcinoma cell line (HeLa), human neuroblastoma cell line (Kelly). Commercially available human brain total RNA was used as positive control for matching primers and polymerase enzyme efficiency. Negative control was obtained by replacing cDNA template by dH₂O. All PCRs were performed in a multiplex manner, as beta-actin amplification was concomitantly achieved. HEK WT and HeLa cells express both MCH-R₁ and -R₂ mRNA, and at a similar level (Fig. 35, panel A). MCH mRNA was not detected in these cells with 50 PCR cycles (Fig. 35, panel B). Kelly neuroblastoma cells express only MCH-R₁ mRNA, as MCH-R₂ mRNA was not detected with 60 PCR cycles (50 PCR cycles experiment in Fig. 35, panel C). MCH mRNA expression was at a similar level to the one found in the positive control (Fig. 35, panel B).

A quantification of the intensity of PCR-amplified fragments was performed with a digital imaging system on more than three independent experiments and the mean ± standard error of the mean (SEM) plotted (Fig. 36). It revealed that MCH-R₁ mRNA is 10 times more abundant in Kelly cells compared to the two non-neuronal control cell lines HEK and HeLa. Statistical interference of the data calculated a p value p < 0.0001.

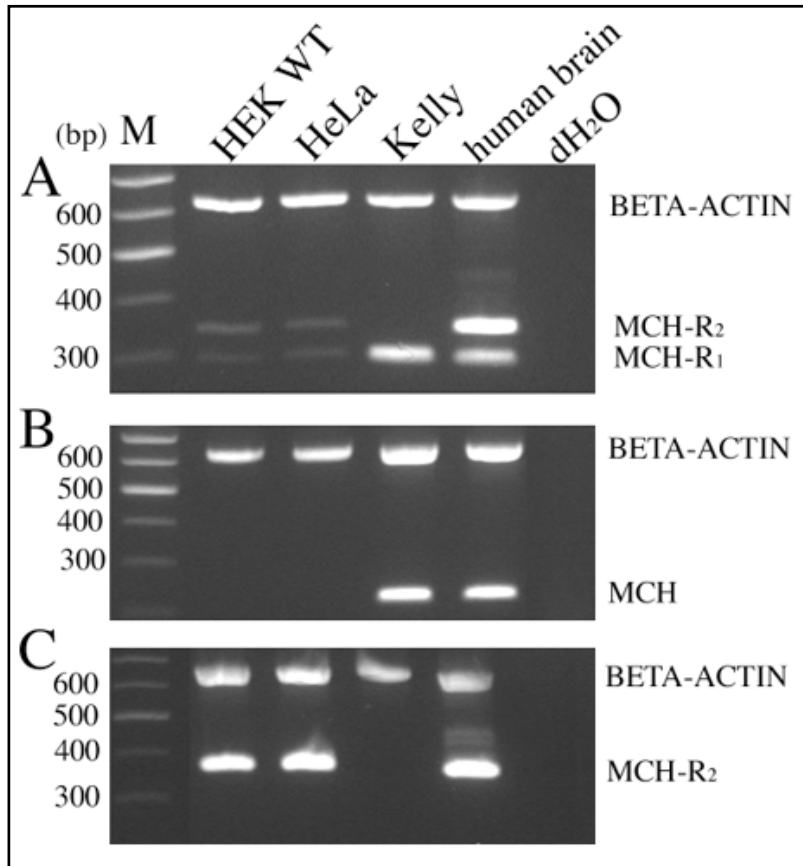


Figure 35. Semi-Quantitative RT-PCR analysis of beta-actin, MCH-R₁, MCH-R₂ and MCH in HEK wild type (WT), HeLa and Kelly cells. Positive control used human brain RNA as template, negative control was obtained by replacing cDNA by dH₂O, photographs of ethidium bromide stained agarose gels of PCR products are shown. (A) 40 PCR cycles; (B) and (C) 50 PCR cycles.

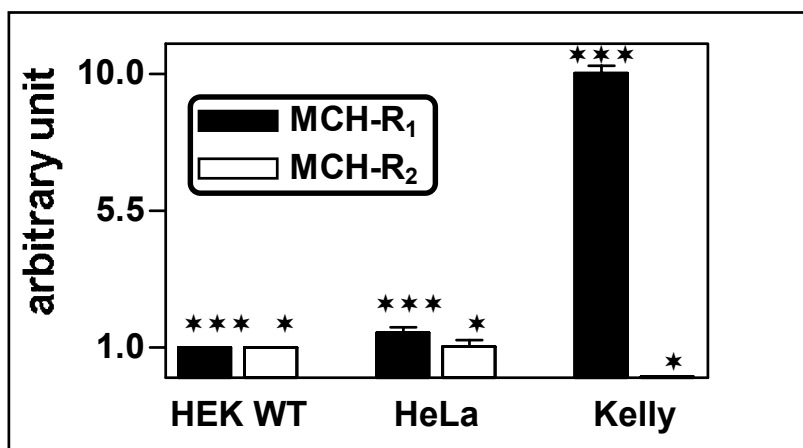


Figure 36. Quantification of the intensity of PCR-amplified fragments, standardised with beta-actin. Intensity quantification of bands was performed with a digital imaging system and results standardised with corresponding beta-actin value. The results are expressed as mean \pm SEM and statistical inference of the data determined by an analysis of variance (ANOVA).

***p < 0.001; * p < 0.01.

3.4.2. MCH-R₁ immunofluorescence staining

The anti-MCH-R₁ rabbit polyclonal antibody raised in our laboratory was used to perform immunostaining of permeabilized HEK wild type (WT), HEK transfected with rat-MCH-R₁ (HEK #33) and Kelly neuroblastoma cells (Fig. 37). A specific fluorescent signal was observed in both HEK #33 and Kelly cells, the background in HEK WT is similar to the one obtained with preimmune serum IgG. The staining in Kelly is localised on both plasmic and nuclear membranes.

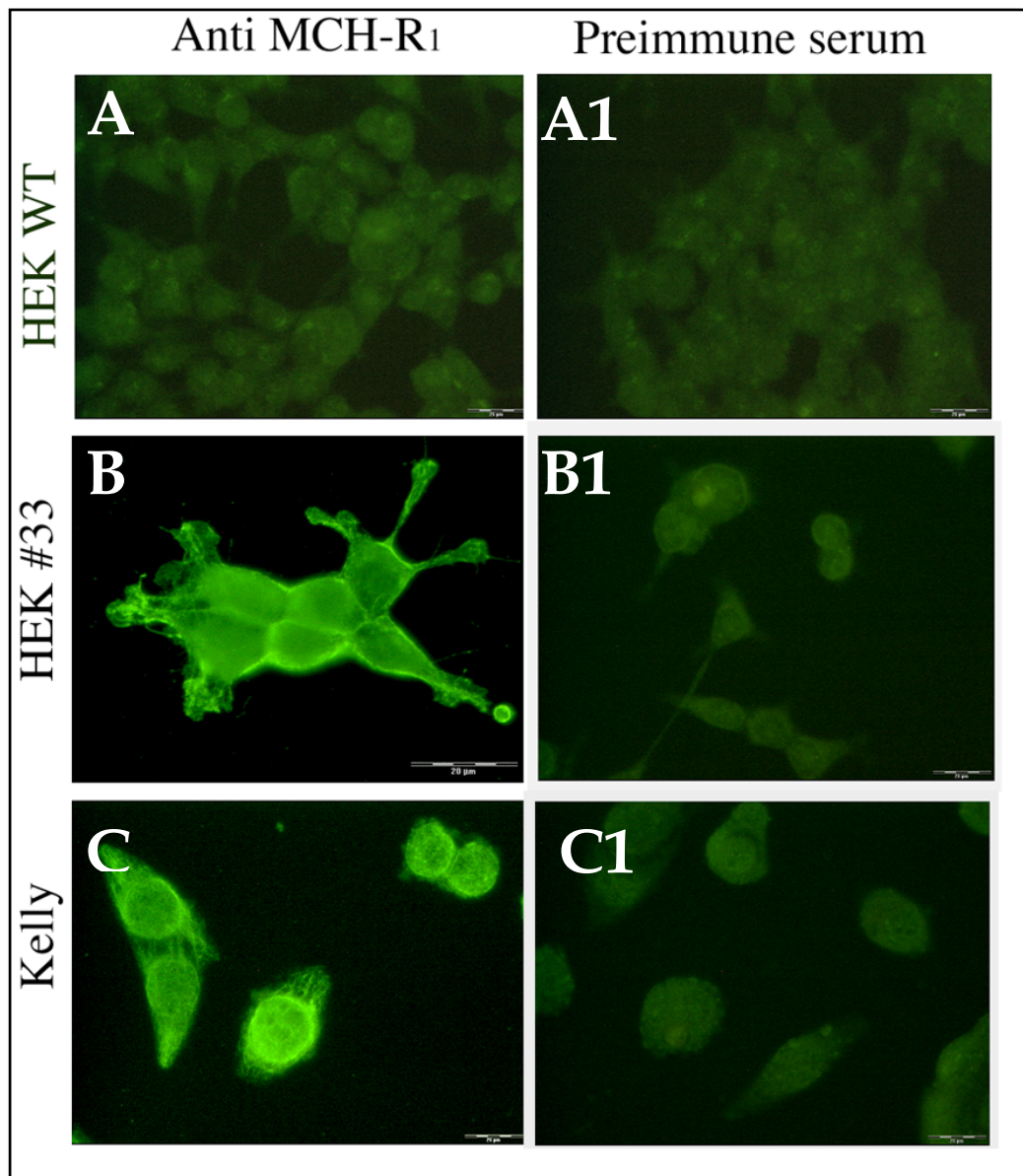


Figure 37. MCH-R₁ visualisation on HEK wild type (WT), HEK transfected with Flag-rat MCH-R₁ (#33) and Kelly cells. A, B, C, immunostaining with MCH-R₁ polyclonal rabbit IgG diluted 1:100. A1, B1, C1, immunostaining with preimmune serum IgG diluted 1:100. Scale bar, 20 μ m. Picture representative of five experiments.

3.4.3. Western blotting

Preliminary result using the anti-MCH-R₁ polyclonal rabbit antibody raised in our laboratory shows the labeling of a specific band migrating between the 45 and 66 kDa protein markers (Fig. 38). The \approx 200 kDa band is not specific as it also appears in the control lane, where preimmune IgG was incubated.

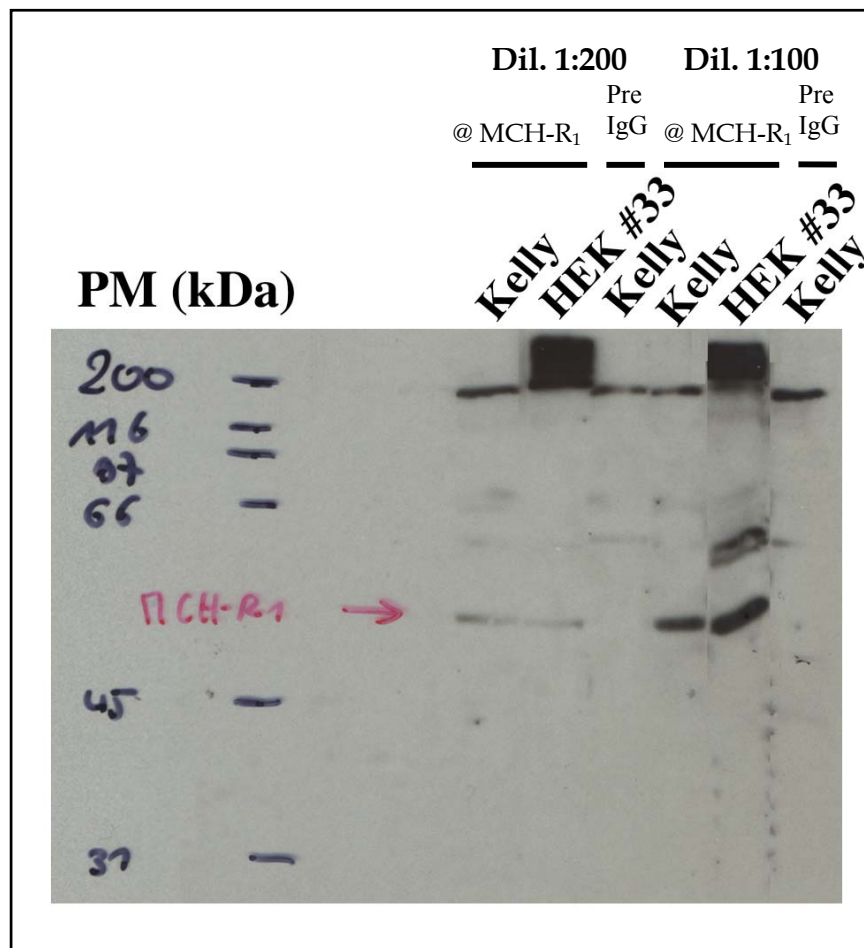


Figure 38. Western blotting of Kelly neuroblastoma and HEK #33 cells extracts. 120 μ g total proteins were loaded in each well, after electrotransfer and Ponceau S staining nitrocellulose membrane was cut into strips and western blotting procedure performed in BioRad mini incubation tray to minimise incubation volume (1ml per lane) in order to spare antibody. @ MCH-R₁, anti r/hMCH-R₁ rabbit polyclonal IgG. Pre IgG, preimmune serum IgG. Secondary antibody was a goat anti rabbit-peroxidase-conjugated (1:2000).

3.4.4. Competition assay with [¹²⁵I]-MCH

[¹²⁵I]-MCH competition binding assays with HEK wild type (WT), HEK transfected with rat-MCH-R₁ (HEK #33) and Kelly neuroblastoma cells showed that MCH had a good affinity for Kelly cells, comparable to the one obtained with HEK #33 (Fig. 39). It is worth noticing that there is slight binding of the radioligand to HEK WT.

Table 13: [¹²⁵I]-MCH competition assay data

Cell line	IC ₅₀ (nM) *	Specific binding (%) *
HEK WT (n=1)	240.5	46
HEK #33 (n=2)	48.8 ± 9.5	72.5 ± 1.5
Kelly (n=2)	76.08 ± 9.9	57.6 ± 5.6

* mean ± SEM in case of n ≥ 2

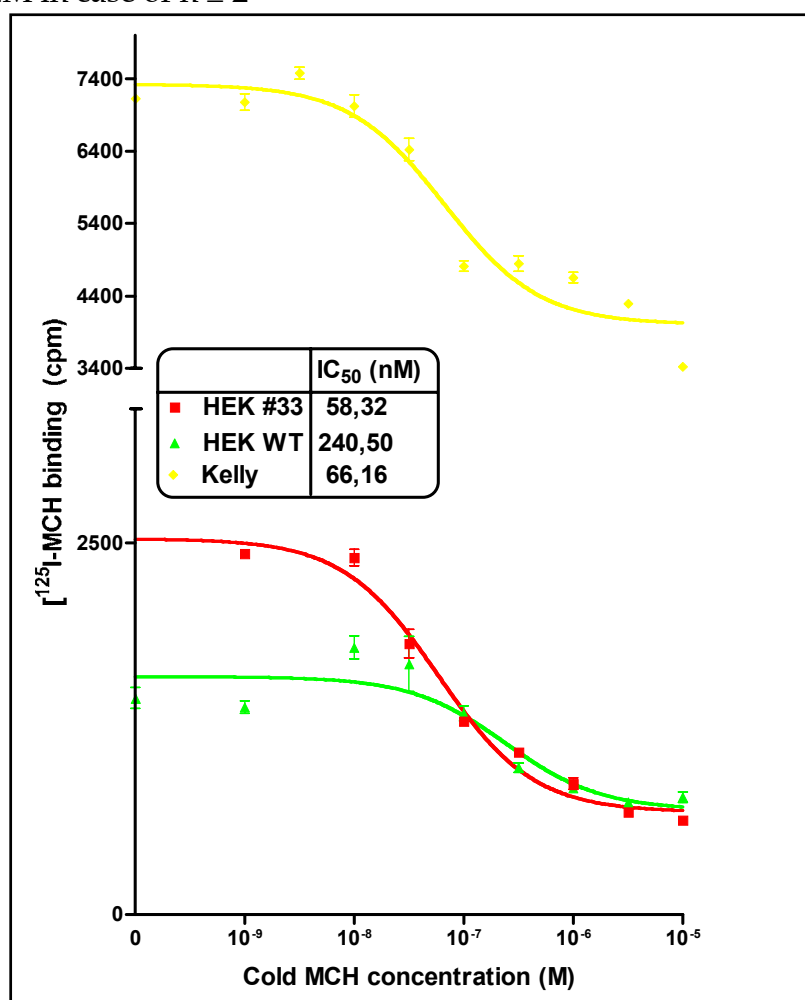


Figure 39. [¹²⁵I]-MCH competition binding assay on HEK wild type (WT), HEK transfected with Flag-rat MCH-R₁ (#33) and Kelly cells. Incubation conditions are 120 min at 20°C. Graph is representative of two experiments.

3.4.5. Cross-linking assay

[¹²⁵I]-MCH cross-linking to HEK wild type (WT), human cervix adenocarcinoma cell line (HeLa) and Kelly neuroblastoma cells allowed the detection of a 50 kDa band in all three cell lines after autoradiography of the SDS-PAGE (Fig. 40).

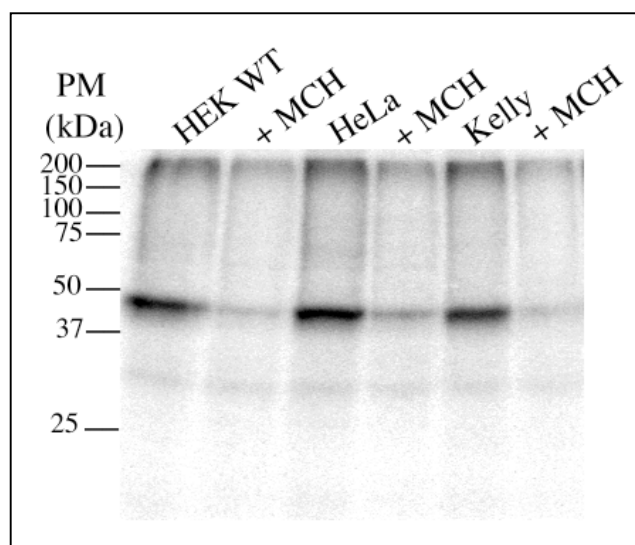


Figure 40. Autoradiography of [¹²⁵I]-MCH cross-linking to HEK wild type (WT), HeLa and Kelly cells. Non-specific binding was obtained by addition of 1 μM MCH. Picture representative of two experiments.

3.4.6. FLIPR assay

Fluorimetric imaging plate reader (FLIPR) assay performed with Kelly cells did not allow the detection of a Ca⁺⁺ signal after stimulation with MCH (Fig. 41). Even in presence of an inhibitor of dye extrusion by multiple drug-resistance pump, no signal could be observed (Fig. 41, panel B). The positive control with CaCl₂ proved that the Ca⁺⁺ system was present and functional in these cells.

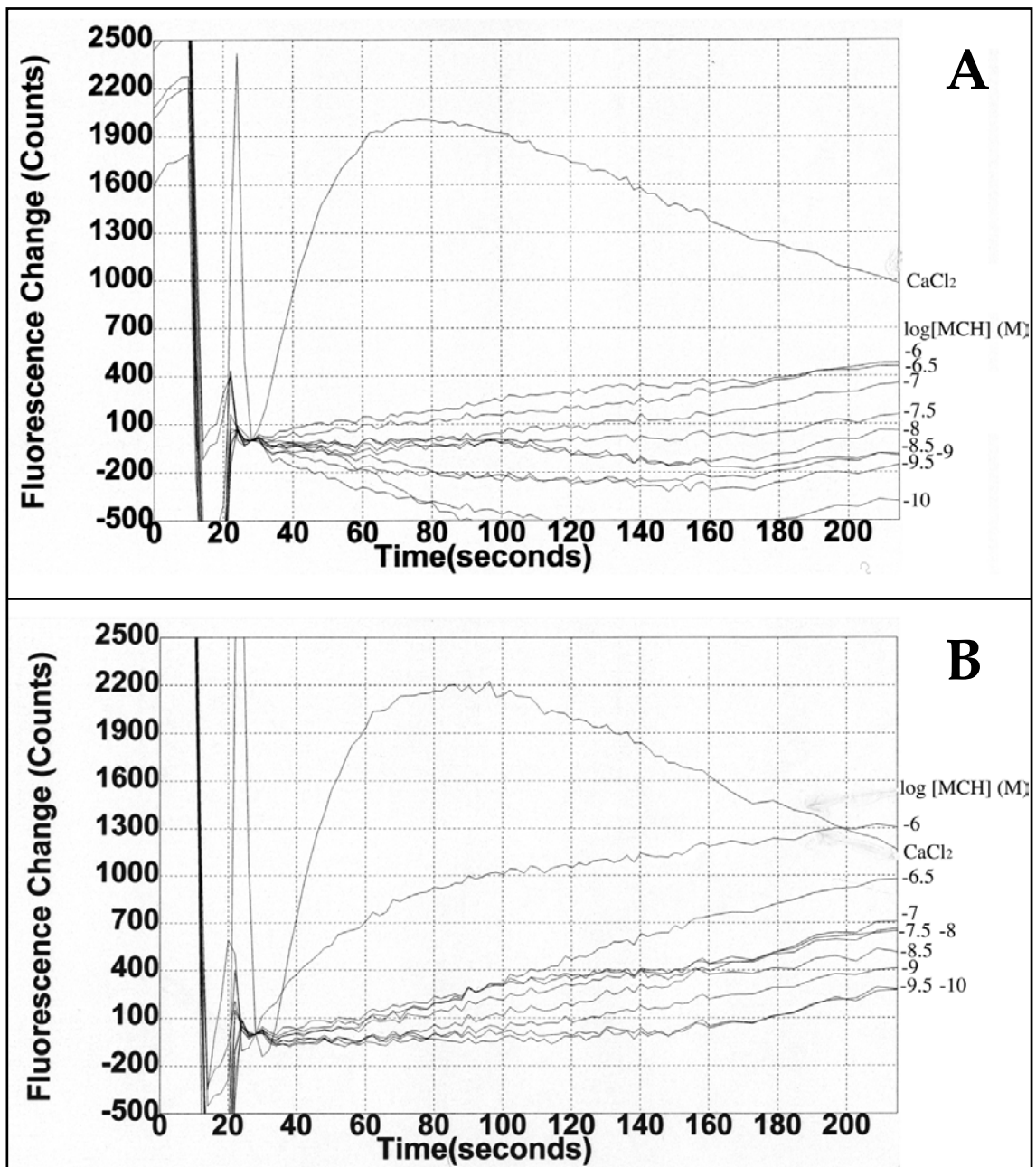


Figure 41. Calcium efflux measurement with fluorimetric imaging plate reader (FLIPR) assay. Kelly cells were stimulated with CaCl₂ (positive control) and increasing concentrations of MCH in absence (A) or presence (B) of an inhibitor of dye extrusion by multiple drug-resistance pump, (probenecid).

4. Discussion

4.1 Choice of the radioligand to find novel MCH binding sites

In autumn 1998, the obvious choice for the MCH radioligand was ^{125}I -[DPhe¹³, Tyr¹⁹]-MCH. This analogue was designed in our laboratory to circumvent the loss of activity of iodinated MCH (^{125}I -Tyr¹³-MCH). It has a D-phenylalanine at position 13, in place of the tyrosine, the D-enantiomer was added to make the radioligand more resistant against proteases, and incidentally abolishing non-specific binding due to ^{125}I -MCH hydrolysed fragments. The ^{125}I -bearing tyrosine replaces the C-terminal valine shifting the ^{125}I atom outside the ring structure formed by the disulfide bridge between cysteines 7 and 16.

This [DPhe¹³, Tyr¹⁹]-MCH radioligand allowed the identification of specific binding sites in the B16 mouse melanoma cells and in the G4F-Cl1 derived from them. The D enantiomer even showed a 7-fold higher binding potency than the L counterpart.

When the ^{125}I -[DPhe¹³, Tyr¹⁹]-MCH binding to G4F-Cl1 is taken the standard, it is not possible to find other cells or brain membranes exhibiting at least the same binding affinity. Human and mouse neuroblastoma cell lines, mouse brain tumour cells and porcine brain were devoid of ^{125}I -[DPhe¹³, Tyr¹⁹]-MCH specific binding.

This lack of specific binding can be explained by later findings, that showed that [DPhe¹³, Tyr¹⁹]-MCH does not bind MCH-R₁ (IC₅₀ = 1,636.7 ± 366.3 nM). Hence RT-PCR experiments performed after MCH-R₁ cloning showed that human neuroblastoma cell lines LAN-5 and Kelly expressed MCH-R₁ but not MCH-R₂, providing an explanation for lack of ^{125}I -[DPhe¹³, Tyr¹⁹]-MCH binding. This hypothesis is reinforced by competition binding experiments performed with ^{125}I -MCH that satisfactorily binds MCH-R₁ on Kelly cells, which gave an IC₅₀ not very much different from the one obtained with HEK transfected with rat MCH-R₁ (76.08 ± 9.9 compared to 48.8 ± 9.5 nM).

Mouse brain tumour or porcine brain cells were not examined for the presence of MCH-R₁ or -R₂ mRNA so no explanation for lack of ^{125}I -[DPhe¹³, Tyr¹⁹]-MCH binding can be given in this case.

On the other hand, even with the L-enantiomer radioligand, ^{125}I -[LPhe¹³, Tyr¹⁹]-MCH that displays good binding affinity and bioactivity for MCH-R₁, no significant specific binding could be obtained with human primary

melanocytes (W400, fig. 10), a cell line in which MCH-R₁ mRNA was detected by RT-PCR (C. Talke-Messerer, unpublished).

As positive control, ¹²⁵I-[LPhe¹³, Tyr¹⁹]-MCH was also used to perform binding assays with G4F-C11 and HEK #33 from which it could be specifically displaced by 1 μM MCH, confirming that it binds MCH-R₁.

Similarly rat embryonic primary hypothalamic neurons displayed a disappointing 40% specific binding with [¹²⁵I]-MCH, even though rat hypothalamus has been shown to be very rich in MCH-R₁ mRNA.

This result is supported by Audinot et al. [83], who report a specific binding of [¹²⁵I]-MCH to rat brain membranes representing only ≈ 30% of total binding. Their attempts to reduce the non-specific binding failed to succeed.

The difference between [¹²⁵I-DPhe¹³, Tyr¹⁹] and [¹²⁵I]-MCH binding is also present in experiments with the porcine brain membranes, [¹²⁵I-DPhe¹³, Tyr¹⁹] giving a higher overall binding than [¹²⁵I]-MCH (between 10,000 and 20,000 cpm for a total input of 200,000 cpm, fig. 12).

Considering cross-linking experiments, both [¹²⁵I]-MCH, [¹²⁵I-LPhe¹³, Tyr¹⁹]-MCH and [¹²⁵I-DPhe¹³, Tyr¹⁹]-MCH allowed the detection of a cross-linked SDS-PAGE band migrating between 45 and 50 kDa, in all cell lines tested. The positive signal found in HEK wild type can be explained by the presence of MCH-R₁ mRNA in these cells. The Chinese hamster ovary cell line as well as other neuroblastoma cell lines were not subjected to RT-PCR analysis.

4.2. Structure/activity of MCH derivatives on MCH-R₁ over-expressing cells

We performed an extensive structure-activity study of twelve MCH derivatives on rat MCH-R₁ expressed by HEK293-T cells (tables 11 and 12). According to their binding affinities and functional potencies the compounds can be classified in three groups:

Group I	Group II	Group III
# 1: h/m/r MCH	# 2: salmon MCH	# 4: [DPhe ¹³]-MCH
# 3: "linear" MCH	# 10: [MetO ^{4,8} , Phe ¹³ , Tyr ¹⁹]-MCH	# 6: [DPhe ¹³ , Tyr ¹⁹]-MCH
# 5: [Phe ¹³ , Tyr ¹⁹] MCH	# 12: [Lys ¹⁹]-MCH	# 9: [Ser ^{4,6} , DPhe ¹³ , Tyr ¹⁹]-MCH
# 7: [des1,2, Phe ¹³ , Tyr ¹⁹]-MCH		# 11: [Ser ^{7,16}]-MCH
# 8: [Val ⁹ , Phe ¹³ , Glu ¹⁸ , Tyr ¹⁹]-MCH		

Group I:

All the peptides of this group (# 1, 3, 5, 7, and 8) have approximately the same characteristics regarding MCH-R₁ as the native MCH peptide. The common factor in these peptides is the Tyr¹³ substitution by phenylalanine and Val¹⁹ by tyrosine. The tyrosine and phenylalanine have a very similar side chain with a phenol ring, it is thus not surprising that MCH properties were not changed. The other modifications lie in residues located outside the ring formed by the cysteines ^{7 and 16} (omission of the residues 1 and 2 in # 7, substitution of Gln¹⁸ by a glutamic acid in # 8), a part that is not necessary for ligand binding as Suply et al. showed that MCH₇₋₁₆ was the minimal sequence retaining potent biological activity (Fig. 1, lower right panel) [46].

The non-cyclic MCH (# 3) is not to be considered as truly linear as spontaneous cyclisation could very well occur when peptide was put into solution as it was treated in normal atmosphere and not under N₂. It is thus not surprising that the compound # 3 behaved almost like MCH.

Group II:

In this group, there are the two peptides with IC₅₀'s and EC₅₀'s that do not correlate well, # 2 and # 12.

Salmon MCH (# 2) has no high affinity for MCH-R₁ but has almost the same functional potency as MCH. Suply et al. report a 10-fold less affinity and potency of salmon MCH on rat MCH-R₁ when compared to MCH [46].

[Lys¹⁹]-MCH (# 12) on the contrary binds MCH-R₁ with a good affinity but has difficulties to induce a functional response.

IC₅₀ and EC₅₀ of compound # 10 correlate, as both binding affinity and functional potency are not optimal.

Group III:

The peptides of this group (# 4, 6, 9, and 11) are both inactive in the FLIPR assay and not able to compete with [¹²⁵I]-MCH in binding assays. The common feature between the three peptides # 4, 6, and 9 is the substitution of

tyrosine¹³ by a D-phenylalanine. The presence of a D-enantiomer in the vicinity of Arg¹¹ can explain this dramatic loss of activity. Indeed Macdonald et al. demonstrated that Arg¹¹ was a critical MCH residue involved in human MCH-R₁ binding and activation [61]. Arg¹¹ is postulated to bind to the receptor via (1) an ion pair between its terminal amino group and one of the carboxylate oxygens in the side chain of Asp¹²³ present in MCH-R₁ (N-H ↔ O=C) and (2) via a hydrogen bond between the Arg¹¹ Nε and the other carboxylate oxygen (C=NH₂⁺ ↔ ⁻O-C). By exchanging Arg¹¹ to D-Arg¹¹ only the ion pair would remain. It can very well be that the presence of D-Phe¹³ distorts the MCH structure thus preventing the interaction with Asp¹²³ of the receptor.

Peptide # 11, a linearised form of MCH, confirmed the need of the ring structure for receptor activation. The synthesis made in our laboratory did not provide enough peptide to perform a binding assay in addition to the three FLIPR assays but Suply et al. who also made a structure-activity study on rat MCH-R₁ found that the replacement of the two cysteines^{7 and 16} by serines led to a compound inactive in both receptor binding and functional assay [46].

They also demonstrated like us, that the less active peptides in the cAMP assay (functional assay) were also the less potent peptides in the [¹²⁵I]S36057 binding assay (correlation coefficient $r = 0.98$, $P < 0.0001$, $n = 10$).

4.3 The case of G4F-C11 mouse melanoma binding site

4.3.1. Binding site

A still unsolved point is the specific binding site for ¹²⁵I-[DPhe¹³, Tyr¹⁹] and ¹²⁵I-[LPhe¹³, Tyr¹⁹] present on B16-derived G4F-C11 mouse melanoma cell line. We and others have shown that the MCH-R₁ mRNA is not present in these cells.

One could hypothesise that this mouse melanoma cell line expresses MCH-R₂. It is not possible to check MCH-R₂ mRNA expression by RT-PCR, northern or southern blot, because the sequence of the mouse ortholog (if it exists) is not yet known.

It is more likely that melanoma cells bear a yet unidentified MCH-R subtype that migrates in SDS-PAGE as MCH-R₁ and -R₂ between 45 and 50 kDa protein markers (cross-linking data). This melanoma MCH-R does not seem to function through the pathways we have tested: MCH could not induce any decrease in adenylyl cyclase activity or mobilisation of intracellular calcium

in B16F1 cells. One explanation for it could be the genetic changes that occurred during the tumourigenic process. It has been reported that human melanocytes (non-transformed cells) were able to respond to MCH with an elevation of intracellular calcium.

4.3.2. Isolation of the \approx 50 kDa cross-linked band

The 2-dimensional SDS-PAGE separation of cross-linked samples has a drawback in that it relies on [^{125}I] which is a γ -emitter and thus radiates in three spatial directions giving a “diffuse” signal. The superposition of an autoradiography image with coomassie stained gel did not indicate a particular coomassie stained spot. It could be that the signal detected by autoradiography came from a protein not detected by coomassie stain. Indeed the two detection systems do not have the same threshold of detection, autoradiography being far more sensitive.

Another difficulty comes from the very constraining rules of sample preparation for mass spectrometry. There should be no salts in the sample, gels should be cut wet after a very time-consuming special coomassie stain. The sample can also not be radioactive so, after identification of the cross-linked spot on coomassie stained gel, one should have reproduced the cross-linking experiment without radioactivity and cut out the corresponding spot (if present!) on this gel. The minimum amount of detectable protein is also limiting, more than 5 mg total proteins should be loaded to have enough material in a single spot. These constraints were so difficult to maintain that we were not able to detect the radioactive spot on the autoradiograph after elution of the 5 mg sample on the desalting column.

4.4 Advantages of FLAGTM tag

Rat MCH-R₁ was transfected into HEK293-T cells together with the FLAGTM tag. This fusion tag consists of eight amino acids (Asp - Tyr - Lys - Asp - Asp - Asp - Asp - Lys). Due to its small size, the marker peptide can be encoded by a single synthetic oligonucleotide. The FlagTM tag is hydrophilic hence water-soluble and is likely to adopt a highly exposed conformation in the three-dimensional folding of the protein to which it is fused. This should facilitate detection by anti-FlagTM antibodies. FlagTM is also a potent immunogenic tag that allows the production of rabbit polyclonal antibodies quite easily. Furthermore, the FlagTM sequence contains the cleaving site of trypsinogen protease (Asp - Asp - Asp - Asp - Lys) which enables the removal of the tag by enterokinase treatment. The FlagTM peptide can equally be fused to either the N- or C-terminus of a given fusion protein.

We used some of these properties to:

- Check exogenous rat MCH-R₁ expression by RT-PCR, by designing the forward primer complementary to the FlagTM sequence. This could eliminate the risk of false positive PCR signal due to the detection of endogenous MCH-R₁ in HEK cells. It has to be remembered that rat and human MCH-R₁ orthologs share 96% amino acid identity.

- Check rat MCH-R₁ protein expression and processing by immunofluorescence staining. The anti-FlagTM M2 antibody stained with high specificity the protein present at the surface of HEK #33 cells. The big advantage was the epitope location at the N-terminal end on the seven-transmembrane receptor. This part is extracellular and thus accessible without permeabilising the cells. One can see the difference with permeabilised cells by looking at both figures 26 and 37. In figure 26, cells are intact and good plasmic membrane staining is to be seen whereas in figure 37 it is diffuse even if predominantly present at the plasma membrane.

- On the other hand, detection of FlagTM-rat MCH-R₁ by western blotting with the same anti-FlagTM M2 antibody did not bring about the expected result. The specific band seen after SDS-PAGE separation is > 200 kDa whereas the predicted size for MCH-R₁ is 56 kDa, suggesting that the receptor did not solubilise and stayed at the end of the stacking gel. This lack of solubilisation cannot be blamed on the FlagTM tag, as it is on the contrary hydrophilic in nature (net charge = -5), while the seven hydrophobic domains of the receptor are more likely to induce this insolubility in aqueous solution.

Preliminary western blot data obtained using our own MCH-R₁ antibody, also demonstrates the staining of a >200 kDa abundant band in the HEK #33 cell extract (Fig. 38).

Perhaps the HEK #33 cells are overburdened by the high number of Flag-rat-MCH-R₁ protein copies produced and are not able to process them properly to the plasma membrane. As MCH mRNA was not detectable in HEK cells, it is unlikely that HEK-released hormone induces a constant Flag-rat-MCH-R₁ internalisation, except if the foetal calf serum that supplements the culture medium contains MCH.

4.5. MCH-R₁ regulation by MCH or leptin

By performing [¹²⁵I]-MCH binding experiments on HEK-T cells expressing rat MCH-R₁ that were incubated for several hours in 200 nM MCH and then acid washed to remove externally bound peptide (Siegrist et al. [84]), we were not able to show a down- or an up-regulation of MCH-R₁ by its natural ligand (data not shown). One could explain such a result by the fact that rat MCH-R₁ is not in its physiological environment, and furthermore all promoter sequences governing MCH-R₁ expression are lacking in HEK #33. Indeed the MCH-R₁ cDNA sequence is located on a plasmid and not integrated in the genome in place of the endogenous MCH-R₁ receptor, as it would be if the transfection strategy would have used a retrovirus to “knock-in” MCH-R₁.

Nevertheless, it has been reported by others [42] that MCH *per se* had no obvious effect on MCH-R₁ expression in mice as MCH-R₁ mRNA levels in MCH knock-out animals and their wild type littermates did not differ.

On the other hand, leptin acts as a negative regulator of MCH-R₁ expression in the mouse brain: leptin deficiency induced by fasting or gene disruption in *ob/ob* mice leads to an up-regulation of MCH-R₁ and MCH expression. Exogenous leptin treatment of these mice (fasted or *ob/ob*) results in lowered MCH-R₁ expression levels. Finally, in *ob/ob* mice (that are leptin deficient), MCH-R₁ mRNA fails to rise with fasting indicating that MCH-R₁ mRNA regulation in mouse brain is due to leptin effects [42].

4.6. Presence of MCH-R₁ in Kelly human neuroblastoma cell line

We show MCH, MCH-R₁ but not MCH-R₂ mRNA expression in the Kelly human neuroblastoma cell line. Others have also reported MCH-R₁ expression in various human neuroblastoma cells of both cell line and tumour tissue origin [45].

Using our own anti MCH-R₁ polyclonal rabbit antibody, a plasma membrane and an intracellular signal was detected by immunofluorescence of cells fixed on a glass slide. The intracellular staining is consistent with the strong [¹²⁵I]-MCH cross-linked band obtained with internal membranes. Others also detected MCH-R₁ protein by western blot using an anti MCH-R₁ antibody produced in rabbit against two peptides corresponding to amino acids 80-110 and 159-180 of the protein. They labelled a 56 kDa band on both crude plasma

membrane and internal membrane fractions, but not on a cytosolic fraction prepared from rat adipocytes [19].

Preliminary data from a western blot experiment performed with our rabbit polyclonal antibody showed the labelling of a band migrating between 45 and 66 kDa (Fig. 38).

The intracellular localisation of MCH-R₁ in Kelly cells could explain the higher non-specific binding of [¹²⁵I]-MCH in these cells. It has thus been demonstrated that MCH radioligand can enter the cells thanks to its hydrophobicity [50]. It is possible that in Kelly cells MCH-R₁ is trapped in the nuclear membrane, neighbouring endoplasmic reticulum or Golgi apparatus. MCH release into culture medium was not assessed, but if the levels are significant this could explain this chronic MCH-R₁ internalisation.

We also showed that the Kelly cell line did not respond to MCH stimulation with an increase of intracellular Ca⁺⁺, in contrast to MCH-R₁ transfected cells. The human melanoma SK-MEL-37 that also expresses MCH-R₁, only couples to Gα_i/Gα_o (no elevation of Ca⁺⁺ levels could be elicited in these cells either) [48]. This would attach more importance to MCH-R₁ naturally expressing cells compared to transfected cell models, if the transfection of MCH-R₁ into HEK or CHO forces the receptor to couple artificially to Gα_q in addition to Gα_i and Gα_o.

4.7. MCH: a promising drug target for obesity and/or anorexia ?

4.7.1. Example of a neuropeptide administration that induced body fat loss in humans

The hypothalamus is the centre for the integration and control of feeding and satiety. The hypothalamic circuits that control food intake and energy expenditure are complex and involve a number of neuropeptides (Table 14).

Table 14: Orexigenic (stimulating food intake) and anorectic (decreasing food intake) hypothalamic neuropeptides implicated in the control of food intake and energy homeostasis (from [85]).

Orexigenic neuropeptides	Anorectic neuropeptides
Agouti-related protein (Agrp)	α melanocyte-stimulating hormone (α -MSH)
Neuropeptide Y (NPY)	Cocaine and amphetamine regulated transcript (CART)
Ghrelin	Glucagon-like peptide (GLP-1, GLP-2)
Melanin-concentrating Hormone (MCH)	oxyntomodulin
Endocannabinoids	

Melanocortins (among them α -MSH), produced by the proteolytic cleavage of the precursor molecule pro-opiomelanocortin (POMC) are anorectic peptides acting through melanocortin receptor 4 (MC₄). Agouti-related protein (Agrp) is an endogenous MC₄ antagonist. Mice lacking MC₄ are hyperphagic and very obese; mice lacking POMC (and consequently α -MSH) or overexpressing Agrp are also obese.

Obesity in humans has already been linked to POMC /melanocortin receptor mutations as inactivating mutations in the human POMC [86] and MC₄ [87] receptor have been identified in extremely obese children. 4% of heterozygous MC₄ receptor mutations were also reported in a large population of morbidly obese patients, which is a high frequency not found in controls [88].

Another correlation between animal models phenotypes and human physiology came with the following functional study [89]:

Twelve normal weight students (six men and six women with a mean body mass index of 21.98 ± 0.34 kg/m²) received 0.5 mg MSH/ACTH₄₋₁₀ (the core sequence of all melanocortins) intranasally twice daily during 6 weeks. Intranasal route of administration was chosen because it was shown that by these means the molecules could directly enter the cerebrospinal fluid compartment within about 60 minutes.

Compared with placebo, MSH/ACTH₄₋₁₀ reduced body fat by 1.68 kg and body weight by 0.79 kg on average. Plasma levels of leptin were decreased by 24% and insulin levels by 20%. It is important to know that the subjects studied were not aware of the real aim of the study and consequently did not change their nutritional habits nor paid more attention to their body weight. This finding may encourage the therapeutic use of melanocortin peptides in the control of adiposity in humans.

4.7.2. Tools to study MCH-MCH-R₁ axis in humans

So far MCH is the only orexigenic peptide whose depletion leads to leanness in mice, as a consequence of hypophagia and increased metabolic rate [30]. For example NPY^{-/-} mice have normal food intake and growth even if NPY is a very potent orexigenic peptide that also decreases energy expenditure and favours fat deposition [31]. All the results obtained with knockout and overexpressing mice suggest that MCH-MCH-R₁ axis is a central target of leptin action in the mammalian brain and may play a crucial role in feeding behaviour and energy balance. Although the pathophysiological roles of the MCH-MCH-R₁ axis in humans are still unknown, the blockade of this signal is an attractive pharmaceutical target for the treatment of obesity.

Takekawa et al. have already described an orally active MCH-R₁ antagonist, T-226296 (Fig. 42) [90]. This compound shows functional antagonistic activities in Chinese hamster ovary (CHO) cells expressing human MCH-R₁ and inhibits MCH-induced food intake in rats. T-226296 is specific for MCH-R₁ (IC₅₀ = 5.5 ± 0.12 nM) and does not display an appreciable affinity for receptors having a high degree of homology with MCH-R₁ (human MCH-R₂, SSTR₁₋₅, etc...) or other receptors involved in feeding behaviour such as: MC₃, MC₄, NPY₁. A 30 mg/kg oral dose of T-226296 given to rats one hour before the 5 µg MCH intracerebroventricular injection suppressed the MCH-stimulated food intake by more than 90%. T-226296 showed good oral bioavailability and brain permeability, suggesting that orally administered T-226296 directly antagonised MCH-R₁ in the rat brain and consequently suppressed food intake. To be certain that the anorectic effect is only mediated by MCH-R₁, the same experiment should be repeated in MCH-R₁ knockout mice. Nevertheless, the description of this MCH-R₁ specific antagonist provides a useful tool for exploring MCH-R₁ putative therapeutic possibilities.

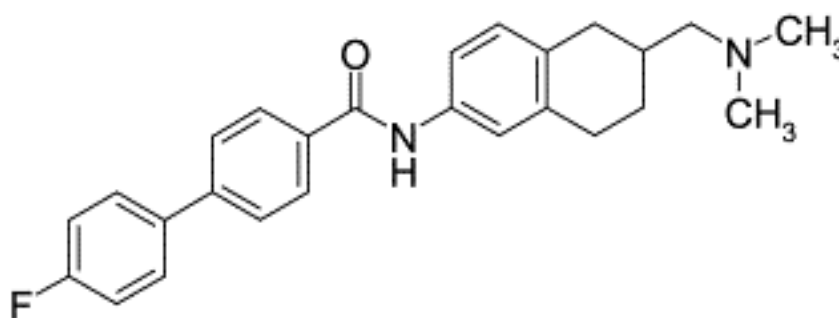


Figure 42. Chemical structure of T-226296.

Starting from a compound of agonist potency similar to that of the full length MCH at both receptors namely Ac-Arg⁶-cyclo(S-S)(Cys⁷-Met⁸-Leu⁹-Gly¹⁰-Arg¹¹-Val¹²-Tyr¹³-Arg¹⁴-Pro¹⁵-Cys¹⁶)-NH₂ (Fig. 1, upper right panel) [91], Bednarek et al. synthesised and tested analogues containing 5-aminovaleric acid (Ava) in positions 9 and 10 or 14 and 15 [92]. They found among others, a fully competitive MCH-R₁ antagonist (IC₅₀ = 14 nM, K_B = 0.9 nM) with more than 1,000-fold selectivity over MCH-R₂, namely Gva⁶-cyclo(S-S)(Cys⁷-Met⁸-Leu⁹-Gly¹⁰-Arg¹¹-Val¹²-Tyr¹³-Ava^{14,15}-Cys¹⁶)-NH₂, (Gva = 5-Guanidinovaleric acid). These peptides could be useful in the evaluation of the physiological role of human MCH-R₁ in vivo.

Another interesting tool was reported recently: a selective, high potency peptide agonist of MCH action at human MCH-R₁ (hMCH-R₁) [93]. This agonist which shows more than 200-fold selectivity with respect to human MCH-R₂ (hMCH-R₂) has the following sequence: Ac-D-Arg⁶-cyclo(S-S)(Cys⁷-Met⁸-Leu⁹-Asn¹⁰-Arg¹¹-Val¹²-Tyr¹³-Arg¹⁴-Pro¹⁵-Cys¹⁶)-NH₂. This compound if converted to an orally active MCH-R₁ agonist could be a useful therapeutic tool for anorexia.

5. Conclusion and perspectives

5.1 Conclusion

Along with the experiments performed in the course of this thesis, we confirmed the “sticky” nature of MCH and its radioligand [^{125}I]-MCH. Even in tissues expressing MCH-R₁ and -R₂ (rat brain, rat hypothalamic neurons), non-specific binding of [^{125}I]-MCH was considerable (60 to 95% of the radioligand could not be displaced by 5 μM MCH in the binding assay with rat hypothalamic neurons). When pipeting [^{125}I]-MCH, one tenth of the radioactivity sucked up stayed in the pipet tip, siliconised tips helped reduce this loss without totally abolishing it.

Due to technical limitations and lack of intracellular response in G4F-C11 mouse melanoma cells, we were not able to identify or clone the MCH binding site detected by binding and cross-linking experiments.

We confirmed the lack of binding of [DPhe¹³, Tyr¹⁹]-MCH to MCH-R₁ with the experiments carried out on Kelly cells (no binding was observed with [^{125}I -DPhe¹³, Tyr¹⁹]-MCH whereas an IC₅₀ of 76.08 ± 9.9 nM was determined with [^{125}I]-MCH). The structure-activity study also revealed that all D-phenylalanine¹³-containing analogues were devoid of activity.

Moreover, with [^{125}I]-MCH we were able to correlate the EC₅₀'s and the IC₅₀'s of nine MCH analogues on the HEK #33 cellular model of MCH-R₁ ectopic expression. For these nine compounds a weaker biological response correlates with a decreased binding affinity.

The characterisation of the human Kelly neuroblastoma cell line provides a good model for the brain MCH system. Besides their human origin, which makes them very attractive for pharmacological studies, these cells mimic some populations of neurons of the CNS as they express the neuropeptide MCH as well as MCH-R₁. One still do not know if this receptor is functional in these cells as no calcium response could be monitored by FLIPR, but it is likely that they behave like the SK-MEL-37 human melanoma cells and do not couple to G α_q .

In conclusion, we demonstrated in this thesis that the choice of the radioligand was of greatest importance, as well as the detection of a bioactivity in the cellular model studied. Even if the G4F-C11 binding site is still

unidentified, the discovery that Kelly cells express MCH-R₁ and MCH is a major step forward for studying the role of MCH in physiological and disease states.

5.2 Perspectives (proposal for future experiments)

5.2.1. With the Kelly human neuroblastoma cell line

Having found a putatively good model for an endogenous MCH-R₁-expressing cell line devoid of MCH-R₂ expression, namely the human neuroblastoma Kelly cell line, one could use this cell line to study:

- The regulation of MCH-R₁ expression under different physiological situations (leptin, insulin or glucose levels mimicking a disease such as diabetes, obesity).
- The effect of newly developed MCH-based anti-obesity drugs on receptor expression.

5.2.2. With MCH-R₁ and -R₂ coding sequences

To study fundamental functioning of former orphan GPCR_s, one often needs to manipulate their cDNA and make the receptors to be expressed by host cell lines. The reason is that the receptor cDNA sequence is known before any self-expressing cell line, and as long as no antibody to detect the receptor is available, one needs to introduce a tag (Myc, Flag) in front of the coding sequence to detect the receptor by western blot or flow cytometry. Some experiments and the information they could yield are listed below:

a. Incellular localisation of MCH-R₁ and -R₂

Western blotting of preparations of crude subcellular fractions of MCH-R₁ or -R₂ expressing cells could enable the localisation of these receptor proteins into the intracellular compartments. Differential centrifugation in sucrose-containing medium can separate:

- Nuclear pellet: nuclei, mitochondria.

- Heavy mitochondrial pellet: principally mitochondria together with few contaminants (lysosomes, peroxisomes, Golgi membranes).
- Light mitochondrial pellet: mitochondria, lysosomes, peroxisomes, Golgi membranes and some endoplasmic reticulum.
- Microsomal pellet: membranes vesicles

It is also possible to fractionate major organelles i.e. Golgi membranes, lysosomes, mitochondria and peroxisomes form a light mitochondrial fraction in a self-generated gradient.

Next, one should solubilise proteins present in the different fractions, subject them to a SDS-PAGE separation and perform western blotting to detect MCH-R₁ and -R₂, and quantify the proportion of receptor present in each sub-cellular compartment.

b. Study of intracellular dynamics of MCH-R₁ and -R₂

- With a fluorescent-labelled MCH, intracellular MCH-R₁ and -R₂ trafficking could be monitored directly under a fluorescence microscope [94].
- With a flow cytometry assay, surface receptors could be labelled with fluorescent antibodies, which in turn would be measured using a flow cytometer. The antibodies could recognise the Flag epitope engineered onto the N-terminus of the GPCR (thus accessible extracellularly).
- One could also examine the putative agonist-induced degradation of Flag-MCH-R₁ expressed in HEK 293-T cells.

c. Study of MCH-R₁ and -R₂ homo- or heterodimerisation (as for somatostatin receptors, glutamate receptor)

In recent years there has been an increasing number of reports describing G protein-coupled receptor (GPCR) homo- and heterodimerisation. Some even speculate that this phenomenon is of greatest importance, as it would induce different second messenger responses depending on the type of interaction. Therefore the same ligand signal could induce different cellular responses depending on the receptor subtypes that are present on the cell surface and on how these receptors dimerise.

The following techniques could be used to demonstrate the existence of GPCR dimers in living cells:

- Bioluminescence resonance energy transfer (BRET) [95]

This newly developed biophysical method examines protein-protein interaction. It has already been used to elegantly demonstrate the existence of GPCR dimers in intact cells (β_2 -adrenoreceptor).

- Fluorescence resonance energy transfer (FRET) [95]

This technique is related to BRET, it measures the Foster resonance energy transfer between two fluorophores that emit fluorescence at non-overlapping wave lengths.

- Photobleaching FRET (pbFRET) [95]

In this FRET-related method, antisera conjugated to two different fluorophores (fluorescein and rhodamine) are used to bind the receptor.

- Co-immunoprecipitation and western blot [96]

Epitope-tagged receptors (c-Myc, Flag™) are co-expressed in HEK293 cells at a 1:1 ratio (checked by quantitative western blot analysis). Cells are or are not treated with the agonist, with reducing reagents or cross-linking agents. Cell lysates are then prepared and subjected to immunoprecipitation. Regular 6% SDS-polyacrylamide gel containing 0.1% is then performed, followed by electroblotting and western blotting.

d. Mapping of the [125 I]-MCH contact point on MCH-R₁ and -R₂

One could use photoreactive MCH analogs containing a *p*-benzoyl-L-phenylalanine (Bpa) in a position where it does not interfere with the binding affinity, to covalently label MCH-R₁ or -R₂. Targeted enzymatic and chemical fragmentation of the photoaffinity labelled receptor could identify a domain specifically labelled by the photoreactive analogue [97].

5.2.3. With the G4F-C11 mouse melanoma cells

To identify the 45-50 kDa binding site labelled with [125 I]-MCH on G4F-C11 cells, one could try to trap it in an affinity column coated with MCH. G4F-C11 cells extracts should first be prepared, then passed through the affinity column and the retained proteins eluted with NaCl 5M or MCH itself. The next step would be to prepare the sample so that it is compatible for mass spectrometry analysis (remove the salts, ions, metals). If the mass found does not correspond to any previously characterised mouse protein, one should sequence a part of the protein and use it to screen mouse protein data bases. As the mouse genome is not yet complete, the protein data base is not likely to contain the isolated protein either.

To monitor MCH functional activity on the melanoma cell receptor, one could examine G₀ linked signaling pathways as only Ca⁺⁺ and cAMP responses have been studied so far and not protein kinase C (PKC) or MAP kinase activation.

6. References

1. Knigge KM, Baxter-Grillo D, Speciale J and Wagner J, Melanotropic peptides in the mammalian brain: the melanin-concentrating hormone. *Peptides* **17**(6): 1063-73, 1996.
2. Rance T and Baker BI, The teleost melanin-concentrating hormone: a pituitary hormone of hypothalamic origin. *Gen Comp Endocrinol* **37**(1): 64-73., 1979.
3. Baker BI, Eberle AN, Baumann JB, Siegrist W and Girard J, Effect of melanin concentrating hormone on pigment and adrenal cells in vitro. *Peptides* **6**(6): 1125-30., 1985.
4. Griffond B and Baker BI, Cell and molecular cell biology of melanin-concentrating hormone. *Int Rev Cytol* **213**: 233-77, 2002.
5. Kawauchi H, Kawazoe I, Tsubokawa M, Kishida M and Baker BI, Characterization of melanin-concentrating hormone in chum salmon pituitaries. *Nature* **305**(5932): 321-3, 1983.
6. Nahon JL, The melanin-concentrating hormone: from the peptide to the gene. *Crit Rev Neurobiol* **8**(4): 221-62, 1994.
7. Viale A, Zhixing Y, Breton C, Pedoutour F, Coquerel A, Jordan D and Nahon JL, The melanin-concentrating hormone gene in human: flanking region analysis, fine chromosome mapping, and tissue-specific expression. *Brain Res Mol Brain Res* **46**(1-2): 243-55, 1997.
8. Parkes D and Vale W, Secretion of melanin-concentrating hormone and neuropeptide-EI from cultured rat hypothalamic cells. *Endocrinology* **131**(4): 1826-31, 1992.
9. Qu D, Ludwig DS, Gammeltoft S, Piper M, Pellemounter MA, Cullen MJ, Mathes WF, Przypek R, Kanarek R and Maratos-Flier E, A role for melanin-concentrating hormone in the central regulation of feeding behaviour. *Nature* **380**(6571): 243-7, 1996.
10. Tritos NA and Maratos-Flier E, Two important systems in energy homeostasis: melanocortins and melanin-concentrating hormone. *Neuropeptides* **33**(5): 339-49, 1999.
11. Jezova D, Bartanusz V, Westergren I, Johansson BB, Rivier J, Vale W and Rivier C, Rat melanin-concentrating hormone stimulates adrenocorticotropin secretion: evidence for a site of action in brain regions protected by the blood-brain barrier. *Endocrinology* **130**(2): 1024-9., 1992.
12. Hervieu G, Volant K, Grishina O, Descroix-Vagne M and Nahon JL, Similarities in cellular expression and functions of melanin-concentrating hormone and atrial natriuretic factor in the rat digestive tract. *Endocrinology* **137**(2): 561-71., 1996.

13. Parkes DG and Vale WW, Contrasting actions of melanin-concentrating hormone and neuropeptide-E- I on posterior pituitary function. *Ann N Y Acad Sci* **680**: 588-90., 1993.
14. Miller CL, Hruby VJ, Matsunaga TO and Bickford PC, Alpha-MSH and MCH are functional antagonists in a CNS auditory gating paradigm. *Peptides* **14**(3): 431-40., 1993.

15. Gonzalez MI, Kalia V, Hole DR and Wilson CA, alpha-Melanocyte-stimulating hormone (alpha-MSH) and melanin-concentrating hormone (MCH) modify monoaminergic levels in the preoptic area of the rat. *Peptides* **18**(3): 387-92, 1997.
16. Gonzalez MI, Vaziri S and Wilson CA, Behavioral effects of alpha-MSH and MCH after central administration in the female rat. *Peptides* **17**(1): 171-7, 1996.
17. Sanchez M, Baker BI and Celis M, Melanin-concentrating hormone (MCH) antagonizes the effects of alpha-MSH and neuropeptide E-I on grooming and locomotor activities in the rat. *Peptides* **18**(3): 393-6, 1997.
18. Tadayyon M, Welters HJ, Haynes AC, Cluderay JE and Hervieu G, Expression of melanin-concentrating hormone receptors in insulin-producing cells: MCH stimulates insulin release in RINm5F and CRI-G1 cell-lines [In Process Citation]. *Biochem Biophys Res Commun* **275**(2): 709-12, 2000.
19. Bradley RL, Kokkotou EG, Maratos-Flier E and Cheatham B, Melanin-concentrating hormone regulates leptin synthesis and secretion in rat adipocytes. *Diabetes* **49**(7): 1073-7, 2000.
20. Kennedy AR, Todd JF, Stanley SA, Abbott CR, Small CJ, Ghatei MA and Bloom SR, Melanin-concentrating hormone (MCH) suppresses thyroid stimulating hormone (TSH) release, in vivo and in vitro, via the hypothalamus and the pituitary. *Endocrinology* **142**(7): 3265-8., 2001.
21. Bayer L, Mairet-Coello G, Risold PY and Griffond B, Orexin/hypocretin neurons: chemical phenotype and possible interactions with melanin-concentrating hormone neurons. *Regul Pept* **104**(1-3): 33-39., 2002.
22. Monzon ME, de Souza MM, Izquierdo LA, Izquierdo I, Barros DM and de Barioglio SR, Melanin-concentrating hormone (MCH) modifies memory retention in rats. *Peptides* **20**(12): 1517-9, 1999.
23. Murray JF, Mercer JG, Adan RA, Datta JJ, Aldairy C, Moar KM, Baker BI, Stock MJ and Wilson CA, The effect of leptin on luteinizing hormone release is exerted in the zona incerta and mediated by melanin-concentrating hormone. *J Neuroendocrinol* **12**(11): 1133-9, 2000.
24. Knigge KM and Wagner JE, Melanin-concentrating hormone (MCH) involvement in pentylenetetrazole (PTZ)-induced seizure in rat and guinea pig. *Peptides* **18**(7): 1095-7, 1997.
25. Monzon ME, Varas MM and De Barioglio SR, Anxiogenesis induced by nitric oxide synthase inhibition and anxiolytic effect of melanin-concentrating hormone (MCH) in rat brain. *Peptides* **22**(7): 1043-7., 2001.
26. Baker BI, Melanin-concentrating hormone updated functional considerations. *TEM* **5**(3): 120-6, 1994.
27. Ludwig DS, Mountjoy KG, Tatro JB, Gillette JA, Frederick RC, Flier JS and Maratos-Flier E, Melanin-concentrating hormone: a functional melanocortin antagonist in the hypothalamus. *Am J Physiol* **274**(4 Pt 1): E627-33, 1998.

28. Hoogduijn, M.J., Ancans, J., and Thody, A.J. Melanin-concentrating hormone may act as a paracrine inhibitor of melanogenesis. British Society for Investigative Dermatology, annual meeting. Warwick, 9-11 April 2001. Abstracts. *Br J Dermatol* **144**(3): 668-669, 2001.
29. Bluet-Pajot MT, Presse F, Voko Z, Hoeger C, Mounier F, Epelbaum J and Nahon JL, Neuropeptide-E-I antagonizes the action of melanin-concentrating hormone on stress-induced release of adrenocorticotropin in the rat. *J Neuroendocrinol* **7**(4): 297-303, 1995.
30. Shimada M, Tritos NA, Lowell BB, Flier JS and Maratos-Flier E, Mice lacking melanin-concentrating hormone are hypophagic and lean. *Nature* **396**(6712): 670-4, 1998.
31. Beck B, KO's and organisation of peptidergic feeding behavior mechanisms. *Neurosci Biobehav Rev* **25**(2): 143-58, 2001.
32. Ludwig DS, Tritos NA, Mastaitis JW, Kulkarni R, Kokkotou E, Elmquist J, Lowell B, Flier JS and Maratos-Flier E, Melanin-concentrating hormone overexpression in transgenic mice leads to obesity and insulin resistance. *J Clin Invest* **107**(3): 379-386, 2001.
33. Civelli O, Nothacker HP, Bourson A, Ardati A, Monsma F and Reinscheid R, Orphan receptors and their natural ligands. *J Recept Signal Transduct Res* **17**(1-3): 545-50., 1997.
34. Kolakowski LF, Jr., Jung BP, Nguyen T, Johnson MP, Lynch KR, Cheng R, Heng HH, George SR and O'Dowd BF, Characterization of a human gene related to genes encoding somatostatin receptors. *FEBS Lett* **398**(2-3): 253-8, 1996.
35. Lakaye B, Minet A, Zorzi W and Grisar T, Cloning of the rat brain cDNA encoding for the SLC-1 G protein-coupled receptor reveals the presence of an intron in the gene. *Biochim Biophys Acta* **1401**(2): 216-20, 1998.
36. Chambers J, Ames RS, Bergsma D, Muir A, Fitzgerald LR, Hervieu G, Dytko GM, Foley JJ, Martin J, Liu WS, Park J, Ellis C, Ganguly S, Konchar S, Cluderay J, Leslie R, Wilson S and Sarau HM, Melanin-concentrating hormone is the cognate ligand for the orphan G- protein-coupled receptor SLC-1. *Nature* **400**(6741): 261-5, 1999.
37. Saito Y, Nothacker HP, Wang Z, Lin SH, Leslie F and Civelli O, Molecular characterization of the melanin-concentrating-hormone receptor. *Nature* **400**(6741): 265-9, 1999.
38. Lembo PM, Grazzini E, Cao J, Hubatsch DA, Pelletier M, Hoffert C, St-Onge S, Pou C, Labrecque J, Groblewski T, O'Donnell D, Payza K, Ahmad S and Walker P, The receptor for the orexigenic peptide melanin-concentrating hormone is a G-protein-coupled receptor. *Nat Cell Biol* **1**(5): 267-71, 1999.
39. Shimomura Y, Mori M, Sugo T, Ishibashi Y, Abe M, Kurokawa T, Onda H, Nishimura O, Sumino Y and Fujino M, Isolation and identification of melanin-concentrating hormone as the endogenous ligand of the SLC-1 receptor. *Biochem Biophys Res Commun* **261**(3): 622-6, 1999.

40. Bachner D, Kreienkamp H, Weise C, Buck F and Richter D, Identification of melanin concentrating hormone (MCH) as the natural ligand for the orphan somatostatin-like receptor 1 (SLC-1). *FEBS Lett* **457**(3): 522-4, 1999.
41. Saito Y, Nothacker HP and Civelli O, Melanin-concentrating Hormone receptor: an orphan receptor fits the key. *TEM* **11**(8): 299-303, 2000.
42. Kokkotou EG, Tritos NA, Mastaitis JW, Sliker L and Maratos-Flier E, Melanin-concentrating hormone receptor is a target of leptin action in the mouse brain. *Endocrinology* **142**(2): 680-6, 2001.
43. Saito Y, Cheng M, Leslie FM and Civelli O, Expression of the melanin-concentrating hormone (MCH) receptor mRNA in the rat brain. *J Comp Neurol* **435**(1): 26-40, 2001.
44. Mori M, Harada M, Terao Y, Sugo T, Watanabe T, Shimomura Y, Abe M, Shintani Y, Onda H, Nishimura O and Fujino M, Cloning of a novel G protein-coupled receptor, slt, a subtype of the melanin-concentrating hormone receptor. *Biochem Biophys Res Commun* **283**(5): 1013-8., 2001.
45. Takahashi K, Totsune K, Murakami O, Sone M, Satoh F, Kitamuro T, Noshiro T, Hayashi Y, Sasano H and Shibahara S, Expression of Melanin-Concentrating Hormone Receptor Messenger Ribonucleic Acid in Tumor Tissues of Pheochromocytoma, Ganglioneuroblastoma, and Neuroblastoma. *J Clin Endocrinol Metab* **86**(1): 369-374., 2001.
46. Suply T, Della Zuana O, Audinot V, Rodriguez M, Beauverger P, Duhault J, Canet E, Galizzi JP, Nahon JL, Levens N and Boutin JA, Slc-1 receptor mediates effect of melanin-concentrating hormone on feeding behavior in rat: a structure-activity study. *J Pharmacol Exp Ther* **299**(1): 137-46., 2001.
47. Hintermann E, Erb C, Talke-Messerer C, Liu R, Tanner H, Flammer J and Eberle AN, Expression of the melanin-concentrating hormone receptor in porcine and human ciliary epithelial cells. *Invest Ophthalmol Vis Sci* **42**(1): 206-9., 2001.
48. Saito Y, Wang Z, Hagino-Yamagishi K, Civelli O, Kawashima S and Maruyama K, Endogenous melanin-concentrating hormone receptor SLC-1 in human melanoma SK-MEL-37 cells. *Biochem Biophys Res Commun* **289**(1): 44-50., 2001.
49. Hintermann E, Tanner H, Talke-Messerer C, Schlumberger S, Zumsteg U and Eberle AN, Interaction of melanin-concentrating hormone (MCH), neuropeptide E-I (NEI), neuropeptide G-E (NGE), and alpha-MSH with melanocortin and MCH receptors on mouse B16 melanoma cells. *J Recept Signal Transduct Res* **21**(1): 93-116., 2001.
50. Kokkotou E, Mastaitis JW, Qu D, Hoersch D, Sliker L, Bonter K, Tritos NA and Maratos-Flier E, Characterization of [Phe(13), Tyr(19)]-MCH analog binding activity to the MCH receptor. *Neuropeptides* **34**(3/4): 240-247, 2000.
51. Hawes BE, Kil E, Green B, O'Neill K, Fried S and Graziano MP, The melanin-concentrating hormone receptor couples to multiple G proteins to activate diverse intracellular signaling pathways. *Endocrinology* **141**(12): 4524-32., 2000.

52. Audinot V, Beauverger P, Lahaye C, Suply T, Rodriguez M, Ouvry C, Lamamy V, Imbert J, Rique H, Nahon JL, Galizzi JP, Canet E, Levens N, Fauchere JL and Boutin JA, Structure activity relationship studies of MCH-related peptide ligands at SLC-1, the human melanin-concentrating hormone receptor. *J Biol Chem* **18**: 18, 2001.
53. Sone M, Takahashi K, Murakami O, Totsune K, Arihara Z, Satoh F, Sasano H, Ito H and Mouri T, Binding sites for melanin-concentrating hormone in the human brain. *Peptides* **21**(2): 245-50, 2000.
54. Marsh DJ, Weingarth DT, Novi DE, Chen HY, Trumbauer ME, Chen AS, Guan XM, Jiang MM, Feng Y, Camacho RE, Shen Z, Frazier EG, Yu H, Metzger JM, Kuca SJ, Shearman LP, Gopal-Truter S, MacNeil DJ, Strack AM, MacIntyre DE, Van Der Ploeg LH and Qian S, Melanin-concentrating hormone 1 receptor-deficient mice are lean, hyperactive, and hyperphagic and have altered metabolism. *Proc Natl Acad Sci U S A* **26**: 26, 2002.
55. Kemp EH, Waterman EA, Hawes BE, O'Neill K, Gottumukkala RV, Gawkrödger DJ, Weetman AP and Watson PF, The melanin-concentrating hormone receptor 1, a novel target of autoantibody responses in vitiligo. *J Clin Invest* **109**(7): 923-30, 2002.
56. An S, Cutler G, Zhao JJ, Huang SG, Tian H, Li W, Liang L, Rich M, Bakleh A, Du J, Chen JL and Dai K, Identification and characterization of a melanin-concentrating hormone receptor. *Proc Natl Acad Sci U S A* **98**(13): 7576-81., 2001.
57. Sailer AW, Sano H, Zeng Z, McDonald TP, Pan J, Pong SS, Feighner SD, Tan CP, Fukami T, Iwaasa H, Hreniuk DL, Morin NR, Sadowski SJ, Ito M, Bansal A, Ky B, Figueroa DJ, Jiang Q, Austin CP, MacNeil DJ, Ishihara A, Ihara M, Kanatani A, Van Der Ploeg LH, Howard AD and Liu Q, Identification and characterization of a second melanin-concentrating hormone receptor, MCH-2R. *Proc Natl Acad Sci U S A* **12**: 12, 2001.
58. Hill J, Duckworth M, Murdock P, Rennie G, Sabido-David C, Ames RS, Szekeres P, Wilson S, Bergsma DJ, Gloger IS, Levy DS, Chambers JK and Muir Al A, Molecular cloning and functional characterisation of MCH2, a novel human MCH receptor. *J Biol Chem* **27**: 27, 2001.
59. Wang S, Bihan J, O'Neill K, Weig B, Fried S, Laz T, Bayne M, Gustafson E and Hawes BE, Identification and pharmacological characterization of a novel human melanin-concentrating hormone receptor, MCH-R2. *J Biol Chem* **17**: 17, 2001.
60. Rodriguez M, Beauverger P, Naime I, Rique H, Ouvry C, Souchaud S, Dromaint S, Nagel N, Suply T, Audinot V, Boutin JA and Galizzi JP, Cloning and molecular characterization of the novel human melanin-concentrating hormone receptor mch2. *Mol Pharmacol* **60**(4): 632-9., 2001.
61. Macdonald D, Murgolo N, Zhang R, Durkin JP, Yao X, Strader CD and Graziano MP, Molecular characterization of the melanin-concentrating hormone/receptor complex: identification of critical residues involved in binding and activation. *Mol Pharmacol* **58**(1): 217-25, 2000.

62. Drozdz R, Siegrist W, Baker BI, Chluba-de Tapia J and Eberle AN, Melanin-concentrating hormone binding to mouse melanoma cells in vitro. *FEBS Lett* **359**(2-3): 199-202, 1995.
63. Burgaud JL, Poosti R, Fehrentz JA, Martinez J and Nahon JL, Melanin-concentrating hormone binding sites in human SVK14 keratinocytes. *Biochem Biophys Res Commun* **241**(3): 622-9, 1997.
64. Kastin AJ, Akerstrom V, Hackler L and Zadina JE, Phe(13),Tyr(19)-melanin-concentration hormone and the blood-brain barrier: role of protein binding. *J Neurochem* **74**(1): 385-91, 2000.
65. Schlumberger SE, Saito Y, Giller T, Hintermann E, Tanner H, Jäggin V, Civelli O and Eberle AN, Different structural requirements for melanin-concentrating hormone (MCH) interacting with rat MCH-R₁ (SLC-1) and mouse B16 cell MCH-R. *J Recept Signal Transd* **22**(4), 2002. (in press).
66. Schlumberger SE, Jäggin V, Tanner H, and Eberle AN, Endogenous receptor for melanin-concentrating hormone in human neuroblastoma Kelly cells. *Biochemical and Biophysical Research Communications* (manuscript in preparation).
67. Biedler JL, Helson L and Spengler BA, Morphology and growth, tumorigenicity, and cytogenetics of human neuroblastoma cells in continuous culture. *Cancer Res* **33**(11): 2643-52, 1973.
68. Seeger RC, Danon YL, Rayner SA and Hoover F, Definition of a Thy-1 determinant on human neuroblastoma, glioma, sarcoma, and teratoma cells with a monoclonal antibody. *J Immunol* **128**(2): 983-9, 1982.
69. Sonnenfeld KH and Ishii DN, Nerve growth factor effects and receptors in cultured human neuroblastoma cell lines. *J Neurosci Res* **8**(2-3): 375-91, 1982.
70. Schwab M, Alitalo K, Klempnauer KH, Varmus HE, Bishop JM, Gilbert F, Brodeur G, Goldstein M and Trent J, Amplified DNA with limited homology to myc cellular oncogene is shared by human neuroblastoma cell lines and a neuroblastoma tumour. *Nature* **305**(5931): 245-8, 1983.
71. Amano T, Richelson E and Nirenberg M, Neurotransmitter synthesis by neuroblastoma clones (neuroblast differentiation-cell culture-choline acetyltransferase- acetylcholinesterase-tyrosine hydroxylase-axons-dendrites). *Proc Natl Acad Sci U S A* **69**(1): 258-63., 1972.
72. Richelson E, Regulation of tyrosine hydroxylase activity in mouse neuroblastoma clone N1E-115. *J Neurochem* **21**(5): 1139-45., 1973.
73. Suri C, Fung BP, Tischler AS and Chikaraishi DM, Catecholaminergic cell lines from the brain and adrenal glands of tyrosine hydroxylase-SV40 T antigen transgenic mice. *J Neurosci* **13**(3): 1280-91., 1993.
74. Gey et al. *Cancer Res.* **12**: 264, 1952.
75. Scherer et al. *J. Exp. Med.* **97**: 695, 1953.
76. *J. Exp. Med.* **108**: 945, 1958.
77. Graham FL, Smiley J, Russell WC and Nairn R, Characteristics of a human cell line transformed by DNA from human adenovirus type 5. *J Gen Virol* **36**(1): 59-74., 1977.

78. Solca FF, Chluba-de Tapia J, Iwata K and Eberle AN, B16-G4F mouse melanoma cells: an MSH receptor-deficient cell clone. *FEBS Lett* **322**(2): 177-80., 1993.
79. Hintermann E, Drozd R, Tanner H and Eberle AN, Synthesis and characterization of new radioligands for the mammalian melanin-concentrating hormone (MCH) receptor. *J Recept Signal Transduct Res* **19**(1-4): 411-22, 1999.
80. Froidevaux S, Meier M, Hausler M, Macke H, Beglinger C and Eberle AN, A microplate binding assay for the somatostatin type-2 receptor (SSTR2). *J Recept Signal Transduct Res* **19**(1-4): 167-80., 1999.
81. Bottenstein JE and Sato GH, Growth of a rat neuroblastoma cell line in serum-free supplemented medium. *Proc Natl Acad Sci U S A* **76**(1): 514-7., 1979.
82. Anderson NL, Esquer-Blasco R, Hofmann JP and Anderson NG, A two-dimensional gel database of rat liver proteins useful in gene regulation and drug effects studies. *Electrophoresis* **12**(11): 907-30., 1991.
83. Audinot V, Lahaye C, Suply T, Beauverger P, Rodriguez M, Galizzi JP, Fauchere JL and Boutin JA, []. *Br J Pharmacol* **133**(3): 371-378., 2001.
84. Siegrist W, Stutz S and Eberle AN, Homologous and heterologous regulation of alpha-melanocyte-stimulating hormone receptors in human and mouse melanoma cell lines. *Cancer Res* **54**(10): 2604-10., 1994.
85. Dhillon WS and Bloom SR, Hypothalamic peptides as drug targets for obesity. *Curr Opin Pharmacol* **1**(6): 651-5., 2001.
86. Krude H, Biebermann H, Luck W, Horn R, Brabant G and Gruters A, Severe early-onset obesity, adrenal insufficiency and red hair pigmentation caused by POMC mutations in humans. *Nat Genet* **19**(2): 155-7., 1998.
87. Yeo GS, Farooqi IS, Aminian S, Halsall DJ, Stanhope RG and O'Rahilly S, A frameshift mutation in MC4R associated with dominantly inherited human obesity. *Nat Genet* **20**(2): 111-2., 1998.
88. Vaisse C, Clement K, Durand E, Hercberg S, Guy-Grand B and Froguel P, Melanocortin-4 receptor mutations are a frequent and heterogeneous cause of morbid obesity. *J Clin Invest* **106**(2): 253-62., 2000.
89. Fehm HL, Smolnik R, Kern W, McGregor GP, Bickel U and Born J, The melanocortin melanocyte-stimulating hormone/adrenocorticotropin(4- 10) decreases body fat in humans. *J Clin Endocrinol Metab* **86**(3): 1144-8., 2001.
90. Takekawa S, Asami A, Ishihara Y, Terauchi J, Kato K, Shimomura Y, Mori M, Murakoshi H, Suzuki N, Nishimura O and Fujino M, T-226296: a novel, orally active and selective melanin-concentrating hormone receptor antagonist. *Eur J Pharmacol* **438**(3): 129-35., 2002.
91. Bednarek MA, Feighner SD, Hreniuk DL, Palyha OC, Morin NR, Sadowski SJ, MacNeil DJ, Howard AD and Van Der Ploeg LH, Short segment of human melanin-concentrating hormone that is sufficient for full activation of human melanin-concentrating hormone receptors 1 and 2. *Biochemistry* **40**(31): 9379-86., 2001.

92. Bednarek MA, Hreniuk DL, Tan C, Palyha OC, MacNeil DJ, Van Der Ploeg LH, Howard AD and Feighner SD, Synthesis and biological evaluation in vitro of selective, high affinity Peptide antagonists of human melanin-concentrating hormone action at human melanin-concentrating hormone receptor 1. *Biochemistry* **41**(20): 6383-90., 2002.
93. Bednarek MA, Tan C, Hreniuk DL, Palyha OC, MacNeil DJ, Van Der Ploeg LH, Howard AD and Feighner SD, Synthesis and biological evaluation in Vitro of a selective, high potency peptide agonist of human melanin-concentrating hormone action at human melanin-concentrating hormone receptor 1. *J Biol Chem* **11**: 11, 2002.
94. Stroh T, Jackson AC, Sarret P, Dal Farra C, Vincent JP, Kreienkamp HJ, Mazella J and Beaudet A, Intracellular dynamics of sst5 receptors in transfected COS-7 cells: maintenance of cell surface receptors during ligand-induced endocytosis. *Endocrinology* **141**(1): 354-65., 2000.
95. Devi LA, G-protein-coupled receptor dimers in the lime light. *Trends Pharmacol Sci* **21**(9): 324-6, 2000.
96. Pfeiffer M, Koch T, Schroder H, Klutzny M, Kirscht S, Kreienkamp HJ, Holtt V and Schulz S, Homo- and heterodimerization of somatostatin receptor subtypes. Inactivation of sst3 receptor function by heterodimerization with sst2A. *J Biol Chem* , 2000.
97. Laporte SA, Boucard AA, Servant G, Guillemette G, Leduc R and Escher E, Determination of peptide contact points in the human angiotensin II type I receptor (AT1) with photosensitive analogs of angiotensin II. *Mol Endocrinol* **13**(4): 578-86., 1999.

7. Appendix

7.1 Acknowledgements

I would like to thank my two Ph.D. supervisors Pr A.N. Eberle and Pr MJ. Freund-Mercier who gave me the opportunity to achieve this thesis "en co-tutelle".

Many thanks to the members of the endocrinology laboratory namely (from left to right, back to front row) Heidi, Sylvie, Olivier, Alex, Anna, Verena, Kerstin and Martine for their either technical help (Heidi: peptide synthesis; Verena: rabbit polyclonal antibody production) or theoretical advice.

I thank E. Helen Kemp, Division of Clinical Sciences (North), University of Sheffield, Northern General Hospital, Sheffield, UK for providing me the reference and the abstract of the poster presented by Hoogduijn M.J. et al. at the British Society for Investigative Dermatology Annual Meeting, Warwick, 9-11 April 2001.

Finally many thanks to Dr J. Baumann for her critical reading of the manuscript.



7.2. Curriculum vitae

7.2.1. Personal information

Name: Sophie SCHLUMBERGER

Address: 47 bis, rue du Dr HURST
68300 Saint Louis, France

Phone: ++ 33 3 89 67 96 04

E-mail: Sophie.Schlumberger@unibas.ch

New address from October 1st, 2002:

50, rue de Village Neuf
68128 Rosenau, France

Phone: ++33 3 89 70 68 55

E-mail: Sophie.Schlumberger@free.fr

Nationality: French

Date of Birth: October 5, 1975

Place of birth: Colmar, France

Languages: French, English, and German

7.2.2. Education

1990-1993: High School: "Baccalauréat C" equivalent to British A-level with emphasis in maths and physics
Lycée Louise Weiss, Ste Marie-aux-Mines, France

1993-1997: Faculty of Sciences, Master degree in Biochemistry
University Louis Pasteur, Strasbourg, France

1997-1998: Faculty of Sciences, "Diplôme d'Études Approfondies" in Cellular and Molecular Biology
University Louis Pasteur, Strasbourg, France

1998-2002: Ph.D. Fellowship

Laboratory of Endocrinology, Department of
Research, University Hospital and University
Children's Hospital, Basel, Switzerland

And

Laboratory of Cellular and Integrated
Neurophysiology, UMR 7519, Institut de Physiologie
et de Chimie Biologique (IPCB), Strasbourg, France

7.2.3. Lectures attended during the Ph.D. fellowship

3425	Cellular signalling; Part II (Prof. Dr.sc.nat. Alex N. Eberle and PD Dr. K. Ballmer-Hofer)
6491	Neurological diseases (Prof. Dr. med. U. Otten)
5426	Experimental Cancer Research; Part II (Dr. med et phil. Max M. Burger)
1244	Developmental neuroscience (Prof. Dr.sc.nat. D. Monard)
2434	Immunology; Part I (Prof. Dr.phil. R. Gisler)
5490	Immunology; Part II (Prof. Dr.phil. R.Gisler)
2431	Disease genes, cell and gene therapy (Prof. Dr. P. Philippsen)
4231	Molecular neurobiology and signaling (Prof. Dr.phil. Markus A. Ruegg)
4538	Novel and emerging technologies in functional genomics (Prof. Dr. P. Philippsen)

7.3. Original publications (P) and poster presentation (PO)

- P-1 Hintermann E., Tanner H., Talke-Messerer C., **Schlumberger S.**, Zumsteg U. & Eberle A.N. Interaction of melanin-concentrating hormone (MCH), neuropeptide E-I (NEI), neuropeptide G-E (NGE), and α -MSH with melanocortin and MCH receptors on mouse B16 melanoma cells. *J. of Receptor & Signal Transduction Research*, 2001 Feb; 21(1): 93-116
- P-2 Hintermann E., Talke-Messerer C., Jäggin V., **Schlumberger S.**, Tanner H. & Eberle A.N. Characterization of receptors for melanin-concentrating hormone (MCH) in the ciliary epithelium of the eye. *Peptides 2000*, 2001 p735-736; EDK, Paris, France.
- P-3 **Schlumberger S.E.**, Talke-Messerer C., Zumsteg U., & Eberle A.N., Expression of receptors for melanin-concentrating hormone (MCH) in different tissues and cell lines. *J. Recept. Signal Transd.*, 2002 ; 22 (1-3): 511-533.
- P-4 **Schlumberger S.E.**, Saito Y., Giller T., Hintermann E., Tanner H., Jäggin V., Civelli O. & Eberle A.N. Different structural requirements for melanin-concentrating hormone (MCH) interacting with rat MCH-R₁ (SLC-1) and mouse B16 cell MCH-R. *J. Recept. Signal Transduct.*, 2002 ; 22 (4) *in press*.
- P-5 **Schlumberger S.E.**, Jäggin V., Tanner H. & Eberle A.N. Endogenous receptor for melanin-concentrating hormone in human neuroblastoma Kelly cells. *Biochemical and Biophysical Research Communications* (manuscript in preparation).
- PO-1 **Schlumberger S.E.**, Talke-Messerer C. & Eberle A.N. Characterization of receptors for melanin-concentrating hormone (MCH) on human Kelly cells. 9th. *Swiss Workshop on Methodology of Receptor Research*, September 2001, Zürich, Switzerland.

Abstract

Melanin-concentrating hormone (MCH), initially isolated from teleost fish as a 17-amino acid peptide, is a potent orexigenic neuropeptide in mammals where it is produced by hypothalamic neurons and participates in the regulation of food intake. In 1999 and 2001, two receptor subtypes for MCH were discovered, MCH-R₁ and -R₂. They are coupled to G-proteins and are mainly expressed in the brain.

The purpose of this thesis was to identify MCH binding sites or receptors in various cell lines and tissues. To this end, stable and potent MCH radioligands were developed and applied: ¹²⁵I-[Phe¹³, Tyr¹⁹]-MCH, ¹²⁵I-[DPhe¹³, Tyr¹⁹]-MCH, and [¹²⁵I]-MCH. Many cell lines and tissues were screened, amongst which 5 human neuroblastoma cell lines, 2 murine neuroblastoma cell lines, human primary melanocytes, mouse brain tumour, rat embryonic hypothalamic cells, rat brain cryostat sections and porcine brain membranes. Even though ¹²⁵I-[Phe¹³, Tyr¹⁹]-MCH and ¹²⁵I-[DPhe¹³, Tyr¹⁹]-MCH revealed specific binding sites in mouse melanoma cells, they were not suitable to find MCH-R₁ or -R₂. We therefore used [¹²⁵I]-MCH to perform a MCH-R₁ structure-activity study with 12 MCH analogues, which was extended to a functional study using the FLIPR assay. For 9 analogues, there was a good correlation between IC₅₀s and EC₅₀s. We also screened different cell lines for MCH-R expression by RT-PCR and identified a promising MCH-R₁-expressing cell line, which also produces MCH: Kelly human neuroblastoma cells. MCH binding sites could be visualised on 2-D gels following crosslinking with MCH radioligand.

In conclusion, these studies demonstrated that MCH receptor subtypes expressed on different cell lines display different ligand recognition profiles and hence require different types of radioligand for binding analysis. The human Kelly cell line appears to be an interesting model for analysis of novel MCH ligands as it endogenously expresses MCH-R.

Caractérisation des récepteurs de l'hormone de mélanocortine (MCH)

L'hormone de mélanocortine (MCH) a été isolée initialement chez les poissons téléostéens sous la forme d'un peptide de 17 acides aminés. Chez les mammifères c'est un puissant neuropeptide orexigénique produit par des neurones hypothalamiques régulant la prise alimentaire. En 1999 et 2001, deux récepteurs de la MCH furent découverts, MCH-R₁ et -R₂, ils sont couplés aux protéines G et exprimés dans le cerveau.

Le but de cette thèse était d'identifier les sites de liaison ou les récepteurs pour la MCH dans différentes lignées cellulaires et tissus. Pour cela, des radioligands stables et efficaces (¹²⁵I-[Phe¹³, Tyr¹⁹]-MCH, ¹²⁵I-[DPhe¹³, Tyr¹⁹]-MCH et [¹²⁵I]-MCH) ont été développés et utilisés. De nombreuses lignées et tissus ont été testés dont 5 lignées de neuroblastome humain et 2 lignées murines, des melanocytes primaires humains, des neurones embryonnaires hypothalamiques de rat, des coupes de cerveau de rat et des membranes de cerveau de porc. ¹²⁵I-[Phe¹³, Tyr¹⁹]-MCH et ¹²⁵I-[DPhe¹³, Tyr¹⁹]-MCH ont mis en évidence des sites de liaison dans le mélanome murin mais se sont révélés inadéquats pour trouver le MCH-R₁ ou -R₂. Nous avons alors effectué avec [¹²⁵I]-MCH une étude de structure-activité du MCH-R₁ avec 12 analogues de la MCH, l'étude fonctionnelle utilisant le FLIPR. Pour 9 analogues il y a eu une bonne corrélation entre les IC₅₀s et les EC₅₀s. Nous avons aussi testé par RT-PCR des lignées pour l'expression des MCH-R et nous en avons trouvé une exprimant le MCH-R₁ et produisant de surcroît la MCH: la lignée de neuroblastome humain Kelly.

En conclusion, ces études ont montré que les sous-types de récepteurs de la MCH exprimés par différentes lignées cellulaires reconnaissent les ligands de façon différente et nécessitaient donc différents types de ligands pour les études de liaison. La lignée de neuroblastome humain Kelly semble être un modèle intéressant pour l'analyse de nouveaux ligands dérivés de la MCH car elle exprime le MCH-R de façon endogène.

Mots-Clés :

Hormone de mélanocortine (MCH) / Récepteur couplé aux protéines G (GPCR) / radioligand / étude de liaison.

Laboratoire d'Endocrinologie
Département de Recherche,
Hôpital cantonal de Bâle
Hebelstrasse 20, CH-4031 BASEL

UMR 7519 CNRS/ULP
Neurophysiologie cellulaire et
intégrée
21, rue René Descartes
67084 STRASBOURG